Durham E-Theses

Dielectric and optical properties of organic photorefractive materials

Farsari, Maria

How to cite:

Farsari, Maria (1996) *Dielectric and optical properties of organic photorefractive materials*, Durham theses, Durham University. Available at Durham E-Theses Online: http://etheses.dur.ac.uk/5226/

Use policy

Dielectric and Optical Properties of

Organic Photorefractive Materials

Maria Farsari

Submitted for the degree of Doctor of Philosophy

University of Durham

Department of Physics

1 0 MAR 1997

1996

Abstract

The work presented in this thesis is derived from experimentation in the field of polymeric photorefractive materials. Low T_g polymeric composites were prepared, based on the well-known photoconductive polymer PVK (maximum 50% w/w), sensitized with TNF (2% w/w) and C_{60} (0.2% w/w), plasticized with ECZ (maximum 49.3% w/w) and doped with the nonlinear optical materials NPP (50% w/w), DAN (20% w/w), DED (5% w/w), DCNQI (0.5% w/w), ULTRA-DEMI (5% w/w) and DI-DEMI (2% w/w), and their dielectric, linear and non-linear optical properties were investigated. All the materials, except DCNQI, exhibited good solubility and sample processibility.

The dielectric properties of the composites at 1 KHz and 1 MHz were determined using a parallel-plate capacitance bridge. The dielectric constant and loss at 10 GHz were measured using a novel adaptation of the resonant cavity technique, which was designed for measurements at ambient and elevated temperatures. The method was used to measure of the dielectric constant and loss of two novel, high T_g, electro-optic polymers at temperatures up to 100 °C. The dielectric properties measured were typical of polymeric materials. The absorption coefficient and the refractive index at different wavelengths were measured us-

ing a spectrophotometer. For the refractive index, an interference fringe analysis was used.
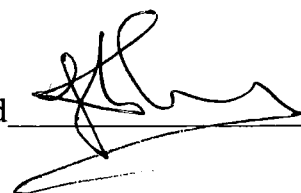
The nonlinear measurements consisted of second harmonic generation, to prove the nonlinearity of the composites, two-beam coupling measurements, to prove their photorefractivity and degenerate four-wave mixing to measure their diffraction efficiency. The NPP, DAN, DED and ULTRA-DEMI doped investigated composites exhibited second order nonlinearity with highest the one of ULTRA-DEMI, at 292 pm/V for 19 kV of corona poling field. The photorefractivity of the NPP, DAN and DED doped composites was proven at 632.8 nm, while ULTRA-DEMI doped composites photooxidized before any measurements were possible. The two-beam coupling coefficients measured were lower than 20 cm^{-1}, while net gain was observed only in the NPP doped composite. The diffraction efficiencies of the NPP, DAN and DED doped composites were measured at 632.8 nm, and were found to be 10^{-5}-10^{-6}.

Declaration
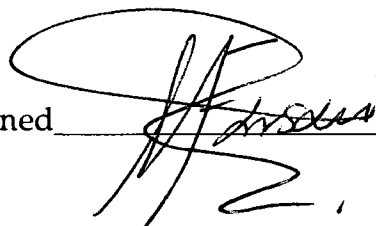
I hereby declare that the work presented in this thessi has not previously been submitted for any degree and is not beeing currently submitted in candidature for any other degree.

Signed_____

The work reported in this thessi was carried out by the candidate. Any work not carried out by the candidate is acknowledged in the main text.

Signed_____

Ph.D. Supervisor

Signed_____

Candidate

Statement of Copyright.

The copyright of this thesis rests with the author. No quotation should be published without the prior written consent and information derived from it should be acknowledged.

Acknowledgments

It has been for me an honour and privilege to be a member of the Nonlinear Optics group of the University of Durham. First and foremost I would like to thank my supervisor Dr. Graham Cross, for his trust, his continuous guidance and for being an inexhaustible source of ideas and inspiration.

I am grateful to Professor David Bloor, for his invaluable advice and Dr. B. L. J. Kulesza for his continuous help and encouragement.

I would also like to thank other member of the department. Dr. Marek Szablewski for the synthesis of nonlinear optical materials; Dr. David Gray for many critical discussions on nonlinear optics; Dr. Tony Axon for his help on laser systems; Dr. Marcus Swann for his help with polymers; Dr. Phil Adams for his advice on solvents; Dr. Anna Thornton for her patience with me in the chemistry lab; and Mr. Phil Thomas for 'keeping an eye' on me during my high-voltage experiments; Mr. Norman Thompson and Mr. David Pattinson for providing the necessary technical support. But mostly I would like to thank these people for making my life in the department interesting and enjoyable.

I would also like to thank the EU for partly financing this project and Dr. C. H. Wang, from Heriot-Watt University, for his help with the photorefractive measurements.

I would also like to thank all the people that made my life in Durham enjoyable. Dr. Mirela Cuculescu for being a friend and a solid support in difficult times; Panos Kokkonis and Panos Giannakos for their unique company; Henry Day for sharing my interest in cinema; Becca Asquith, Jörg Mosig and Zenén Santana for being wonderful housemates; Rob and Vinda Gray for being my family in this country.

Last, but not least, I would like to thank my parents and my sister for their unconditional love and support.

ITHAKA

As you set out for Ithaka
hope your road is a long one,
full of adventure, full of discovery.
Laistrygonians, Cyclops,
angry Poseidon-don't be afraid of them;
you'll never find things like that on your way,
as long as you keep your hopes raised high,
as long as a rare excitement
stirs your spirit and your body.
Laistrygonians, Cyclops,
angry Poseidon-you won't encounter them
unless you bring them along inside your soul,
unless your soul sets them up in front of you.

Hope your road is a long one.
May there be many summer mornings when,
with what pleasure, what joy,
you enter harbours you see for the first time;
may you stop at Phoenician bazaars
to buy fine things,
mother of pearl and coral, amber and ebony,
sensual perfume of every kind-
as many sensual perfumes as you can;
and may you visit many Egyptian cities,
to learn and go on learning from their scholars.

Keep Ithaka always in your mind.
Arriving there is what you are destined for.
But don't hurry the journey at all.
Better if it lasts for years,
so you are old when you reach the island,
wealthy with what you've gained on the way,
not expecting Ithaka to make you rich.

Ithaka gave you the marvellous journey.
Without her you wouldn't have set out.
She has nothing left to give you now.

And if you find her poor, Ithaka won't have fooled you.
Wise as you will be, so full of experience,
you'll understand by then what these Ithakas mean.

K.P. Kavafis

Contents

List of Figures

List of Tables

Important Symbols

η	diffaction efficiency
Γ	two-beam coupling coefficient
α	absorbtion coefficient
$\mathbf{E}$	electric field
$\mathbf{P}$	polarization
$\mathbf{D}$	dielectric displacement
E_{sc}	space-charge field
λ	wavelength
ε_r	relative dielectric constant ($\varepsilon_r = \varepsilon_r' + i\varepsilon_r''$)
$\chi^{(n)}$	n order susceptibility
χ_{eff}	effective susceptibility
r	linear electro-optic coefficient
r_{eff}	effective electro-optic coefficient

ω frequency

t time

k wavenumber

n refractive index

U energy density

η impermeability tensor

Λ_G grating wavelength

$\mathbf{K}_G$ grating vector

$\phi(E)$ photocarrier geneartion quantum yield

n_q free carrier density

J current density

N_A acceptor density

N_D donor density

N_D^+ density of ionized donors

D diffusion constant

μ_q carrier mobility

e elementary charge

q carrier charge

β_T thermal degeneration rate

s_I photoionization constant

γ recombination constant

I irradiance

m modulation depth

β_0 beam ratio

γ_0 two-beam coupling ratio

d film thickness

L path length

T_g glass transition temperature

μ dipole moment

β hyperpolarizability

C capacitance

Q_c resonant cavity quality factor

Q electro-optic quality factor

V volume

D_ω frequency dispersion

f local field factor

Abbreviations

nlo	nonlinear optical
TCNQ	7,7,8,8-tetracyanoquinodimethane
PVK	poly(N-vinylcarbazole)
TNF	2,4,7-trinitro-9-fluorenone
ECZ	N-Ethyl Carbazole
NPP	N-(4-nitrophenyl)-(L)-prolinol
DAN	2-(N, N,-dimethylamino)-5-nitroacetanilide
DED	7,7 bis-diethylamino,-8, 8 dicyanoquinodimethane
DCNQI	2-(4-dicyanomethylenecyclohexa-2, 5-dienylidine)-imidazolidine
ULTRA-DEMI	Propanedinitrile {4-[1-cyano-2(1-acetaldehyde diethyl acetal-3(ØH)-2 -piperideine) ethylidene]-2, 5-cyclohexadiene-1-ylidene}

DI-DEMI   Propanedinitrile [4-[1-cyano-3-dicyclohexylamino)-2-
                propenylidene]-2, 5-cyclohexadiene-1-ylidene]

DCM   dichloromethane

TMU   N, N - tetramethylurea

DMF   N, N-dimethylformamide

THF   etrahydofluran

TPC   1,2,3-trichloropropane

Chapter 1

Introduction

1.1 Introduction

The photorefractive effect is a phenomenon in which the index of refraction of an optical medium is changed due to the optically induced redistribution of charges. The effect arises when carriers, photo-excited by a spatially-modulated light intensity, separate and become trapped to produce nonuniform space-charge distribution. The resulting space-charge field then modulates the refractive index via the electro-optic effect to create a phase grating that can diffract a light beam. The necessary components to produce a photorefractive phase hologram are therefore: photo-ionizable charge generator, transporting medium, trapping sites and electric field dependent refractive index.

The effect was first discovered in 1966, when A. Ashkin and coworkers were studying the transmission of laser beams through electro-optic crystals, hoping that they would produce second harmonic generation [1].

The presence of laser beams inside some electro-optic crystals such as $LiNbO_3$ and $LiTaO_3$ led to an index inhomogeneity which distorted the wavefront of the transmitted laser beam. The effect was then referred to as 'Optical Damage' [1] and was thought to pose serious limitations in the use of $LiNbO_3$ and $LiTaO_3$ in nonlinear experiments requiring high light irradiancies. F. S. Chen et al first suggested that this 'Optical Damage' could be used to advantage to form a holographic recording in applications where a material that gives refractive index change on exposure would be desirable [2]. Since then, the effect has been observed in many inorganic electro-optic crystals such as $Bi_{12}SiO_{20}$, $BaTiO_3$, GaAs and CdTe [3-18].

Photorefractive materials change rapidly when exposed to bright light, respond slowly when exposed to dim light and capture sharp detail when struck by some pattern of light. For these reasons, a variety of novel applications have been proposed and demonstrated on a laboratory scale, including photorefractive phase conjugation, novelty filtering, beam fanning and optical limiters [19-30]. However, inorganic crystals are costly to grow, their photorefractive properties vary from crystal to crystal and they require a fairly powerful laser source as a pump. All these considerations make devices based on photorefractive crystals rather impractical and have prevented them from reaching commercialization on a broad basis.

Until 1990, all the materials exhibiting the photorefractive effect were inorganic crystals. The first organic material in which the photorefractive effect was observed was a carefully grown nonlinear crystal 2-(cyclooctylamino)-5-nitropyridine (COANP) doped with 7,7,8,8-tetracy-

anoquinodimethane (TCNQ) [31,32]. The preparation, however, of high optical quality, doped organic crystals containing reasonably large concentrations of dopants, is a very difficult process because most of them are expelled during the crystal growth. Consequently, the strength of the photorefractive effect observed in this crystal was small. Further, in order for a crystal to exhibit the electro-optic effect it must have a non-centrosymmetric crystal structure, which is a relatively rare case in organics.

The first polymeric photorefractive material appeared in 1991, composed of the nonlinear polymer bisphenol-A-diglycidylether 4-nitro-1,2-phenylenediamine (bisA-NPDA) made photoconductive by doping with the hole transport agent diethylaminobenzaldehyde-diphenylhydrazone (DEH) [33]. The response of the material was slow and had a diffraction efficiency of the order of 10^{-6}, but it did serve to demonstrate that the simultaneous requirements of optical nonlinearity, charge generation and trapping could be combined in a single polymeric material to produce photorefractivity.

A milestone in polymer photorefractivity was reached in 1994, when Peyghambarian and co-workers managed to increase the maximum recorded diffraction efficiency of a polymeric photorefractive material to nearly 100% [34]. They used a polymer composite based on the photoconductor poly(N-vinylcarbazole) (PVK). Photosensitivity in the visible part of the spectrum was provided by the charge transfer complex PVK forms with 2,4,7-trinitro-9-fluorenone (TNF). The azo-dye 2,5-dimethyl-4-(nitrophenylazo) anisole (DMNPAA) was used as the electro-optic active chromophore, at a concentration of 50% w/w. This material proved very unstable, however, mainly

because of the crystalline nature and the high concentration of the nonlinear optical dopant [43]. Since then, a lot of progress has been made in improving virtually all response parameters in polymeric photorefractive materials, and they can compete with inorganic photorefractive crystals in diffraction efficiency and speed. In Table 1.1 a list of the diffraction efficiencies η of some existing photorefractive polymers are given. In this table are also included the net gain coefficient (Γ-α), where Γ and α are the two-beam coupling and the absorption coefficient respectively, the applied voltage E, the film thickness and operating wavelength which, as it will become clear in the following chapters, are important parameters for the characterization of a photorefractive polymer.

There are many mechanisms that can cause the diffraction of an incident optical beam including photochromism, thermochromism, thermorefraction, excited state generation and the Kerr effect [43]. The photorefractive effect, however, possesses a combination of characteristics which make it unique. Diffraction efficiencies approaching 100% can be achieved even with weak laser beams as a consequence of the integrating nature of the effect. The resulting refractive index gratings are reversible, as uniform illumination will erase the space charge field. Another very important characteristic, as it is explained in detail in Chapter 2, is the existence of a spatial phase shift between the illumination pattern and the refractive index grating. This is the genuine 'fingerprint' of the photorefractive effect; no other local or non-local mechanism can produce a phase-shifted grating. The existence of this phase

Table 1.1 Photorefractive properies of some polymeric photorefractive materials

Material	Two-beam coupling net gain			diffraction efficiency				Ref.
	Γ -α (cm^{-1})	E (V/μm)	λ (nm)	η	E (V/μm)	d(μm)	λ (nm)	
DMNPAA:PVK:ECZ:TNF	200	90	675	86×10^{-2}	61	105	675	[34]
DMNPAA:Polysiloxane:TNF	$\approx$200	80	650	60×10^{-2}	80	40	650	[35]
PDCST:PVK:TNF	5.5	32	753	3.7×10^{-3}	32	125	753	[36]
FDEANST:PVK:TNF	5.6	32	753	4.5×10^{-4}	32	125	753	[36]
MBANP:PVK:TNF	1.7	32	753	1.7×10^{-4}	32	125	753	[36]
MTFNS:PVK:TNF	0.6	32	753	1.2×10^{-5}	32	125	753	[36]
DEANMST:PVK:TNF	no net gain			1.5×10^{-3}	32	125	753	[36]

Material	Two-beam coupling net gain			diffraction efficiency				Ref.
	Γ-α (cm^{-1})	E (V/μm)	λ (nm)	η	E (V/μm)	d(μm)	λ (nm)	
DEACST:PVK:TNF	no net gain	32	753	2.0×10^{-4}	32	125	753	[36]
DEABNB:PVK:TNF	no net gain	32	753	9.9×10^{-5}	32	125	753	[36]
DTNBI:PVK:TNF	no net gain	32	753	3.8×10^{-4}	32	125	753	[36]
FDEANST:PVK:p-dci	$\approx$2	32	753	4.0×10^{-4}	32	125	753	[36]
FDEANST:PVK:p-dci	2.1	32	753	2.1×10^{-3}	32	125	753	[36]
DEANST:PVK:TPY	7*	62.5	703	11×10^{-3}	62.5	160	703	[37]
DEANST:PVK:C$_{60}$	4*	50	645	2×10^{-2}	50	250	633	[38]

* Γ instead of Γ-α

Material	Two-beam coupling net gain			diffraction efficiency				Ref.
	$\Gamma - \alpha$ (cm^{-1})	E (V/μm)	λ (nm)	η	E V/μm	$d(\mu$m)	λ (nm)	
EHDNPB:PVK:TNF	120	60	676	60×10^{-2}	60	250	676	[39]
PMMA:DTNBI:C$_{60}$	34	40	676	8×10^{-3}	40	125	676	[40]
PRODAN:TTA:PC:C$_{60}$	12.9	70	633	1.4×10^{-2}	80	140	633	[41]
PRODAN:TTA:PC:C$_{60}$	13.3	85	515	0.6×10^{-2}	80	140	515	[41]
PRODAN:TTA:PC:C$_{60}$	13	85	488	-	-	-	-	[41]
NPP:TTA:PC:C$_{60}$	19.6	42.5	633	14×10^{-2}	75	100	633	[41]
EPNA:PVK:TNF	18	10 kV*	633	2×10^{-3}	10 kV	65	633	[42]

* Corona-poled sample

shift gives rise to an asymmetric beam transfer between two laser beams which is the basis for several specific applications.

Polymeric materials cost less, are easy to manufacture and are more versatile than crystalline materials. They can be doped with molecules of different sizes and can easily be formed into a variety of thin film and waveguide configurations. Furthermore, unlike crystalline materials, where a non-centrosymmetric structure is essential, in polymeric materials the second order optical nonlinearity can be introduced by electric field poling. However, the low cost and the ease of manufacture are not the only reasons for pursuing the development of polymeric photorefractive materials. In organic materials a potentially better performance in terms of refractive index change per incident energy is expected compared to inorganic crystals, because of the lower dielectric constant, which allows a higher space charge field for the same charge trapped. In inorganics, the optical nonlinearity is mainly driven by ionic polarizability, which results in large electro-optic coefficient being accompanied by large dielectric constant. On the other hand, in organic electro-optic materials the optical nonlinearity is a molecular property arising from the nonuniform electronic charge distribution and the dielectric constant does not vary much from material to material.

1.2 Aim and Outline of this Thesis

The field of organic photorefractive materials is one of the fastest growing in the area of optoelectronics. There is however a limited approach to the subject. In most cases only the photorefractivity and the diffraction efficiency of each candidate photorefractive material are investigated. Other optical pa-

rameters such as the refractive index and the electro-optic response are ignored. The same applies to the dielectric properties of the candidate photorefractive material at low and high frequencies, quantities that become increasingly important as the response time of the photorefractive materials becomes faster.

In this work, a more complete approach to the subject was attempted. Polymeric composites based on the well-known photoconductive polymer poly (N-vinylcarbazole) sensitized with C_{60}, plasticized with ECZ and doped with several nonlinear optical materials were prepared and the dielectric, linear and nonlinear properties of these composites were investigated.

In Chapter 2 the theory behind the electro-optic and photorefractive effects is discussed. The relation between the second order nonlinear optical coefficient and the electro-optic coefficient is established. The principle of operation and an up-to-date approach to the theory of the photorefractive effect are presented and the basic theory of the two-beam coupling and four-wave mixing experiments is outlined.

Chapter 3 gives an introduction to the general characteristics of photoconductive and electro-optic materials and a detailed description of the materials investigated. In addition, there is a description of two electro-optic polymers investigated for their dielectric properties.

Chapter 4 describes the experimental techniques employed. In order to measure the dielectric constant at different microwave frequencies, a parallel-plate dielectric bridge was used and a new adaptation of the resonant cavity method that would allow the measurement of the dielectric properties

at high temperatures was devised. The optical absorption and refractive index were measured using a spectro-photometer. The second order permittivity were measured using second harmonic generation. In order to show the asymmetric two-beam energy transfer and thus prove the photorefractivity of the material, as well as measure the two-beam coupling gain coefficient, a two-beam coupling experiment was setup. The diffraction efficiency was measured with a degenerate four-wave mixing experiment.

Chapter 5 give a detailed description of the preparation of the different sample.

Chapter 6 gives the results of the linear experiments described in Chapter 4. The dielectric constant was measured at 1 KHz and 1 MHz and the dielectric constant and loss at 10 GHz. In addition the dielectric constant and loss at 10 GHz up to a temperature of 100 °C of the two electro-optic polymers described in Chapter 3 was measured. The optical absorption and refractive index were measured at all the operating wavelengths.

In Chapter 7 the results of the nonlinear optical experiments described in Chapter 4 are given. The second order susceptibility was measured at 1064 nm and the electro-optic coefficient at the required wavelengths was inferred from this. The two-beam coupling gain and the diffraction efficiency were measured as functions of the applied field.

1.3 References

[1]   A. Ashkin, G. D. Boyd, J. M. Dziedzic, R. G. Smith, A. A. Ballman, H. J. Levinstein, and K. Nassau, 'Optically induced refractive index inhomogeneities in LiNbO$_3$ and LiTaO$_3$', *App. Phys. Lett.*, vol. 9, pp. 72-74, **1966**.

[2]   F. S. Chen, J. T. LaMacchia, and D. B. Fraser, 'Holographic storage in Lithium Niobate', *App. Phys. Lett.*, vol. 13, pp. 223-225, **1968**.

[3]   Z. Q. Wang, W. A. Gillespie, and C. M. Cartwright, 'Holographic-recording improvement in a bismuth silicon oxide crystal by the moving-grating technique', *Applied Optics*, vol. 33, pp. 7627-7633, **1994**.

[4]   C. X. Yang, Y. H. Zhang, X. M. Yi, P. C. Yeh, Y. Zhu, M. J. Hui, and X. Wu, 'Intensity-dependent absorption and photorefractive properties in cerium-doped BaTiO$_3$ crystals', *J. Appl. Phys.*, vol. 78, pp. 4323-4330, **1995**.

[5]   M. Zgonik, K. Nakagawa, and P. Günter, 'Electro-optic and dielectric properties of photorefractive BaTiO$_3$ and KNbO$_3$', *J. Opt. Soc. Am. B*, vol. 12, pp. 1416-1421, **1995**.

[6]   J. Y. Chang, M. H. Garrett, H. P. Jenssen, and C. Warde, 'Intensity-dependent photorefractive properties in an *n*-type BaTiO$_3$', *J. Appl. Phys.*, vol. 75, pp. 43-48, **1994**.

[7]   R. Müller, L. Arizmendi, M. Carrascosa, and J. M. Cabrera, 'Time evolution of grating decay during photorefractive fixing processes in LiNbO$_3$', *J. Appl. Phys.*, vol. 77, pp. 308-312, **1995**.

[8]   B. Guo, L. Yan, H. Y. Zhang, X. H. He, and Y. H. Shih, 'Near-infrared response of photorefractive crystals $(K_{0.5} Na_{0.5})_{0.2} (Sr_{0.75}Ba_{0.25})_{0.9} Nb_2O_6$:Cu and LiNbO$_3$:Fe', *J. Appl. Phys.*, vol. 79, pp. 72-76, **1996**.

[9] M. Zgonik, C. Medrano, M. Ewart, H. Wüest, and P. Günter, 'KNbO$_3$ crystals for photorefractive applications', *Optical Engineering*, vol. 34, pp. 1930-1935, **1995**.

[10] N. V. Kukhtarev, T. Kukhtareva, H. J. Caulfield, P. P. Banerjee, H. L. Yu, and L. Hesselink, 'Broadband dynamic, holographically self-recorded, and static hexagonal scattering patterns in photorefractive KNbO$_3$:Fe', *Optical Engineering*, vol. 34, pp. 2261-2265, **1995**.

[11] V. Levya, D. Engin, X. L. Tong, M. Tong, A. Yariv, and A. Agranat, 'Fixing of photorefractive volume holograms in $K_{1-y}Li_yTa_{1-x}O_3$', *Optics Letters*, vol. 20, **1995**.

[12] Y. Tomita, J. Bergquist, and M. Shibata, 'Photorefractive properties of undoped, Cr-doped, and Cu-doped potassium sodium strontium barium niobate crystals', *J. Opt. Soc. Am. B*, vol. 10, pp. 94-99, **1993**.

[13] M. D. Ewbank, R. A.Vazquez, R. R. Neurgaonkar, and F. Vachss, 'Contradirectional two-beam coupling in absorptive photorefractive materials: application to Rh-doped strontium barium niobate (SNB:60)', *J. Opt. Soc. Am. B*, vol. 12, pp. 87-98, **1995**.

[14] H. C. Pedersen and P. M. Johansen, 'Parametric oscillation in photorefractive media', *J. Opt. Soc. Am. B*, vol. 12, pp. 1065-1073, **1995**.

[15] S. Mailis, L. Boutsikaris, and N. A. Vainos, 'Multiplexed static and dynamic photorefraction in $Bi_{12}SiO_{20}$ crystals at 780-nm', *J. Opt. Soc. Am. B*, vol. 11, pp. 1996-1999, **1994**.

[16] J. -Y. Moisan, N. Wolffer, O. Moine, P. Gravey, G. Martel, A. Aoudia, E. Repka, Y. Marfaing, and R. Triboulet, 'Characterization of photorefractive CdTe-V - high two-wave mixing gain with an optimum low-frequency periodic external electric- field', *J. Opt. Soc. Am. B*, vol. 11, pp. 1655-1667, **1994**.

[17] C. Özkul, S. Jamet, P. Gravey, K. Turki, and G. Bremond, 'Photorefractive effect in InP:Fe dominated by holes at room- tem-

perature - influence of the indirect transitions', *J. Opt. Soc. Am. B,* vol. 11, pp. 1668-1673, **1994.**

[18] W. Feng, Y. Yu, H. Chen, Q. Huang, and J. M. Zhou, 'Low-temperature AlGaAs/GaAs multiple-quantum-well structure and its application to photorefractive devices', *Appl. Phys. Lett.,* vol. 68, pp. 812-814, **1996.**

[19] A. Yariv, 'Phase conjugate optics and real-time holography', *IEEE Journal of Quantum Electronics,* vol. QE-14, pp. 650-660, **1978.**

[20] P. C. Yeh, 'Photorefractive phase conjugators', *Proceedings of the IEEE,* vol. 80, pp. 436-450, **1992.**

[21] D. Engin, M. Segev, S. Orlov, and A. Yariv, 'Double-phase conjugation', *J. Opt. Soc. Am. B,* vol. 11, pp. 1708-1717, **1994.**

[22] M. Sedlatschek, T. Rauch, C. Denz, and T. Tschudi, 'Demonstrator concepts and performance of a photorefractive optical novelty filter', *Optical Materials,* vol. 4, pp. 376-380, **1995.**

[23] M. Sedlatschek, T. Rauch, C. Denz, and T. Tschudi, 'Generalized theory of the resolution of object tracking novelty filters', *Optics Communications,* vol. 116, pp. 25-30, **1995.**

[24] H. C. Pedersen, P. E. Andersen, and P. M. Johansen, 'Observation of spontaneously frequency-shifted beam fanning in photorefractive $Bi_{12}SiO_{20}$', *Optics Letters,* vol. 20, pp. 2475-2477, **1995.**

[25] A. A. Zozulya, M. Saffman, and D. Z. Anderson, 'Propagation of light beams in photorefractive media - fanning, self-bending and formation of self-pumped four-wave-mixing phase conjugation geometries', *Phys. Rev. Lett.,* vol. 73, pp. 818-821, **1994.**

[26] H. Tuovinen, A. A. Kamishilin, R. Ravattinen, V. V. Prokofiev, and T. Jaaskelainen, 'Two-wave mixing and fanning effect in $Bi_{12}TiO_{20}$

under an alternating electric field', *Optical Engineering*, vol. 34, pp. 2641-2647, **1995.**

[27] M. Snowbell, M. Horowitz, and B. Fischer, 'Dynamics of multiple 2-wave mixing and fanning in photorefractive materials', *J. Opt. Soc. Am. B*, vol. 11, pp. 1972-1982, **1994.**

[28] M. Cronin-Golomb and A. Yariv, 'Optical limiters using photorefractive nonlinearities', *J. Appl. Phys.*, vol. 57, pp. 4906-4910, **1985.**

[29] T. F. Boggess, A. L. Smirl, J. Dubard, A. G. Cui, and S. R. Skinner, 'Single-beam and multiple-beam optical limiters using semiconductors', *Optical Engineering*, vol. 30, pp. 629-635, **1991.**

[30] G. L. Wood, W. W. Clark, III, G. J. Salamo, A. Mott, and E. J. Sharp, 'Fluence limiting via photorefractive 2-beam coupling', *J. Appl. Phys.*, vol. 71, pp. 37-44, **1992.**

[31] K. Sutter, J. Hullinger, and P. Günter, 'Photorefractive effects observed in the organic crystal 2-(cyclooctylamino)-5-nitropyridine doped with 7,7,8,8-tetracyanoquinodimethane', *Solid State Communications*, vol. 74, pp. 867-870, **1990.**

[32] K. Sutter and P. Günter, 'Photorefractive gratings in the organic-crystal 2-cyclooctylamino-5-nitropyridine doped with 7,7,8,8-tetracyanoquinodimethane', *J. Opt. Soc. Am. B*, vol. 7, pp. 2274-2278, **1990.**

[33] S. Ducharme, J. C. Scott, R.J. Twieg, and W. E. Moerner, 'Observation of the photorefractive effect in a polymer', *Phys. Rev. Lett.*, vol. 66, pp. 1846-1849, **1991.**

[34] K. Meerholz, B. L. Volodin, Sandalphon, B. Kippelen, and N. Peyghambarian, 'A photorefractive polymer with high optical gain and diffraction efficiency near 100%', *Nature*, vol. 371, pp. 497-500, **1994.**

[35] O. Zobel, M. Eckl, P. Strohlieg, and D. Haarer, 'A polysiloxane-based photorefractive polymer with high optical gain and diffraction efficiency', *Adv. Mater.*, vol. 7, pp. 911-914, **1995.**

[36] S. M. Silence, M. C. J. M. Donckers, C. A. Walsh, D. M. Burland, R. J. Twieg, and W. E. Moerner, 'Optical properties of poly(N-vinylcarbazole)-based guest-host photorefractive polymer systems', *Applied Optics*, vol. 33, pp. 2218-2222, **1994.**

[37] Y. Zhang, C. A. Spencer, S. Ghosal, M. K. Casstevens, and R. Burzynski, 'Thiapyrylium dye sensitization of photorefractivity in a polymer composite', *App. Phys. Lett.*, vol. 64, pp. 1908-1910, **1994.**

[38] M. E. Orczyk, J. Zieba, and P. N. Prasad, 'Fast photorefractive effect in PVK-C_{60}-DEANST polymer composite', *J. Phys. Chem.*, vol. 98, pp. 8699-8704, **1994.**

[39] A. M. Cox, R. D. Blackburn, D. P. West, T. A. King, F. A. Wade, and D. A. Leigh, 'Crystallization-resistant photorefractive polymer composite with high diffraction efficiency and reproducibility', *Appl. Phys. Lett.*, vol. 68, pp. 2801-2803, **1996.**

[40] S. M. Silence, J. C. Scott, J. J. Stankus, W. E. Moerner, C. R. Moylan, G. C. Bjorklund, and R. J. Twieg, 'Photorefractive polymers based on dual-function dopants', *J. Phys. Chem.*, vol. 99, pp. 4096-4105, **1995.**

[41] R. Burzynski, Y. Zhang, S. Ghosal, and M. K. Casstevens, 'Photorefractive composites with high-band-gap second-order nonlinear optical chromophores', *J. Appl. Phys.*, vol. 78, pp. 6903-6907, **1995.**

[42] G. G. Malliaras, V. V. Krasnikov, H. J. Bolink, and G. Hadziioannou, 'Photorefractive polymer composite with net gain and subsecond response at 633 nm', *App. Phys. Lett.*, vol. 65, pp. 262-264, **1994.**

[43] C. Poga, D. M. Burland, T. Hanemann, Y. Jia, C. R. Moylan, J. J. Stankus, R. J. Twieg, and W. E. Moerner, 'Photorefarctivity in new organic polymeric materials', *SPIE Proceedings*, vol. 2526, pp. 82-93, **1995**.

[44] W. E. Moerner and S. M. Silence, 'Polymeric photorefractive materials', *Chem. Rev.*, vol. 94, pp. 127-155, **1994**.

Chapter 2

The Electro-Optic and Photorefractive Effect

2.1 Introduction to the Electro-Optic Effect

The electro-optic effect occurs when the refractive index of a material is changed by the application of a d.c. or low frequency electric field. When the refractive index change is linearly proportional to the electric field amplitude, the effect is known as the linear electro-optic effect, or Pockels effect.

The linear electro-optic effect is a second order non-linear optical process and can occur only for materials that are non-centrosymmetric [1]. Although it can be described in terms of a second-order non-linear susceptibility, historically a very different mathematical formalism has been used. This formalism, as well as the relation between the electro-optic coefficient and the second-order non-linear susceptibility is described in § 2.1.1.

The linear electro-optic effect has been studied extensively and has proved to be one of the most important technological applications of both organic and inorganic materials. In contrast to pure electronics or photonics, where the information carriers are electrons and photons respectively, in devices employing electro-optic material both electrons and photons interact with each other. Optoelectronic devices can replace many of the purely electronic functions in communication and measurement systems such as modulation and information storage [2].

2.1.1 Relation between the Electro-Optic Coefficient and the Second Order Nonlinear Optical Susceptibility

When an electric field is applied across a dielectric material, the molecules are subjected to a polarization that lowers the internal field by the factor $1+\varepsilon_r$, where ε_r is the relative permittivity of the medium [1]. In terms of susceptibility, $\chi^{(1)}$, the polarization can be expressed as

$$P = \varepsilon_0 \chi^{(1)} E \tag{2.1}$$

where P is the dipole moment per unit volume and E the applied electric field. The susceptibility is related to the permittivity by

$$\chi^{(1)} = \varepsilon_r - 1 \tag{2.2}$$

The dielectric displacement of the medium is defined as

$$D = E + \frac{P}{\varepsilon_0} = \varepsilon_r E \qquad (2.3)$$

At optical frequencies, the permittivity is related to the linear optical susceptibility by an equation analogous to (2.2). The optical response of the medium is represented by its refractive index. Therefore, for an isotropic medium,

$$n_0{}^2 = \varepsilon_r = 1 + \chi^{(1)} \qquad (2.4)$$

If the field strength is intense, but still weak compared to intermolecular binding forces, the non-linear polarization can be expressed as a power series of the electric field strength, E

$$P = \varepsilon_0 \left(\chi^{(1)} E + \chi^{(2)} E^2 + \chi^{(3)} E^3 ... \right) \qquad (2.5)$$

where the equation is in SI units. $\chi^{(1)}$ is the linear susceptibility and $\chi^{(2)}$, $\chi^{(3)}$ are the quadratic and cubic susceptibilities respectively.

If the total field consists of a DC field (or a very low frequency) and a fast time varying optical field then

$$E = E(0) + E(\omega) = E(0) + E_0 cos(\omega t - kz) \qquad (2.6)$$

where ω is the frequency, t the time, z the propagation direction and k the wavenumber. The polarization is then given by

$$P = \varepsilon_0 \left\{ \chi^{(1)} \left[E(0) + E_0 cos(\omega t - kz) \right] + \right.$$

$$\chi^{(2)} \left[E(0) + E_0 cos(\omega t - kz) \right]^2 +$$

$$\left. \chi^{(3)} \left[E(0) + E_0 cos(\omega t - kz) \right]^3 + ... \right\} \qquad (2.7)$$

Expansion and collection of the terms that describe oscillation at frequency ω gives

$$P(\omega) = \varepsilon_0 \left[\chi^{(1)} E_0 cos(\omega t - kz) + 2\chi^{(2)} E(0) E_0 cos(\omega t - kz) + \right.$$

$$\left. 3\chi^{(3)} E^2(0) E_0 cos(\omega t - kz) + \tfrac{3}{4} \chi^{(3)} E_0^3 cos(\omega t - kz) \right] \qquad (2.8)$$

$$= \varepsilon_0 \chi_{eff} E(0) E_0 cos(\omega t - kz)$$

where χ_{eff} is the effective susceptibility.

An equation similar to (2.4) can describe the non-linear refractive index, n

$$n^2 = 1 + \chi_{eff} \qquad (2.9)$$

which combined with equation (2.8) gives

$$n^2 = 1 + \left[\chi^{(1)} + 2\chi^{(2)} E(0) + 3\chi^{(3)} E^2(0) + \tfrac{3}{4} \chi^{(3)} E_0^2 \right] \qquad (2.10)$$

Combination of equations (2.4) and (2.10) gives

$$n^2 - n_0^2 = 2\chi^{(2)} E(0) + 3\chi^{(3)} E(0)^2 + \tfrac{3}{4} \chi^{(3)} E_0^2 \qquad (2.11)$$

The first term on the right hand side of equation (2.11) corresponds to the linear electro-optic effect, while the second and the third term correspond to quadratic effects.

If anisotropic media are to be examined, the polarization response is also in directions other than the applied field [1]. This requires rewriting equation (2.7) using tensor notation

$$P_i = \varepsilon_0 \left(\chi_{ij}^{(1)} E_j + \sum_j \sum_k \chi_{ijk}^{(2)} E_j E_k + \sum_j \sum_k \sum_l \chi_{ijkl}^{(3)} E_j E_k E_l + ... \right) = \qquad (2.12)$$

$$= P_i^{(1)} + P_i^{(2)} + P_i^{(3)} ...$$

The relation between the field vectors **D** and **E** is

$$D_i = \sum_j \varepsilon_{ij} E_j \qquad (2.13)$$

or, in matrix form

$$\begin{bmatrix} D_x \\ D_y \\ D_z \end{bmatrix} = \begin{bmatrix} \varepsilon_{xx} & \varepsilon_{xy} & \varepsilon_{xz} \\ \varepsilon_{yx} & \varepsilon_{yy} & \varepsilon_{yz} \\ \varepsilon_{zx} & \varepsilon_{zy} & \varepsilon_{zz} \end{bmatrix} \begin{bmatrix} E_x \\ E_y \\ E_z \end{bmatrix} \qquad (2.14)$$

A suitable rotation of the coordinate system (x,y,z) can always be chosen such that all the off-diagonal terms go to zero [3]. Under this coordinate system (X,Y,Z), equation (2.14) takes the much simpler form

$$\begin{bmatrix} D_X \\ D_Y \\ D_Z \end{bmatrix} = \begin{bmatrix} \varepsilon_{XX} & 0 & 0 \\ 0 & \varepsilon_{YY} & 0 \\ 0 & 0 & \varepsilon_{ZZ} \end{bmatrix} \begin{bmatrix} E_X \\ E_Y \\ E_Z \end{bmatrix} \qquad (2.15)$$

The energy density per unit volume is

$$U = \frac{1}{8\pi} \mathbf{D} \cdot \mathbf{E} = \frac{1}{8\pi} \sum_i \sum_j \varepsilon_{ij} E_i E_j \qquad (2.16)$$

which, combined with (2.15), can be represented as

$$U = \frac{1}{8\pi} \left[\frac{D_X^2}{\varepsilon_{XX}} + \frac{D_Y^2}{\varepsilon_{YY}} + \frac{D_Z^2}{\varepsilon_{ZZ}} \right] \qquad (2.17)$$

Equations of the form $\dfrac{x^2}{a^2} + \dfrac{y^2}{b^2} + \dfrac{z^2}{c^2} = 1$ describe surface ellipsoids.

In the case of equation (2.17), ellipsoids represent the surfaces of constant energy density.

If $\quad X = \left(\dfrac{1}{8\pi U} \right)^{1/2} D_X, \quad Y = \left(\dfrac{1}{8\pi U} \right)^{1/2} D_Y \quad$ and $\quad Z = \left(\dfrac{1}{8\pi U} \right)^{1/2} D_Z$

equation (2.17) becomes

$$\frac{X^2}{\varepsilon_{XX}} + \frac{Y^2}{\varepsilon_{YY}} + \frac{Z^2}{\varepsilon_{ZZ}} = 1 \qquad (2.18)$$

The surface described by this equation is known as the index ellipsoid. The equation describing the index ellipsoid has the above form in

the principal axis system (X,Y,Z). In any other coordinate system, it is described by the general expression for an ellipsoid,

$$\left(\frac{1}{n^2}\right)_1 x^2 + \left(\frac{1}{n^2}\right)_2 y^2 + \left(\frac{1}{n^2}\right)_3 z^2 + 2\left(\frac{1}{n^2}\right)_4 yz$$
$$+2\left(\frac{1}{n^2}\right)_5 xz + 2\left(\frac{1}{n^2}\right)_6 xy = 1 \qquad (2.19)$$

The coefficients $\left(\frac{1}{n^2}\right)_i$ are optical constants that describe the index ellipsoid in a particular coordinate system.

The index ellipsoid can be used to describe the optical properties of an anisotropic material by means of the following procedure [3]. For any given direction of propagation within the material, a plane perpendicular to the propagation vector and passing through the centre of the ellipsoid is constructed. The curve formed by the intersection of this plane with the index ellipsoid forms an ellipse (c. Figure 2.1). The semi-major and the semi-minor axes of this ellipse give values of the refractive index for this particular direction of propagation, while the orientation of the axes gives the polarization directions of the D vector associated with these refractive indices.

When the material is subjected to an electric field, the index ellipsoid is modified and this change is described by the impermeability tensor, which is defined by the relation
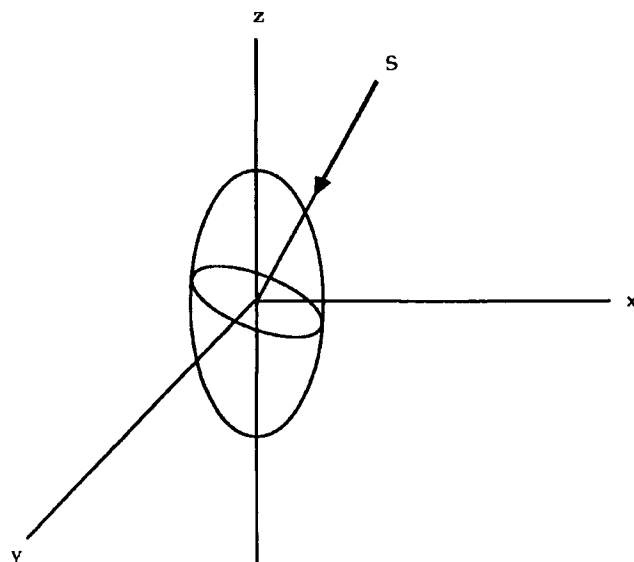
Figure 2.1 The refractive index ellipsoid where s indicates the direction of an incident light beam. The semi-major and the semi-minor axes of the ellipse formed by the intersection of the ellipsoid with a plane perpendicular to the incident light beam give the values of the refractive index for this particular direction of propagation.

$$E_i = \sum_j \eta_{ij} D_j \qquad\qquad (2.20)$$

This relation is the inverse of that given by equation (2.3), hence $\eta_{ij} = \left(\varepsilon^{-1}\right)_{ij}$. The index ellipsoid can be expressed in terms of the elements of the impermeability tensor by noting that the energy density is equal to

$$U = \frac{1}{8\pi} \mathbf{D} \cdot \mathbf{E} = \frac{1}{8\pi} \sum_{ij} \eta_{ij} D_i D_j \qquad\qquad (2.21)$$

If $\quad x = \left(\dfrac{D_x^2}{8\pi U}\right)^{-1/2}, \quad y = \left(\dfrac{D_y^2}{8\pi U}\right)^{-1/2}$ and $\quad z = \left(\dfrac{D_z^2}{8\pi U}\right)^{-1/2},$

then the expression for U as a function of $\mathbf{D}$ becomes

$$\eta_{11}x^2 + \eta_{22}y^2 + \eta_{33}z^2 + 2\eta_{12}xy + 2\eta_{23}yz + 2\eta_{13}xz = 1 \qquad (2.22)$$

By comparison of this expression with (2.19) it can be seen that

$$\left(\frac{1}{n^2}\right)_1 = \eta_{11} \qquad \left(\frac{1}{n^2}\right)_2 = \eta_{22} \qquad \left(\frac{1}{n^2}\right)_3 = \eta_{33}$$

$$\left(\frac{1}{n^2}\right)_4 = \eta_{23} = \eta_{32} \qquad \left(\frac{1}{n^2}\right)_5 = \eta_{13} = \eta_{31} \qquad \left(\frac{1}{n^2}\right)_6 = \eta_{12} = \eta_{21}$$

$$(2.23)$$

The quantity η_{ij} can be expressed as a power series in the strength of the components E_k of the applied field as

$$\eta_{ij} = \eta_{ij}^{(0)} + \sum_k r_{ijk}E_k + \sum_k \sum_l s_{ijkl}E_k E_l + \ldots \qquad (2.24)$$

The tensor r_{ijk} describes the linear electro-optic effect and the tensor s_{ijkl} the quadratic electro-optic effect. Since the dielectric permeability tensor ε_{ij} is real and symmetric in regions far from resonances, its inverse η_{ij} must also be real and symmetric and consequently the electro-optic tensor r_{ijk} must be symmetric in its two indices (Kleinman symmetry). For this reason, the third-rank tensor r_{ijk} is often represented as a two-dimensional matrix r_{ij} using contracted notation. Then the lowest-order modification of the optical constants $\left(\frac{1}{n^2}\right)_i$ for the index ellipsoid can be expressed as

$$\Delta\left(\frac{1}{n^2}\right)_i = \sum_j r_{ij} E_j \tag{2.25}$$

The left side of the equation can be expanded as

$$\Delta\left(\frac{1}{n^2}\right) = \frac{1}{n_0^2} - \frac{1}{n^2} = \frac{n^2 - n_0^2}{n_0^2 n^2} \approx \frac{n^2 - n_0^2}{n_0^4} \tag{2.26}$$

Substituting n_0 and $n^2 - n_0^2$ from equations (2.11) and (2.4) and using the appropriate tensor indices leads to the relationship between r_{ij} and $\chi_{ij}^{(2)}$:

$$-r_{ij} \approx \frac{2\chi_{ij}^{(2)}}{n_0^4} \tag{2.27}$$

The above expression of the electro-optic coefficient is valid only in regions far from resonances, where Kleinman symmetry can be applied. It is a very important relation since in practice it is often the case that $\chi_{ij}^{(2)}$ is measured and r_{ij} is calculated using equation (2.27).

2.2 Introduction to the Photorefractive Effect

The photorefractive effect is defined as the change in the refractive index of an electro-optic material that results from the optically induced redistribution of charges. It differs from the other non-linear optical effects in that it cannot be described by a non-linear susceptibility $\chi^{(n)}$ for any value

of n; special methods must be employed to describe it. The most commonly used, degenerate four-wave mixing is described in Section 2.2.3.

The photorefractive grating formation is illustrated schematically in Figure 2.2. The photorefractive material is illuminated by two beams of light of the same wavelength and polarization, which interact to produce the spatially modulated light intensity distribution shown in Figure 2.2a. This time-independent intensity pattern consisting of light and dark planes throughout the intersection region has a spatial wavelength, Λ_G, given by

$$\Lambda_G = \frac{\lambda_0}{2n\sin[\theta/2]} \qquad (2.28)$$

where θ is the angle between the two beams.

Charge generation occurs at a rate proportional to the local value of the irradiance. The mobile photogenerated charges, holes in the case of most organics, then migrate by diffusion or drift into dark zones leaving behind a stationary ionic site of opposite charge (Figure 2.2b). In the dark areas the carriers are trapped due to a mechanism that is not exactly known in polymeric materials (Figure 2.2c), but it is believed to be shallow traps which empty thermally and deeper traps from molecules or ionic impurities with several stable oxidation states. The space-charge field that is generated by this charge redistribution leads to a refractive index grating via the electro-optic effect (Figure 2.2d).
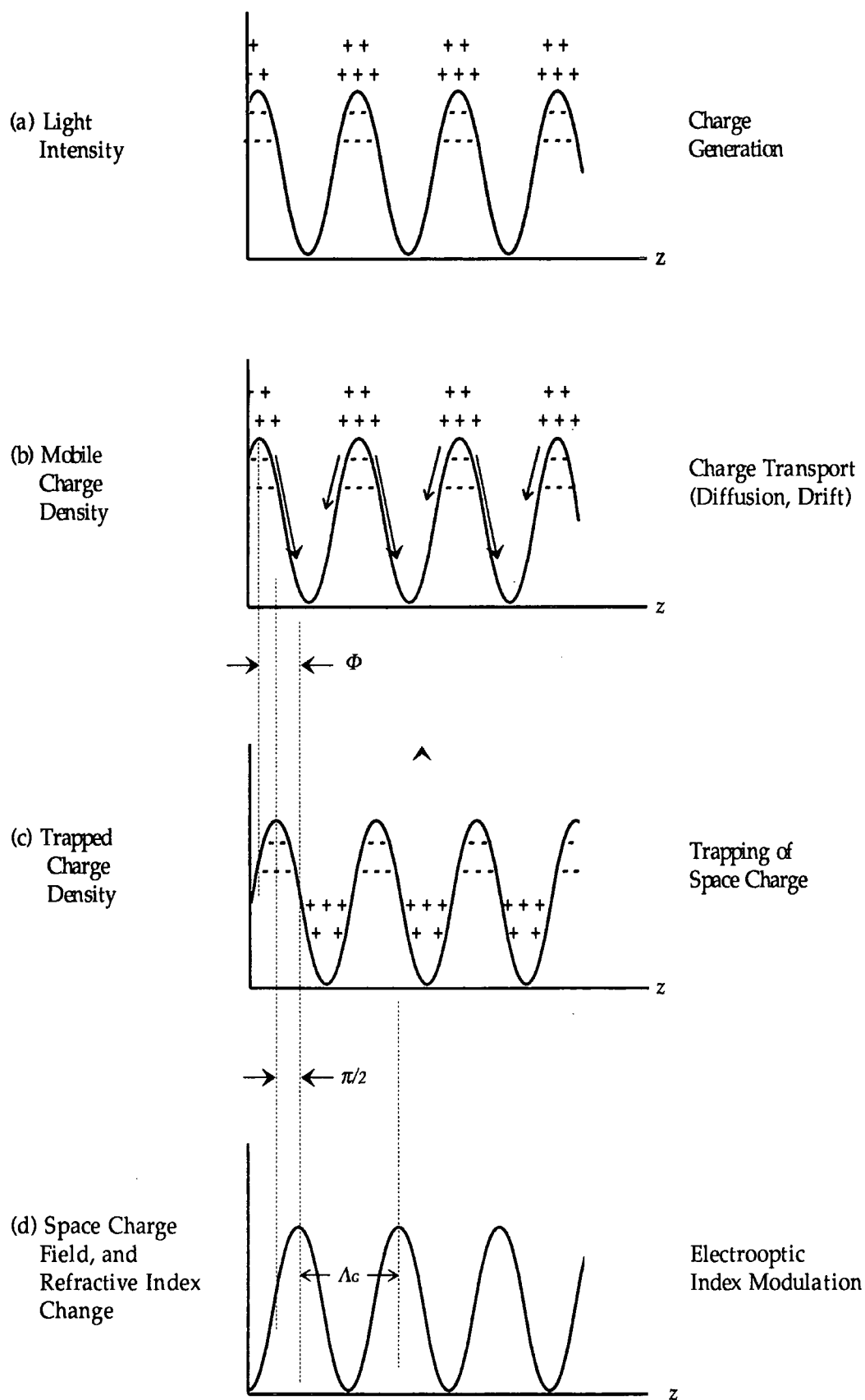
Figure 2.2 Illustration of photorefractive grating formation [4]

The phase of the space-charge field is shifted by angle Φ from the light intensity pattern. In inorganic materials, where charge diffusion is dominant (with zero external field), $\Phi = \pi/2$. When an external field is applied and drift rises, Φ can depart from $\pi/2$, but at high fields, as the ones required to produce the photorefractive effect in polymeric materials, drift is again the dominant mechanism and Φ approaches $\pi/2$. This 90^0 phase shift between the light intensity distribution and the refractive index modulation has the important consequence that it can lead to the transfer of energy between the two incident beams. This transfer of energy is called two-beam coupling and is described in Section 2.2.2. Such a non-local grating formation cannot occur by any non-photorefractive local mechanism, as charge transport over a macroscopic distance is required. Therefore, two-beam coupling experiments are used to test the photorefractivity of materials that are both electro-optic and photoconducting.

In Figure 2.3 a schematic representation of the space charge field formation in a guest-host photorefractive polymer in the context of charge generation, transport and trapping processes is given. Indicated are the highest occupied and lowest unoccupied molecular orbitals (HOMO and LUMO respectively) of the polymer, the charge generating (CG) agent and the nonlinear optical chromophore (EO), together with the HOMO's of the charge transport (CT) and trapping sites (TS). A hole is generated through illumination and is transferred to a charge transport site from where it migrates until it becomes trapped in a low ionization potential

Polymer LUMO

EO

CG

hv

CT CT TS
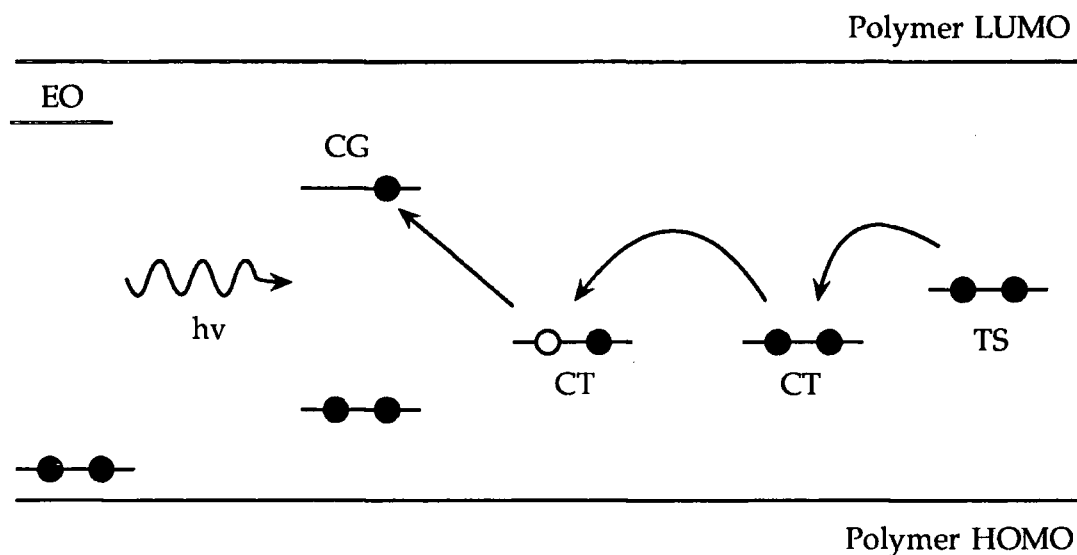
Polymer HOMO

Figure 2.3 A schematic representation of the space charge field formation process in a guest-host photorefractive polymer. Indicated are the highest occupied and lowest unoccupied molecular orbitals (HOMO and LUMO respectively) of the polymer, the charge generating (CG) agent and the nonlinear optical chromophore (EO), together with the HOMO's of the charge transport (CT) and trapping sites (TS).

site. The mathematical description of the space charge field formation is given in § 2.2.1.

2.2.1 The Transport Equations

The initial effort to describe the space-charge field due to non-uniform illumination was made by Kukhtarev et al. in 1979 [5]. The set of equations that Kukhtarev derived included a current equation, a continuity equation for a single charge carrier, Poisson's equation to relate the internal field to the charge density, and a rate equation for one species of ions. The Kukhtarev model [5] provided a solid framework and a starting point for further theoretical work, however, it contains several shortcomings

when organic materials are considered. It did not include the high field dependence of photocarrier generation quantum yield $\phi(E)$ [6,7], the effects of field dependent mobility, the possibility that the recombination and trapping rates may be mobility-dependent (Langevin recombination [8]) and the possibility that in a polymeric photorefractive material the diffusion coefficient may not be related to the carrier mobility by the usual Einstein relation [9].

A more sophisticated model of charge-carrier generation was presented by Onsager in 1938 [10]. Onsager calculated the probability that a pair of ions of given initial separation will recombine with each other under action of the mutual Coulombic attractive force. The photocarrier generation quantum yield is strongly dependent upon both the temperature and the electric field.

In 1989, Twarowski [11] used the Onsager model for initial recombination of charged pairs to describe the photogeneration process and introduced a quantum yield that is a function of both electric field and temperature into the Kukhtarev model [5]. However, he still failed to address the above mentioned shortcomings.

Despite all these deficiencies, the Kukhtarev model [5] has proven rather useful in understanding and predicting trends [12]. A basic description of the equations that describe it is given here. For the derivation of these equations the following important assumptions were made:

1) Charge transport is dominated by only one carrier species.

2) Only one trap level exists.

3) The efficiency of carrier generation does not depend on the irradiance

   I.

4) The efficiency of carrier generation does not depend on the space

   charge field.

5) No photovoltaic currents.

$$J = e\mu_q n_q E - qD\frac{\partial n}{\partial x} \tag{2.29}$$

$$q\frac{\partial}{\partial t}\left(n_q - N_D^+\right) + \frac{\partial J}{\partial x} = 0 \tag{2.30}$$

$$\frac{\partial}{\partial x}\left(\varepsilon_r\varepsilon_0 E\right) = q\left(n_q + N_A - N_D^+\right) \tag{2.31}$$

$$\frac{\partial N_D^+}{\partial t} = \left(\beta_T + s_I I\right)\left(N_D - N_D^+\right) - \gamma N_D^+ n_q \tag{2.32}$$

with

n_q: free carrier density

J: current density

E: electric field

N_A: acceptor density

N_D: donor density

N_D^+:   density of ionized donors

D: diffusion constant ($D=\mu k_B T/e$, k_B: Boltzmann's constant)

μ_q: carrier mobility

e: elementary charge

q: carrier charge(for electrons: $q=-e$)

β_T: thermal degeneration rate

s_i: photoionization constant

γ: recombination constant

ε_r: dielectric constant of the photorefractive material

ε_0:   vacuum permittivity

I: irradiance

The assumed optical intensity pattern is

$$I = I_0\left(1 + m\cos(K_G z)\right) \tag{2.33}$$

where m is the contrast of the interference pattern and $K_G = 2\pi/\Lambda_G$ is the grating vector.

In order to solve this set of equations, specific models must be assumed for the field dependence of the quantum efficiency, mobility and recombination rate constants. It is therefore clear that there cannot be a

general solution. Approaches through both linearization and numerical solution have been demonstrated by Schildkraut et al. [13,14].

2.2.2 Photorefractive Two-Beam Coupling

A typical geometry for studying two-beam coupling is shown in Figure 2.4. Two mutually coherent beams of the same polarization are spatially overlapped and interact to form a non-uniform intensity distribution within the material. Due to the electro-optic response of the material, this non-uniform intensity distribution produces a refractive index grating at the illuminated part of the material. This grating is shifted by 90° from the light intensity pattern. As a result, the light scattered from beam B into beam A interferes constructively with beam A, while the light scattered from beam A into beam B interferes destructively with beam A. The power of beam A is increased while the power of beam B is equally decreased.

From the increase in the irradiance of beam A the two-beam coupling ratio $\gamma_0 = I_{signal,with\ pump}/I_{signal,without\ pump}$ can be calculated, where I_{signal} is the measured irradiance of the beam under consideration. The normalized energy transfer coefficient (or more usually the two-beam coupling coefficient) is defined as [15]

$$\Gamma = \frac{1}{L}\left[\ln(\gamma_0\beta_0) - \ln(\beta_0 + 1 - \gamma_0)\right] \qquad (2.34)$$
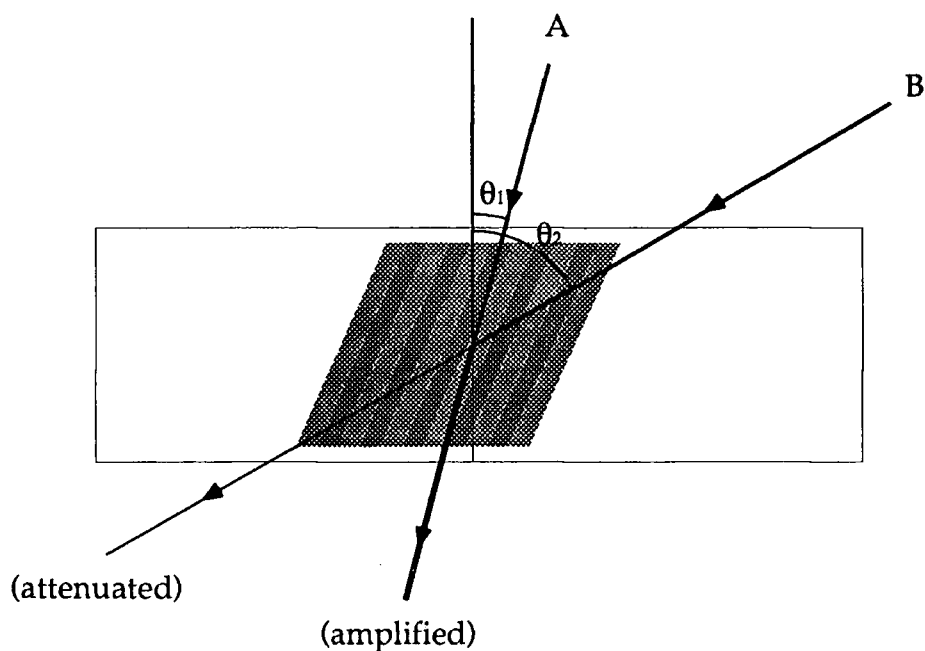
Figure 2.4 Photorefractive two-beam coupling

where β_0 is the ratio of the powers of the beams and L is the optical path length of beam A. Different path lengths and absorption and reflection losses for the two beams have been neglected.

Net gain is achieved when the two-beam coupling coefficient Γ exceeds the absorption coefficient α of the material at the operating wavelength. In applications, where two beam coupling is used as a mechanism to amplify a weak beam, net gain and beam ratios $\beta \gg 1$ are usually required.

2.2.3 Degenerate Four-Wave Mixing

Although photoconductivity and electro-optic response are necessary elements for photorefractivity in a given polymeric mixture, they are not
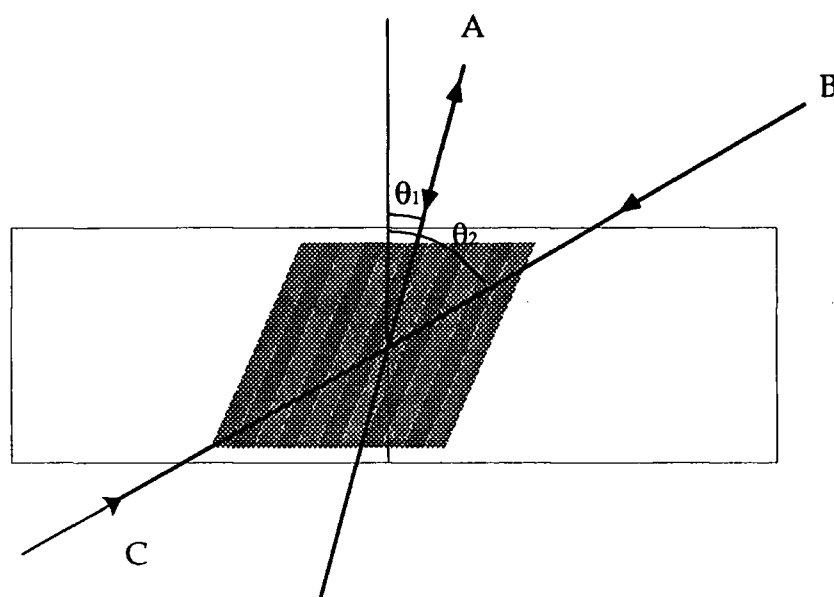
Figure 2.5 Degenerate four-wave mixing

sufficient. The presence of the photorefractive effect must be demon-strated by writing gratings in the material. A number of holographic techniques have been developed to write and read gratings, most com-monly used the degenerate four-wave mixing technique.

Degenerate four-wave mixing is a sensitive measurement method that generates a diffraction grating in the material and reads that grating with a suitably positioned probe beam (Figure 2.5). Two coherent pump beams of the same polarization are interfered in the material, forming a grating. A third, much weaker beam of the same wavelength is used to probe the grating. The read beam is diffracted by the grating with an effi-ciency η, which is defined as the ratio of the diffracted beam to the incom-ing beam. The maximum diffraction efficiency for a certain geometry is given by [16]

$$\eta = \sin^2\left(\frac{\pi n^3 r_{eff} E_{SC} d \cos(\theta_2 - \theta_1)}{2\lambda(\cos\theta_2 \cos\theta_1)^{1/2}}\right) \qquad (2.35)$$

where n is the refractive index, r_{eff} the effective electro-optic coefficient, E_{SC} the space charge field, d the film thickness and θ_1 and θ_2 the angle between the sample normal and beams 1 and 2 respectively. Equation (2.35) can be used to calculate the space charge field, once the diffraction efficiency of the material has been determined experimentally.

2.3 References

[1] P. N. Prasad and D. J. Williams, 'Introduction to nonlinear optical effects in molecules & polymers': pp. 8-34, John Wiley & Sons, 1991.

[2] P. N. Prasad and D. J. Williams, 'Introduction to nonlinear optical effects in molecules & polymers': pp.272-294, John Wiley & Sons, 1991.

[3] R. W. Boyd, 'Nonlinear Optics', pp. 399-411, Academic Press, 1992.

[4] G. C. Valley and M. B. Klein, 'Optimal properties of photorefractive materials for optical data processing', Optical Engineering, vol. 22, pp. 704-711, 1983.

[5] N. V. Kukhtarev, V. B. Markov, S. G. Odulov, M. Soskin, and V. L. Vinetskii, 'Holographic storage in electro-optic crystals. I. Steady state', Ferroelectrics, vol. 22, pp. 949-960, 1979.

[6] P. J. Melz, 'Photogeneration in trinitrofluorenone-poly(N-vinylcarbazole)', J. Chem. Phys., vol. 57, pp. 1694-1699, 1972.

[7] A. Mozumder, 'Effect of an external electric field on the yield of free ions. General results from the Onsager theory', *J. Chem. Phys.*, vol. 60, pp. 4300-4304, **1974**.

[8] P. Langevin, 'L'ionisation des gaz', *Ann. Chim. Phys.*, vol. 287, pp. 289-385, **1903**.

[9] L. Pautmeier, R. Richter, and H. B ssler, 'Anomalous time-independent diffusion of charge carriers in a random potential under a bias field', *Philos. Mag. B*, vol. 63, pp. 587-601, **1991**.

[10] L. Onsager, 'Initial recombination of ions', *Phys. Rev.*, vol. 54, pp. 554-557, **1938**.

[11] A. Twarowski, 'Geminate recombination in photorefractive crystals', *J. Appl. Phys.*, vol. 65, pp. 2833-2837, **1989**.

[12] S. Durcharme, 'Applicability of the band transport (Kukhtarev) model to photorefractive polymers', *Proceedings SPIE*, vol. 2526, pp. 144-154, **1995**.

[13] J. S. Schildkraut, 'Zero-order and first-order of the formation of space charge gratings in photoconductive polymers', *J. Appl. Phys.*, vol. 72, pp. 5055-5060, **1992**.

[14] J. S. Schildkraut, 'Theory and simulation of the formation and erasure of space-charge gratings in photoconductive polymers', *J. Appl. Phys.*, vol. **72**, pp. 1888-1893, **1992**.

[15] J. P. Huignard and A. Marrakchi, 'Coherent signal beam amplification in two-wave mixing experiments with photorefractive $B_{12}SiO_{20}$ crystals', *Optics Communications*, vol. 38, pp. 249-254, **1981**.

[16] W. E. Moerner and S. M. Silence, 'Polymeric photorefractive materials', *Chem. Rev.*, vol. 94, pp. 127-155, **1994**.

Chapter 3

Material Systems

3.1 Introduction

A potential photorefractive material should contain the necessary elements for photorefractivity, that is, photo-induced charge generation, charge transport, trapping and field-dependent refractive index [1]. A polymeric material can be made photorefractive by either incorporating these properties into a polymer, or by doping a host polymer with guest molecules that possess the required properties.

Several matters have to be taken into consideration when the different components of a photorefractive material are chosen in order to achieve optimum photorefractive response. Since charge generation is required for the photorefractive effect to take place, the material must be absorbing at the operating wavelength. However, absorption by any component other than the charge generator may increase the production of photochromic gratings and also the overall absorption of the material,

which competes with the two-beam coupling gain. It is important therefore that the photorefractive composite is absorbing at the operating wavelength, but that this absorption is due only to the charge generator.

There are four approaches to providing the required functionality in a polymeric photorefractive material. The first approach consists of a polymer as a host, while the groups responsible for optical nonlinearities, charge transport, charge generation and trapping exist as guest molecules in the polymer matrix [2,3]. In the second approach the nonlinear group is incorporated into the polymer, while the remaining functional groups exist as guest molecules in the polymer [4,5]. A third method uses a host polymer where the charge transport occurs along the polymer chain, while the remaining functional groups exist as guest molecules [6,7,8]. Finally, a fourth approach involves covalent attachment of all the required functional groups to the polymer backbone [9,10,11].

3.2 Systems Studied

In this study the third approach was adopted, where a photoconducting polymer was used as a host, while the nonlinear molecules existed as guests in the polymer matrix. The polymer used is poly(N-vinylcarbazole) (PVK), a material studied extensively for its photoconducting properties, particularly at short visible and in the ultraviolet. In the present work the polymer has been sensitized in the red and near infra-red regions of the spectrum by the addition of two different charge generating molecules, 2,4,7-trinitro-9-fluorenone (TNF), and fullerene (C_{60}). In order to increase the mechanical tolerance of the composite as well as decrease the glass

transition temperature (T_g) of the material N-Ethyl Carbazole (ECZ) was added as a plasticizer. Several compounds were investigated to provide the optical nonlinearity. These are:

- N-(4-nitrophenyl)-(L)-prolinol (NPP)

- 2-(N, N,-dimethylamino)-5-nitroacetanilide (DAN)

- 7,7 bis-diethylamino,-8, 8 dicyanoquinodimethane (DED)

- 2-(4-dicyanomethylenecyclohexa-2, 5-dienylidine)-imidazolidine (DCNQI)

- Propanedinitrile {4-[1-cyano-2(1-acetaldehyde diethyl acetal-3(ØH)-2 -piperideine) ethylidene]-2, 5-cyclohexadiene-1-ylidene} (ULTRA-DEMI)

- Propanedinitrile [4-[1-cyano-3-dicyclohexylamino)-2-propenylidene]-2, 5-cyclohexadiene-1-ylidene] (DI-DEMI)

In addition to the different photorefractive composites, two novel silicon containing electro-optic polymers were investigated for their dielectric properties [12]. This was to assist the setup of a novel adaptation of the resonant cavity method for the measurement of the dielectric constant and at elevated temperatures, in the region of 10 GHz. These two polymers, refered to as polymer (I) and polymer (II), were ideal for this purpose because they are thermally stable in air to at least 200°C.

The chemical structures of the materials are shown in Figure 3.1.

PVK

ECZ

TNF

C$_{60}$

NPP

DAN
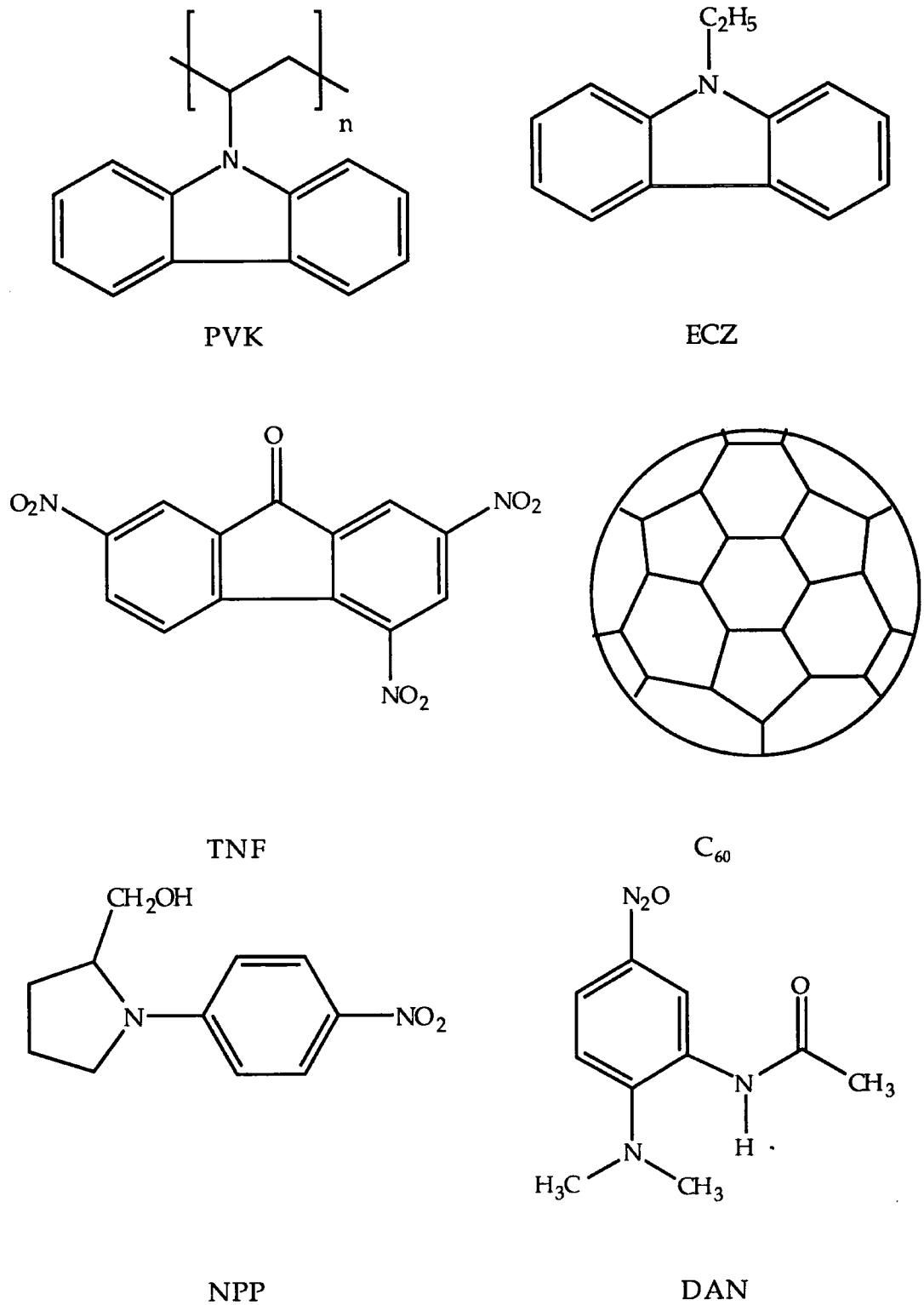
Figure 3.1 Materials Investigated (continued in next page)
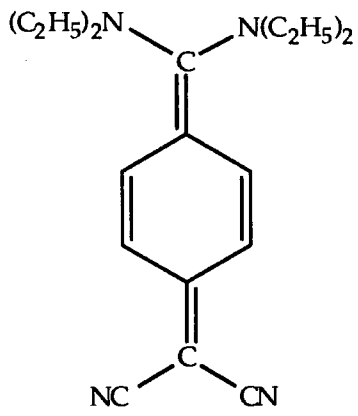
DED
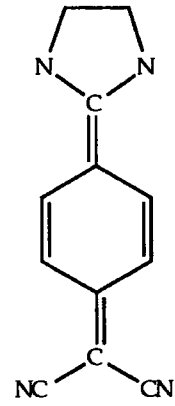
DCNQI
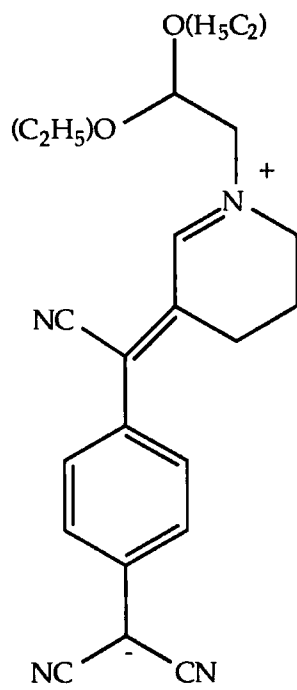
ULTRA-DEMI
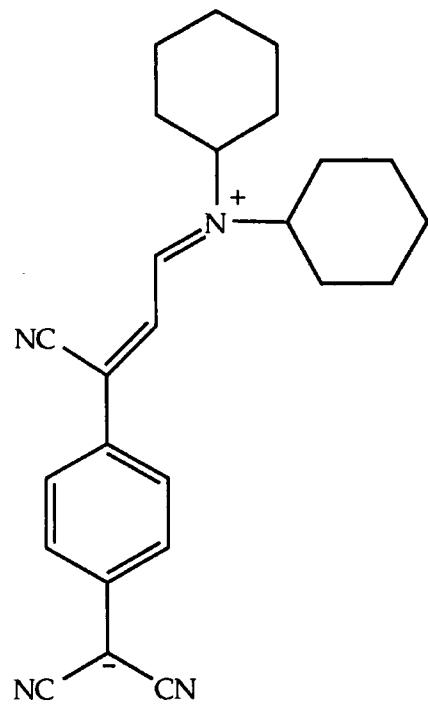
DI-DEMI
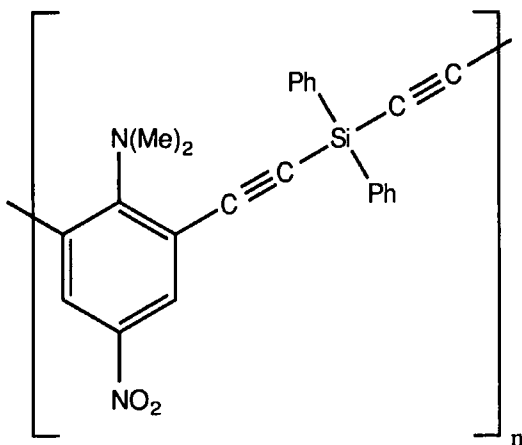
polymer (I)
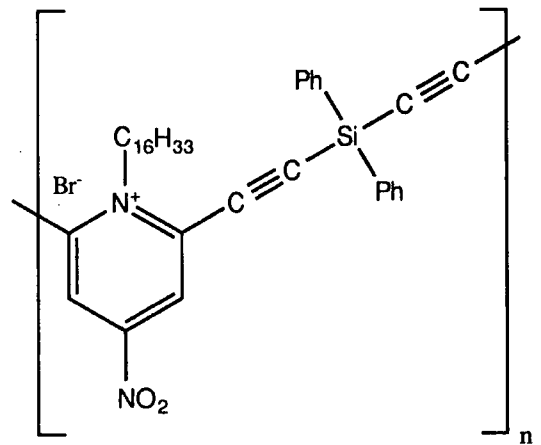
polymer (II)

3.3 The Photoconducting Composites

Photoconductivity in polymeric materials consists of two processes; photogeneration of charges and their subsequent transport and trapping in the material. Poly(N-vinylcarbazole) was one of the first polymers to be investigated for its photo-conductive properties and today it still remains one of the most reliable and easy to use [13,14,15].

The optical absorption of PVK is shown in Figure 3.2. According to Regensburgen [15], the charge generation spectrum is similar in shape to the absorption spectrum. It can be seen, therefore, that PVK is particularly
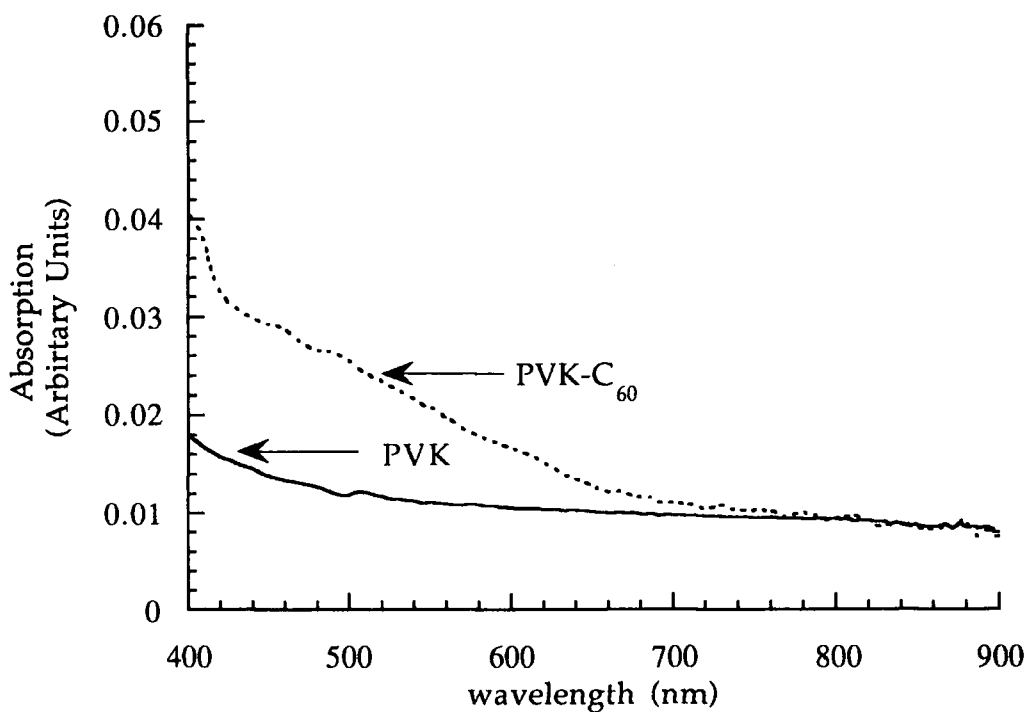
Figure 3.2 Absorption spectrum of PVK and PVK-C_{60}. It can be seen that the addition of C_{60} as a sensitizer increases the absorption, and therefore the photogeneration, at the red part of the spectrum.

photoconducting in a spectral region only up to 450 nm. In order to extend the photoconductivity region to higher wavelengths [15], C_{60} has been used as a charge sensitizer[16]. The addition of a charge sensitizer not only provides control over the material's spectral sensitivity, but also increases the charge generation quantum efficiency, which enhances the speed and magnitude of the photorefractive response. There are several examples of PVK:TNF and PVK:C_{60} mixtures used as hosts in photorefractive polymers. Compared to TNF-sensitized composites, C_{60}-sensitized composites demonstrate an enhancement of the photorefractive effect by almost an order of magnitude [16,17].

PVK as a polymer is a good host and doping levels as high as 67% have been reported [18]. When undoped, PVK has a glass transition temperature (T_g) of 200 °C and a hard and fragile texture, which does not allow the preparation of uniform thick films. In order to avoid that, ECZ has been added as a plastisizer [18]. Since the electronic structure of ECZ is similar to PVK, the plastisization does not disturb strongly the space charge field formation process.

There is another reason to want to plastisize the composite, so as to lower its T_g to room temperature to enable ambient temperature poling. Moerner and co-workers [19] have shown that low T_g materials demonstrate an improved performance due to an orientational enhancement mechanism in which both the birefringence of the sample and the electro-optic coefficient are periodically modulated by the space-charge field itself.

PVK, ECZ, TNF and C_{60} were obtained from Aldrich and used without further purification.

During the course of this work the production and use of TNF was banned as an explosive and extreme carcenogenic. For this reason, only the linear characterization of the different composites was completed and is presented in Chapter 6.

3.4 The Nonlinear Molecules

It has been known for many years that certain organic materials exhibit exceptionally large electro-optic responses. For example, the organic crystal MNA[20] has an electro-optic coefficient of 67 pm/V, at 632.8 nm, compared to 32.2 pm/V for $LiNbO_3$ [21]. The general pattern for these materials is that they consist of molecular units containing alternate σ and π bonds in chain or ring systems and additional electron donor and electron acceptor groups on opposite ends of the molecules.

The wide variety of the properties of organic materials is due to the versatility of the carbon atom to form different bonds with itself and many other elements. There are two types of bonding, and they differ considerably in the localization of electron charge density [22]. A two electron covalent σ bond is spatially confined along the inter-atomic axis of the carbon-carbon bond, while π bonds are regions of delocalized electrons above and below the inter-atomic axis. Because of this delocalization, the electrons of π bonds are much more mobile than the electrons of σ bonds.

If the perturbation to the electronic distribution caused by an intense optical field is asymmetric, then second order nonlinearity occurs. The magnitude of the unpertrubed asymmetric distribution is measured by the dipole moment μ while the ease of asymmetric redistribution in response to an externally applied field by the first hyperpolarizability β.

The ground state asymmetric electron distribution can be enhanced with the addition of appropriate functional groups at either ends of the molecule. The functional groups are divided into two categories based on their ability to donate or accept electrons. Typical donor substituents are $-N(CH_3)_2$, $-NH_2$ and $-OCH_3$ and typical acceptor substituents are $-NO$, $-NO_2$ and $-CHO$.

The optical nonlinearity of an organic molecule can also be enhanced by increasing the conjugated length of the system. According to Oudar and co-workers [23], the hyperpolarizability is proportional to the cube of the length of the molecule ($\beta \propto L^3$).

The presence of long chains and very polar groups however, introduces a negative effect referred to as a 'transparency-efficiency trade-off' [24]. The increase of conjugation by linking double bonds and increasing the polarity using stronger donor and acceptor groups usually leads to a red shift of the spectrum and loss of transparency in the visible and near infra red regions.

A lot of effort has gone into the optimization of the properties of second order nonlinear optical materials. A general framework now ex-

ists for determining the second order nonlinearity as a function of functional group properties and spacer lengths between donor and acceptor groups. However, there are still many problems to overcome, such as transparency at the desired wavelengths, solubility, photochemical and chemical stability.

The nonlinear optical molecules investigated are described in the following paragraphs.

3.4.1 NPP

NPP is a nitroaniline derivative [25,26]. Its donor group is cyclic amine and its acceptor group is ($-NO_2$). The theoretical value of its gas phase dipole moment is 6.81 Debyes, calculated using the Nemesis Software. When dissolved in 1,4 dioxane NPP demonstrated maximum absorption at 386 nm, while the experimental value of the dipole moment was found to be 6.7 ± 0.4 Debyes and the hyperpolarizability at 1064 nm was found to be $28 \pm 5 \; 10^{-30}$ esu [30].

NPP is soluble in a variety of solvents such as dichloromethane (DCM), cyclohexanone, chloroform and N, N - tetramethylurea (TMU).

NPP, 99.9 %, was obtained from Merck Ltd. and used without further purification.

3.4.2 DAN

DAN is another nitroaniline derivative and has been extensively studied for both its molecular and bulk properties [27,28,29]. Its donor group

is ($-NMe_2$) and its acceptor group is ($-NO_2$). The theoretical value of its

gas phase dipole moment is 10.16 Debyes. When dissolved in 1,4 dioxane

it demonstrated maximum absorption at 355 nm while the experimental

value of the dipole moment was found to be 9.2±0.6 Debyes and the first

hyperpolarizability at 1064 nm was found to be 34±3 10^{-30} esu [30].

DAN is soluble in several solvents such as DCM, chlorobenzene,

TMU and cyclohexanone.

DAN, 96%, was obtained from BDH Chemicals Ltd. To remove any

contamination, DAN was re-crystallized in ethanol.

3.4.3 DED

DED is a derivative of the electron acceptor 7, 7, 8, 8 - tetracyanoquinodi-

methane (TCNQ). DED demonstrates negative solvatochromism (Table

3.1) which is a proof of zwitterionic behaviour. As a result, in certain

Solvent	ε_r [31]	DED λ_{max} (nm)	ULTRA-DEMI λ_{max} (nm)	DI-DEMI λ_{max} (nm)
1,4 dioxane	2.21	484	719	720
chloroform	4.08	481	727	726
DCM	8.39	459	718	725
DMF	36.71	433	679	712

Table 3.1 The maximum absorption wavelength λ_{max} of DED, ULTRA-DEMIand
DI-DEMI in different solvents. It can be seen that, unlike conventional
materials, as the polarity of the solvent increases, the λ_{max} shifts to
lower wavelengths, which is a proof of the zwitterionic nature of these
materials [32,33].

media the cyano (-CN) groups can act as electron donors, while the

(-N(C$_2$H$_5$)$_2$) groups act a electron acceptors. The theoretical gas phase

value of the dipole moment is 13.16 Debyes.

DED can be dissolved adequately only in very polar solvents such

as N, N-dimethylformamide (DMF) and TMU.

DED was synthesized and recrystallized in the laboratory. For the

preparation [34], to a hot solution of TCNQ (1g) in tetrahydofluran (THF)

(200 ml) was added triethylamine(3-4 ml, excess), dropwise through a sy-

ringe. The mixture was refluxed briefly and then left to cool. The purple

coloured solution changed to green/brown. The volume of the solution

was reduced by rotary evaporation to approximately 30 ml and this re-

mainder was transferred to a freezer for two days. The yellow solid prod-
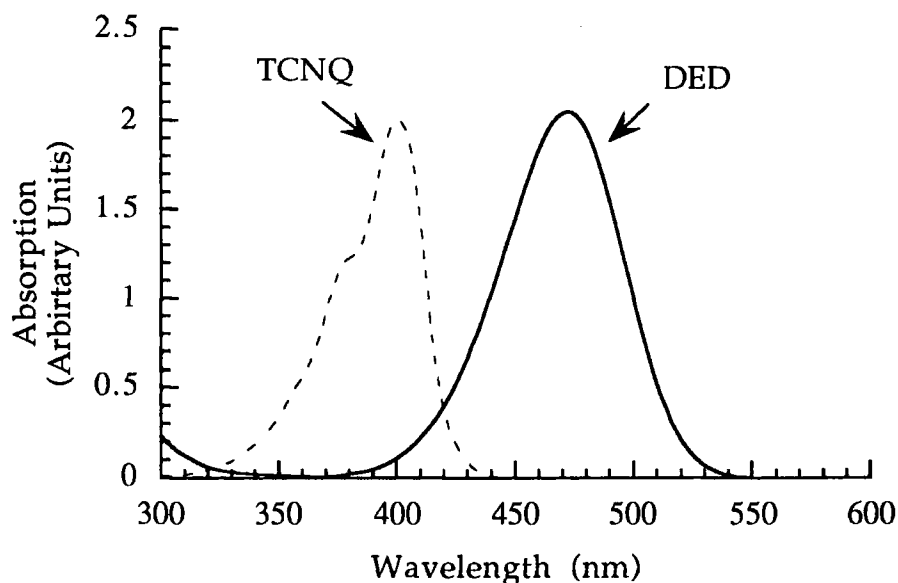
Figure 3.3 The spectra of TCNQ and its product, DED, when dissolved in chloro-
form. The dissapearence of an absorption peak in the UV part of the
spectrum is an indication of the purity of the DED product.

uct was filtered by suction and washed with toluene and then ether and dried. Recrystallization of the product was achieved from methanol. The structure of the product was confirmed with UV/VIS spectroscopy (λ_{max}=471 nm in chloroform, c. Figure 3.3), IR. spectroscopy, proton NMR and X-ray crystallography [35]. For 1 g of TCNQ, approximately 125 mg of DED were obtained (less than 10% yield).

3.4.4 DCNQI

DCNQI is another TCNQ derivative, similar to DED. In the molecule the-cyano (-CN) groups act as electron donors, while the (-NH-) groups act a electron acceptors. Its second order nonlinear nature has been proven with electric field induced second harmonic (EFISH) experiments [36]. Its main characteristic, however, is that it is extremely insoluble. Only very small quantities (1.5 mg in 10 ml maximum) can be dissolved in extremely polar solvents such as TMU and DMF.

DCNQI was produced and recrystalized in the laboratory[37].

3.4.5 ULTRA-DEMI

ULTRA-DEMI is another zwitterionic TCNQ product (Table 3.1) and belongs to a new class of materials that exhibit absorption at the red and infra-red and a 'window' of transparency at the blue region of the spectrum (Figure 3.4) [38,39,40,41]. The cyano (-CN) groups act as electron donors, while the ($-N(C_2H_5)_2$) groups act a electron acceptors. Due to its zwitterionic nature and its long chain of alternating σ and π bonds, a high dipole moment and hyperpolarizability are expected.
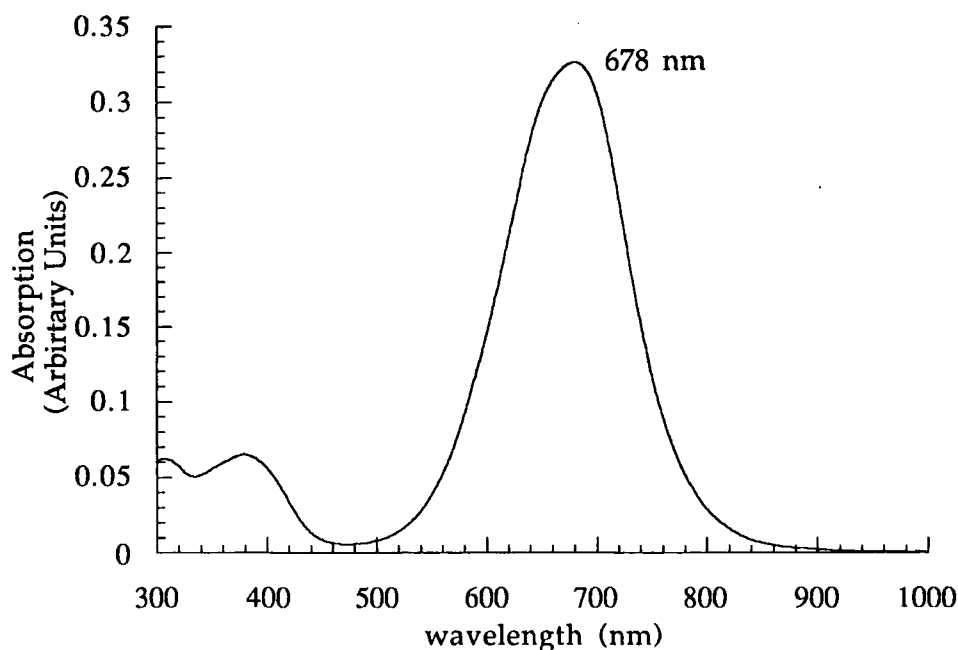
Figure 3.4 The absorption spectrum of ULTRA-DEMI, when dissolved in ace-
tonitrile. In can be seen that, unlike all the other investigated materi-
als, ULTRA-DEMI is absorbing at the red part of the spectrum, but
has a 'window' of low absorption in the blue, which allows optical
measurements at those wavelengths.

ULTRA-DEMI is soluble in a variety of solvents such as DCM, ace-

tonitrile, TMU and DMF. It was synthesized and recrystallized in the labo-

ratory [37].

3.4.6 DI-DEMI

DI-DEMI is another zwitterionic 'blue window' material (Table 3.1). The

cyano (-CN) groups act as electron donors, while the -NH groups act a

electron acceptors. Unlike ULTRA-DEMI, DI-DEMI is fairly insoluble in

most solvents and small quantities of it (a few mg in 10ml) can be dis-

solved in very polar solvents such as DMF and TMU.

DI-DEMI was prepared and recrystallized in the laboratory [37].

3.5 The electro-optic polymers

The first polymer (I) has previously been shown by us to exhibit stable second-order non-linear properties [42,43]. The dimethylaminonitrobenzene chromophore is situated in a rigid segment of polymer chain forming a rigid 'V' section between adjacent silicon atoms. Such a situation would enforce collective re-orientation of the chain to allow the chromophore to re-orient in the applied poling field. The low electro-optic coefficients obtained in previous study suggested that only chain ends could contribute significantly to the polar order.

The second material (II) is an ionic organosilane polymer. The long aliphatic chain on the chromophore acts primarily to aid the solubility of the material. Materials such as these are unusual in that they contain free counter-ions which might be expected to disrupt the poling process but similar polymers containing N-alkylopyridinium salts have been reported to exhibit second-order nonlinear optical properties [44].

Both polymers are soluble only in small quantities in THF and 1,2,3-trichloropropane (TCP).

3.5 References

[1]   W. E. Moerner, and S. M. Silence, 'Polymeric photorefractive materials', *Chem. Rev.*, vol. 94, pp. 127-155, **1994**.

[2]   K. Yokohama, K. Arishima, T. Shimada, and K. Sukegawa, 'Photorefractive effect in a polymer doped with low-molecular-weight compounds', *Jpn. J. Appl. Phys.*, 33, pp. 1029-1033, **1994**.

[3]   S. M. Silence, J. C. Scott, J. J. Stancus, W. E. Moerner, C. R. Moylan, G. C. Bjorklund, and R. J. Twieg, 'Photorefractive polymers based on dual-function dopants', *J. Phys. Chem.*, 99, pp. 4096-4105, **1995**.

[4]   S. Ducharme, J. C. Scott, R. J. Twieg, and W. E. Moerner, 'Observation of the photorefractive effect in a polymer', *Phys. Rev. Lett.*, 66, pp. 1846-1849, **1991**.

[5]   S. M. Silence, C. A. Walsh, J. C. Scott, T. J. Matray, R. J. Twieg, F. Hache, G. C. Bjorklund, and W. E. Moerner, 'Subsecond grating growth in a photorefractive polymer', *Optics Letters*, 17, pp. 1107-1109, **1992**.

[6]   S. M. Silence, M. C. J. M. Donckers, C. A. Walsh, D. M. Burland, R. J. Twieg, and W. E. Moerner, 'Optical properties of poly(N-vinylcarbazole)-based guest-host photorefractive polymer systems', *Applied Optics*, Vol. 33, pp. 2218-2222, **1994**.

[7]   O. Zobel, M. Eckl, P. Strohlieg, and D. Haarer, 'A polysiloxane-based photorefractive polymer with high optical gain and diffraction efficiency', *Adv. Mater.*, vol. 7, pp. 911-914, **1995**.

[8]   A. M. Cox, R. D. Blackburn, D. P. West, T. A. King, F. A. Wade, and D. A. Leigh, 'Crystallization-resistant photorefractive polymer composite with high diffraction efficiency and reproducibility', *Appl. Phys. Lett.*, vol. 68, pp. 2801-2803, **1996**.

[9] L. Yu, W. Chan, and Z. Bao. 'Photorefractive polymers. 2. structure design and property characterization', *Macromolecules*, vol. 26, pp. 2216-2221, **1993**.

[10] Z. H. Peng, Z. N. Bao, and L. P. Yu, 'Large photorefractivity in an exceptional thermostable multifunctional polyimide', *J . Am. Chem. Soc.*, vol. 116, pp. 6003-6004, **1994**.

[11] L. P. Yu, Y. M. Chen, and W. K. Chan, 'Detailed studies on a new conjugated photorefractive polymer', *J. Phys. Chem.*, vol. 99, pp. 2797-2802, **1995**.

[12] W. E. Douglas, University of Montpellier, France. Private Communication.

[13] M. Stolka, and D. M. Pai, 'Polymers with photo-conductive properties', *Advances in Polymer Science*, vol. 29, pp. 1-45, **1978**.

[14] J. Pearson, 'Photoconductive polymers', *J. Pure & Appl. Chem.*, vol. 49, pp. 463-477, **1977**.

[15] P. J. Regenburger, 'Optical sensitization of charge carrier transport in poly(N-vinylcarbazole)', *Photochem. & Photobiol.*, vol. 8, pp. 429-440, **1968**.

[16] S. M. Silence, C. A. Walsh, J. C. Scott, and W. E. Moerner, 'C_{60} sensitization of a photorefractive polymer', *App. Phys. Lett.*, vol. 61, pp. 2967-2969, **1992**.

[17] S. M. Silence, M. C. J. M. Donckers, C. A. Walsh, D. M. Burland, R. J. Twieg, and W. E. Moerner ' Optical properties of poly(N-vinylcarbazole)-based guest-host photorefractive polymer systems', *Applied Optics*, vol. 33, pp. 2218-2222, **1994**.

[18] K. Meerholz, B. L. Volodin, Sandalphon, B. Kippelen, and N. Peyghambarian, 'A photorefractive polymer with high optical gain and diffraction efficiency near 100-percent', *Nature*, vol. 371, pp. 497-500, **1994**.

[19] W. E. Moerner, S. M. Silence, F. Hache, and G. C. Bjorklund, 'Orientationally enhanced photorefractive effect in polymers', *J. Opt. Soc. Am. B*, vol. 11, pp. 320-330, **1994**.

[20] G. F. Lipscomb, A. F. Garito and R. S. Narang, 'An exceptionally large linear electro--optic effect in the organic solid MNA', *J. Chem. Phys.*, vol. 75, pp. 1509-1516, **1981**.

[21] Landolt-Börnstein, *Elastische, piezoelektrische, piezooptische Konstanten und nichtlineare dielektrische Suszeptibilitaten von Kristallen, Band III/11*, Springer-Verlang, **1979**.

[22] P. N. Prasad and D. J. Williams, *Introduction to nonlinear optical effects in molecules & polymers*, pp. 36-38, John Wiley & Sons, **1991**.

[23] J. L. Oudar and D. S. Chemla, 'Theory of second-order optical susceptibilities of benzene substituents', *Optics Communications*, vol. 13, pp. 164-168, **1975**.

[24] C. Bosshard, K. Sutter, P. Prêtre, J. Hulliger, M. Flörsheimer, P. Kaatz, and P. Günter, *Organic Nonlinear Optical Materials*: pp.3-5, Gordon and Breach, **1995**.

[25] J. Zyss, J. F. Nicould, and M. Coquillay, 'Chirality and hydrogen bonding in molecular crystals for phased-matched second-harmonic generation: N-(4-nitrophenyl)-(L)-prolinol (NPP)', *J. Chem. Phys.*, vol. 81, pp. 4160-4167, **1984**.

[26] I. Ledoux, C. Lepers, A. Perigaud, J. Badan, and J. Zyss, ' Linear and nonlinear optical properties of N-(4-nitrophenyl)-(L)-prolinol single crystals', *Optics Communications*, vol. 80, pp. 149, **1990**.

[27] P. A. Norman, D. Bloor, J. S. Obhi, S. A. Karavlov, M. B. Hursthouse, P. V. Kolinsky, R. J. Jones, S. R. Hall, 'Efficient second-harmonic generation in single crystals of 2-(N,N,-dimethylamino)-5-nitroacetanilide', *J. Opt. Soc. Am. B*, pp. 1013-1016, **1987**.

[28] P. V. Kolinsky, R. J. Chad, R. J. Jones, S. R. Hall, P. A. Norman, D. Bloor, and J. S. Obhi, 'Second-harmonic generation in single crystals of 2 - (N, N, - dimethylamino) - 5 - nitroacetanilide (DAN) at 1. 3', *Electronics Letters*, vol. 23, pp. 791-792, **1987**.

[29] J. C. Baumert, R. J. Twieg, G. C. Bjorklund, J. A. Logan, and C. W. Dirk, 'Crystal growth and characterization of 4 - (N, N - dimethylamino) - 3 - acetamidonitrobenzene, a new organic material for nonlinear optics', *App. Phys. Lett.*, vol. 51, pp. 1484, **1987.**

[30] D. Gray, Molecular Organic Photonics, *Ph. D. Thesis*, University of Durham, **1995**.

[31] J. A. Riddick, W. B. Bunger, and T. K. Sakano, *Organic Solvents; Physical Properties and Methods of Purification*, John Wiley & Sons, **1986**.

[32] E. Bungel and S. Rajagopal, 'Solvatochromism and solvent polarity scales', *Acc. Chem. Res.*, vol. 23, pp. 226-231, **1990**.

[33] C. Reichard, 'Solvatochromic dyes as solvent polarity indicators', *Chem. Rev.*, vol. 94, pp. 2319-2358, **1994**.

[34] W. R. Hertler, H. D. Hartzler, D. S. Acker, and R. E. Benson, 'Substituted quinodimethans. III. Displacement reactions of 7,7,8,8-tetracyanoquinodimethan', *J. Am. Chem. Soc.*, vol. 84, pp. 3387-3393, **1962**.

[35] J. Cole, G.H. Cross, M. Farsari, J.A.K. Howard and M. Szablewski, 'Structural studies of a series of organic non-linear optical materials'. Accepted for publication, *Acta Crystalographica B*.

[36] S. J. Lalama, K. D. Singer and N. Garito, 'Exceptional second-order nonlinear optical susceptibilities of quinoid systems', *App. Phys. Lett.* vol. 39, pp. 940-942, **1981**.

[37] M. Szablewski, University of Durham, UK. Personnal Communication.

[38] M. Szablewski, 'Novel reactions of TCNQ: Formation of zwitterions for nonlinear optics by reaction with enamines', *J. Org. Chem.*, vol. 59, pp. 954-956, **1994**.

[39] M. Szablewski, and G. H. Cross, 'High dipole blue window chromophore for frequency doubling', *Abstracts of Papers of the American Chemical Society*, vol. 208, pp. 254-POLY, **1994**.

[40] J. C. Cole, J. A. K. Howard, G. H. Cross, and M. Szablewski, '(Z)-(4-[1-cyano-3-(diethyliminio)-1-propenylphenyl) dicyanomethanide, a novel blue window zwitterionic molecule for nonlinear optics', *Acta Crystallographica C*, vol. 51, pp. 715-718, **1995**.

[41] G. H. Cross, D. Bloor, T. L. Axon, M. Farsari, D. Gray, D. Healy, M. Swann, and M. Szablewski, 'High dipole, high β-molecules with blue window transparency', *SPIE Proceedings*, vol. 2285, pp. 11-16, **1994**.

Chapter 4

Experimental Methods

4.1 Introduction

In determining the suitability of a polymeric material for photorefractive applications, a set of fundamental properties need to be known. These are:

- The dielectric constant ε_r

- The optical absorption spectrum

- The refractive indices at the operating wavelengths

- The second order nonlinearity $\chi^{(2)}$

- The two beam coupling gain coefficient Γ

- The diffraction efficiency η

The dielectric constant is an indication of the internal space charge distribution [1]. The dielectric constant at 1 KHz and 1 MHz was measured

using an capacitance bridge. For the high frequency dielectric measurements at 10 GHz, a resonant cavity measurement technique was suitably adapted.

Knowledge of the linear absorption spectrum is essential in order to determine a suitable wavelength for the photorefractive measurements and applications. It is also needed for the determination of the second order nonlinear optical coefficient and the two beam coupling net gain coefficient. It can be measured with a spectro-photometer and knowing the thickness of the polymeric film, the absorption coefficient α can be calculated for any wavelength of interest. A Perkin Elmer Lambda 9 spectro-photometer was used for the measurements.

Knowing the refractive index at the various operating wavelengths is essential in order to determine the second order nonlinear optical coefficient $\chi^{(2)}$ and the electro-optic coefficient r. For the measurement, an interference fringe method [8] was employed.

The second order nonlinear optical coefficient $\chi^{(2)}$ is needed in order to be able to calculate the electro-optic coefficient. To demonstrate second order nonlinearity, the centrosymmetry of the polymer films was removed with *in situ* room temperature corona poling and second harmonic light was produced using a Nd:Yag laser. $\chi^{(2)}$ was measured using the Maker fringes technique [18,19].

As discussed, the two beam coupling gain coefficient Γ, with units cm^{-1}, is a fundamental photorefractive term. In applications, it is often re-

quired that the two beam coupling gain exceeds the absorption at the operating wavelength. In addition, two beam coupling experiments provide the only conclusive measurement for whether or not an electro-optic and photoconductive material is photorefractive.

Finally, in order to establish the suitability of a material for photorefractive applications, the diffraction efficiency η is needed to be known. For this purpose a degenerate four wave mixing experiment at 632.8 nm was setup.

4.2 Dielectric Measurements

In order to measure the materials' response at high frequencies, the dielectric measurements were performed at 1 KHz, 1 MHz and 10 GHz. The experimental techniques are described at § 4.2.1 and § 4.2.2.

4.2.1 Low Frequency Dielectric Measurements

In order to calculate the dielectric constant of the materials at 1 KHz and 1 MHz, the capacitance of a two-dielectric parallel capacitor was measured. The experimental setup is shown in Figure 4.1. A Hewlett-Packard LCR meter was employed for the capacitance measurements. From the expression of the total capacitance of a two dielectric parallel plate capacitor the dielectric constant can be found. This kind of equipment, however, is designed for the measurement of materials that do not need a substrate to support them, which is not the case with polymeric films. For this reason in this case the bottom plate of the capacitor is the conducting Indium Tin Oxide (ITO) glass substrate of the polymer film, while the top plate is the

top electrode of the LCR meter. The total capacitance C_t can be expressed as the sum of capacitors in series through the equation

$$\frac{1}{C_t} = \frac{1}{C_g} + \frac{1}{C_s}$$
(4.1)

where C_g is the capacitance of the air gap and C_s is the capacitance of the dielectric sample. Using the formula for a parallel plate capacitor [2] the following formula can be obtained.

$$\frac{1}{C_t} = \frac{1}{\dfrac{\varepsilon_0 A}{(d_g - d_s)}} + \frac{1}{\dfrac{\varepsilon_r \varepsilon_0 A}{d_s}}$$
(4.2)

or, rearranging
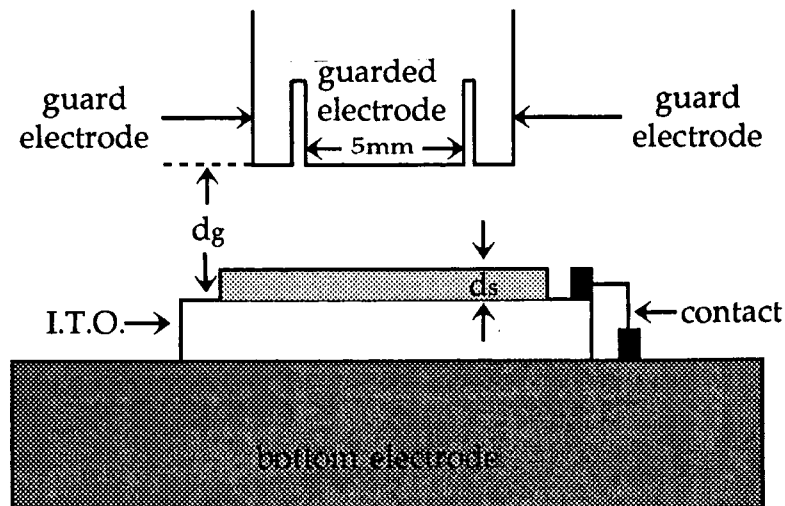
Figure 4.1 Experimental set-up for low frequency dielectric measurements

$$\frac{1}{C_t} = \frac{1}{\varepsilon_0 A} d_g + \frac{d_s(1-\varepsilon_r)}{\varepsilon_r \varepsilon_0 A} \tag{4.3}$$

where the various distances are defined in Figure 4.1, ε_r is the dielectric constant of the polymeric composite, and the dielectric constant of air is assumed to equal 1. A plot of $\frac{1}{C_t}$ vs. d_g shows that the intercept κ is

$$\kappa = \frac{d_s}{\varepsilon_r \varepsilon_0 A} - \frac{d_s}{\varepsilon_0 A} \tag{4.4}$$

Rearranging equation (4.4) gives the following expression for the dielectric constant of the polymer

$$\varepsilon_r = \frac{d_s}{\varepsilon_0 A \kappa + d_s} \tag{4.5}$$

From equation (4.3), the gradient of the line is

$$gradient = s = \frac{1}{\varepsilon_0 A} \tag{4.6}$$

Substituting s into equation (4.5) gives the following expression for the dielectric constant

$$\varepsilon_r = \frac{d_s}{\dfrac{\kappa}{s} + d_s} \qquad\qquad (4.7)$$

In order to accurately calibrate the gap between the two electrodes of the capacitance bridge, the capacitance of the air gap is measured. Assuming that the effective distance $d_{effective}$ between the two electrodes is

$$d_{effective} = d_{measured} + d_{correction} \qquad\qquad (4.8)$$

where $d_{measured}$ is the distance measured using the bridge micrometer and $d_{correction}$ the distance correction factor. The effective distance between the two electrodes can be calculated as a function of the total capacitance C_{total} according to the equation

$$d_{effective} = d_{measured} + d_{correction} = \frac{\varepsilon_0 A}{C_{total}} \qquad\qquad (4.9)$$

4.2.2 High Frequency Dielectric Measurements

The measurement of the dielectric constant and loss at GHz frequencies of polymeric materials is a complicated subject. Most methods either require a free-standing sample [3], or complicated sample preparation and specialized equipment [4]. For the dielectric measurement at 10 GHz of polymeric materials which require a substrate support, a novel adaptation of the resonant cavity method has been employed.

When a sample of dielectric material is introduced into a resonant cavity, the cavity resonance is altered by a small amount and its cavity quality factor, Q_c, is lowered. If the changes are small, as would be expected for polymeric materials, the relation between changes in resonant frequencies and cavity Q_c - factor, and the material dielectric properties can be obtained using perturbation theory [5].

The real and the imaginary parts of the relative permittivity, ε_r' and ε_r'', respectively, are related to the changes in cavity resonance frequency, $\Delta\omega$ and change in the quality factor through the following equations

$$\varepsilon_r' = 1 + 2\frac{\Delta\omega}{\omega}\frac{V_o}{V_s}F(x,y,z) \tag{4.10}$$

$$\varepsilon_r'' = \left(\frac{1}{Q_{c1}} - \frac{1}{Q_{c0}}\right)\frac{V_0}{V_s}F(x,y,z) \tag{4.11}$$

where V_0 is the total volume of the cavity, V_s the volume of the specimen, and Q_{c0} and Q_{c1} are the cavity quality factors before and after the insertion of the material. The factor $F(x, y, z)$ is defined as

$$F(x,y,z) = \frac{V_s}{V_0}\frac{\int_{V_0}|\overline{E}_0|^2\,dv}{\int_{V_s}E_0E_1\,dv} \tag{4.12}$$

By moving the micrometer, the size and therefore the resonant frequency of the cavity changes

Sample entrance

Frequency Synthesizer

Scalar Analyzer

(a)

Waveguide

Thermocouple

Polymer Film

Heater

Heat insulator

Teflon disc

Copper

(b)
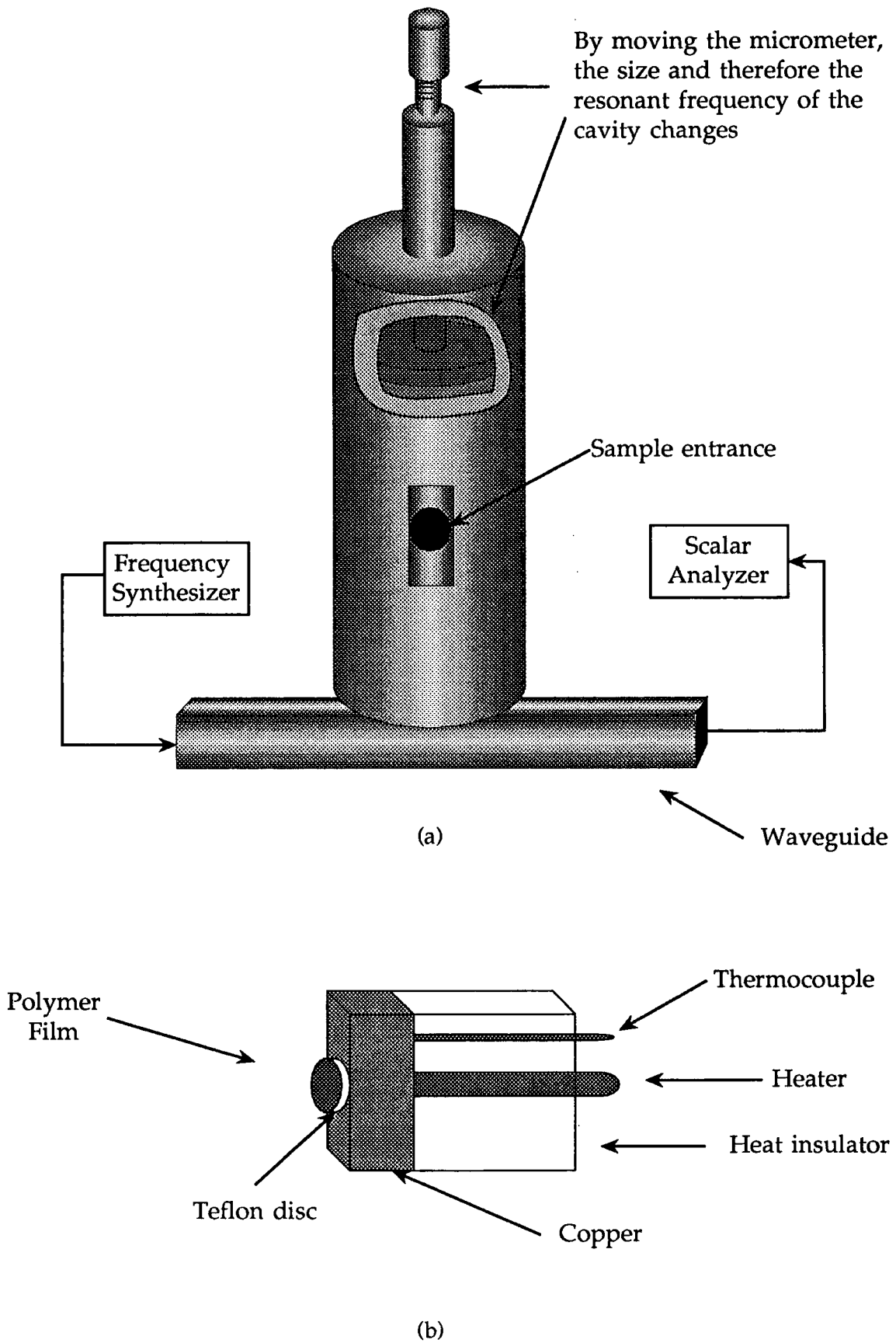
Figure 4.2 (a) The microwave cavity and (b) the sample holder (not to scale)

where E_0 and E_1 are the electric fields in the rest of the cavity and in the sample, respectively.

For the experiment, a Wiltron model 6747A-20 sweep frequency synthesizer was used to excite the modes of an H_{011} cylindrical cavity. The responses were measured using a Wiltron model 561 network scalar analyzer. A sample holder was designed to present the thin film sample at the cylindrical inner wall of the cavity (Figure 4.2).

The sample holder was modified so that high frequency dielectric measurements could be performed at elevated temperatures. A resistive heater and a thermocouple were introduced, as shown in Figure 4.2. The method was confirmed with the investigation of the dielectric properties of the two high T_g organosilane polymers described in Chapter 3.

It should be pointed out that the sample holder was designed to fit exactly the specific cavity used in this experiment; for any different cavity, designed to operate at any frequency, a new holder would have to be designed.

4.3 Linear Optical Measurements

The linear optical measurements consisted of the different optical absorption measurements of the polymeric composites and the measurement of the refractive index at the required wavelengths. The method for measuring the refractive index is described below.

4.3.1 Refractive Index Measurements

The refractive index is most important for the evaluation of the nonlinear optical properties of a material. Depending on the circumstances several methods can be used [6,7]. In the case of photorefractive materials, however, there are a lot of limitations because of the high absorption at the required wavelengths. In this work, an interference fringe method was used [8]. A thin polymeric film on a glass substrate is placed at normal incidence to the beam of a spectrometer. The beam incident on the film gives rise to two reflected beams; one from the film/substrate interface and the other from the film/air interface. If d is the thickness of the film, n the refractive index and λ the wavelength, the transmitted intensity measured in the spectrometer will have a modulation of the form $\cos(2dn/\lambda)$. The refractive index of the film can be derived from the separation of the interference minima or maxima, according to the equation

$$n = \frac{1}{2d\left(\dfrac{1}{\lambda_2} - \dfrac{1}{\lambda_1}\right)} \qquad (4.13)$$

4.4 Nonlinear Optical Measurements

The nonlinear optical measurements performed on the candidate photorefractive materials consisted of second harmonic generation, to prove the nonlinearity of the materials, two-beam coupling, to prove their photorefractivity and four-wave mixing, to measure their diffraction effi-

ciency. Before any measurements were performed, the bulk centrosymmetry of the materials had to be removed with corona poling. The methods for the corona poling and the different nonlinear optical measurements are described in the following sections.

4.4.1 Corona Poling

There are two ways of poling; contact poling and corona poling. For this experiment, where, because of the low glass transition temperature of the polymeric composites the orientation of the dipolar groups lasts only while the electric field is on, and where generally very high fields have to be applied, the method of *in situ* corona poling at room temperature was chosen [9,10]. This technique offers the advantage of easier sample preparation, as sandwiching the polymer between two electrodes is not necessary [11,12]. Furthermore, a high electric field can be applied across the material without causing catastrophic electrical breakdown. More importantly, corona poling deposits stable charged species, unlike in forced contacts, where charge injection of either free electrons or holes can occur. This can lead to electrolysis, a common problem in materials such as DED, DCNQI, ULTRA-DEMI and DI-DEMI [13]. One drawback, however, is that the precise value of the electric field is not known, as it depends on the surface charge capacitance of the material and specific environmental conditions, such as temperature and humidity. The experimental setup is shown in Figure 4.3.

4.4.2 Second-Harmonic Generation: the Maker-Fringe Technique

To characterize fully a photorefractive material, its electro-optic coefficient needs to be known. The most commonly used methods for the measurement of the electro-optic coefficient are the ones developed by Teng and Man [14], and by Schildkraut [15]. These methods cannot be employed however in the case of materials with room temperature glass transition temperature [16]. For this reason, the second order susceptibility of the polymeric composites was measured and the electro-optic coefficient was inferred from these measurements.

For the measurement of the second order susceptibility the Maker fringe technique was employed. The Maker fringe method provides a powerful tool for making precise relative measurements of nonlinear optical coefficients. It was introduced first by Maker and co-workers in 1962 [17] and it was discussed in detail by Jerphangnon and Kurtz in 1970 [18]. The final form for thin polymeric films on a substrate was given by Herman and Hayden in 1995 [19].

Using the Maker-fringe technique a parallel film of a nonlinear optical material is placed perpendicular to an incoming beam (c. Figure 4.4). By varying the incidence angle of the beam, the intensity of the second harmonic generated is found to oscillate in a periodic fashion. The nonlinear optical coefficient can be deduced from the measurement of the second harmonic intensity from the film and its comparison with the second harmonic intensity of a reference crystal, usually quartz.
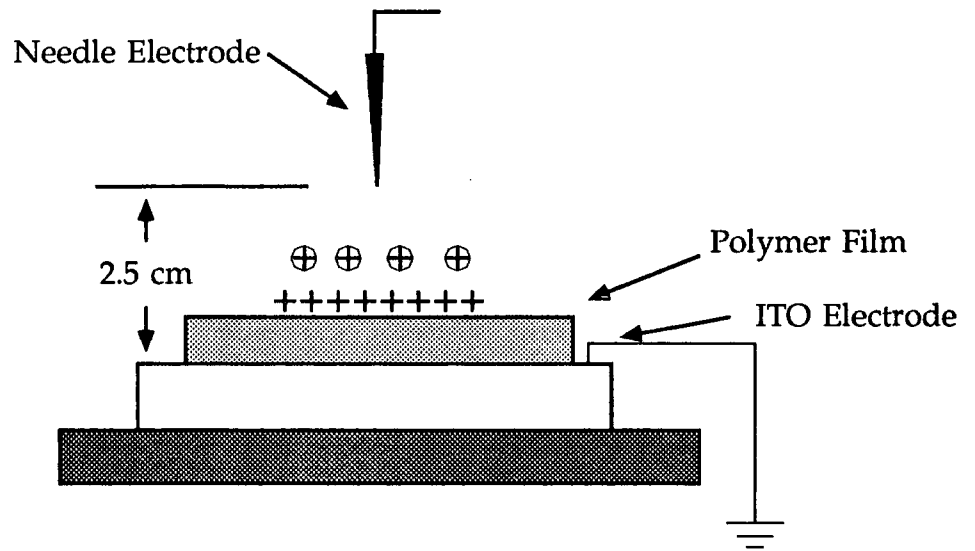
Figure 4.3 Corona poling set-up
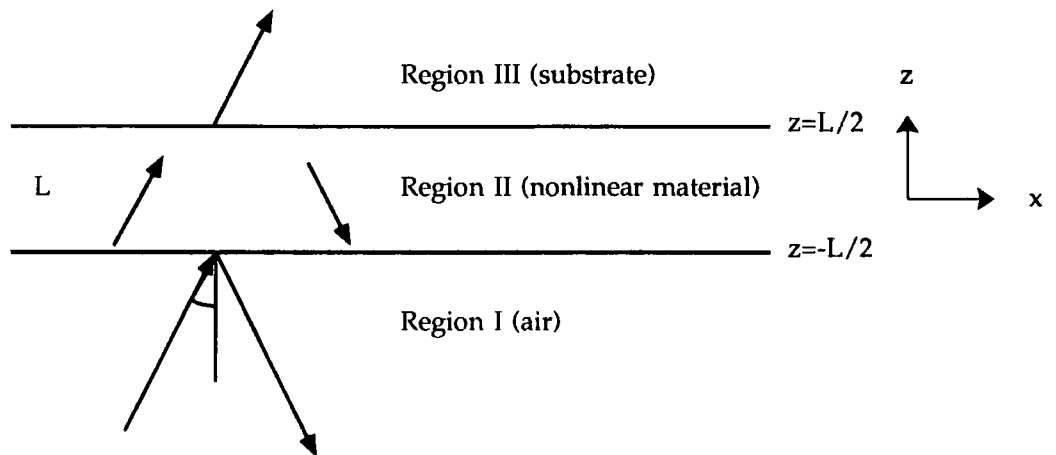
Figure 4.4 Propagation of a laser beam in a material

In order to calculate $\chi^{(2)}$, assume a fundamental laser beam of angular frequency ω and fixed power P_ω incident on a nonlinear polymeric thin film of thickness d (see Figure 4.4). Inside the polymer film, the electric field E_ω induces a nonlinear polarization which radiates electromagnetic waves of angular frequency 2ω. In addition to the bound 'harmonic' wave there is a 'free' harmonic wave (2ω) generated at the input surface. These 'bound' and 'free' waves have in general different velocities, giving rise to interference fringes in the harmonic power $P_{2\omega}$ as the film is rotated. Let θ be the incidence angle for the laser beam and n_ω, $n_{2\omega}$, α_ω and $\alpha_{2\omega}$ the refractive index and optical absorption at the fundamental and second harmonic frequencies respectively. The transmitted second order harmonic power is [19]

$$P_{2\omega} = \frac{128\pi^3}{cA} \frac{\left[t_{af}\right]^4 \left[t_{fs}\right]^2 \left[t_{sa}\right]^2}{n_{2\omega}^2 c_2^2} P_\omega^2 \left(\frac{2\pi d}{\lambda}\right)^2 \left(\frac{\chi_{\mathit{eff}}^{(2)}}{2}\right)^2$$
$$\times \exp\left[-2(\delta_1 + \delta_2)\right] \frac{\sin^2 \Psi + \sinh^2 \chi}{\Psi^2 + \chi^2} \tag{4.14}$$

where t's are standard Fresnel transmission coefficients at the air-film, film-substrate and substrate-air interfaces for the appropriate polarizations and frequencies and c_1 and c_2 are terms related to the wave vectors [19]. κ_1 and κ_2 are the extinction coefficients defined as

$$\kappa_1 = \frac{\lambda \alpha_\omega}{2\pi n_\omega} \qquad (4.15)$$

$$\kappa_2 = \frac{\left(\frac{\lambda}{2}\right)\alpha_{2\omega}}{2\pi n_{2\omega}} \qquad (4.16)$$

The dispersion factor Ψ is

$$\Psi = \frac{2\pi d}{\lambda}\left(n_\omega c_1 - n_{2\omega} c_2\right) \qquad (4.17)$$

and the absorption terms δ_1 and δ_2 are

$$\delta_1 = \frac{\pi d}{\lambda}\frac{n_\omega \kappa_1}{c_1} \qquad (4.18)$$

$$\delta_2 = \frac{\pi d}{\left(\frac{\lambda}{2}\right)}\frac{n_{2\omega} \kappa_2}{c_2} \qquad (4.19)$$

Finally, χ is defined as

$$\chi = \delta_1 - \delta_2 \qquad (4.20)$$

The effective second order nonlinear optical coefficient χ_{eff} can be calculated when the output is compared with the second harmonic of a reference crystal whose nonlinear optical coefficient is known. The most

common choice is quartz. In this work, the value used is $\chi_{11}^{(2)}$=0.6 pm/V

[20]. The χ_{33} coefficient can then be calculated using the following equation

$$\chi_{eff} = \chi_{33}\left\{R\cos\theta_{2\omega}\sin(2\theta_{\omega}) + \sin\theta_{2\omega}\left[R\cos^2\theta_{\omega} + \sin\theta_{\omega}\right]\right\} \qquad (4.\ 21)$$

where $R = \dfrac{\chi_{31}}{\chi_{33}}$.

For the experiment, a Nd:Yag laser was employed using light at

1.064 μm to produce a second harmonic at 532 nm, while a He-Ne laser

operating at the red part of the spectrum was used to help in the align-

ment (c. Figure 4.5). The beam was focused on the sample using a lens.

The power of the fundamental beam was measured by a fast response sili-

con photo-diode (rise time 500 ps). The second harmonic was detected

with a photo-multiplier tube which was pre-filtered with an infra-red

blocking filter (KG3), to prevent any damage because of the high power of

the fundamental. A boxcar integrator was used to measure the reference

and the second harmonic. Two polarizers were used, the first to adjust the

polarization of the beam and the second to control the power of the beam.

4.4.3 Two-Beam Coupling Measurements

In order to establish whether the investigated material is photorefractive

or not, a two beam coupling experiment has to be performed. In this ex-

periment, two coherent beams of the same polarization and wavelength
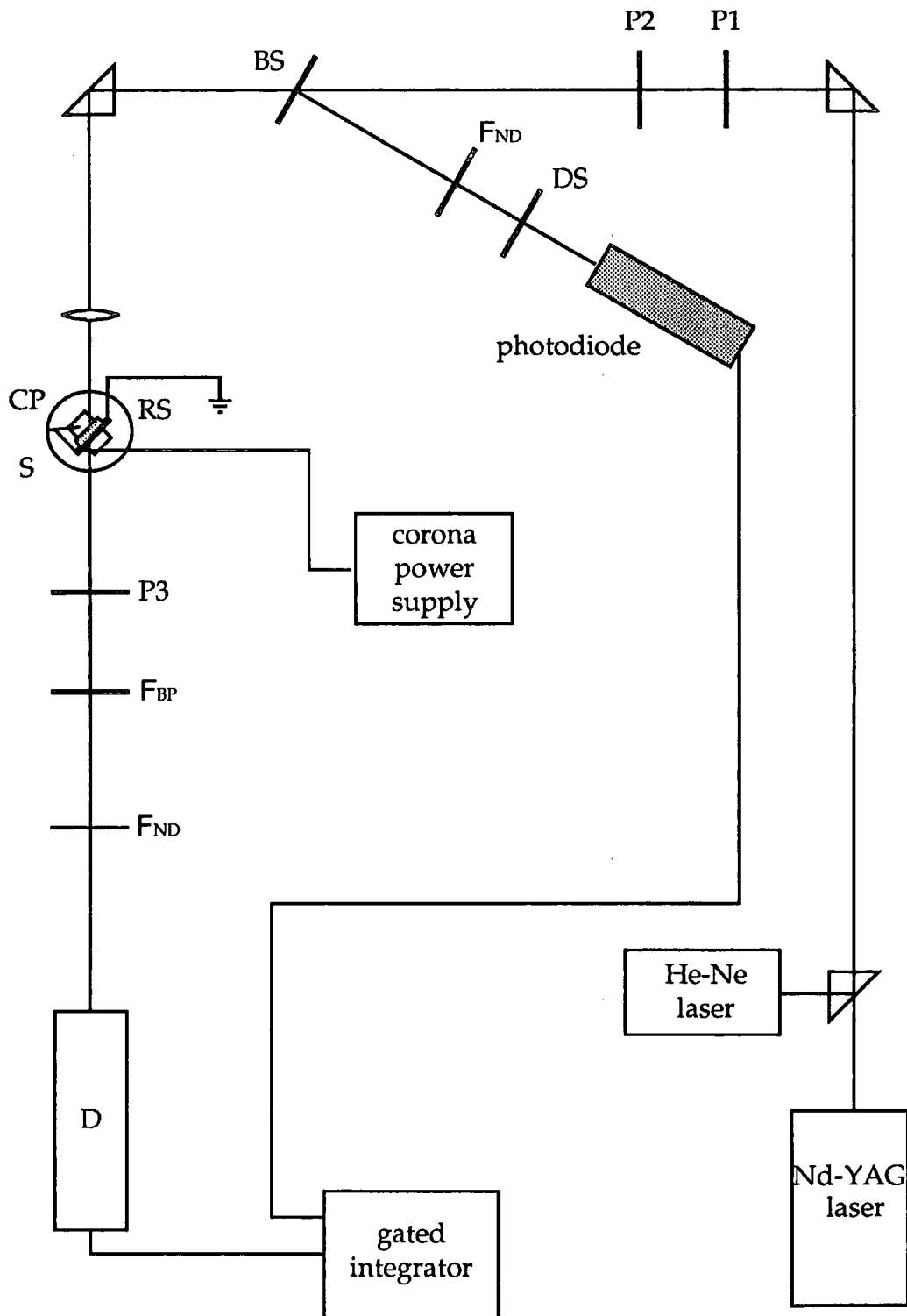
Figure 4.5 Experimental set-up for second harmonic generation. P = polarizer,
PMT = Photomultiplier tube, BS = beam splitter, F = filter, DS = diffusion
screen, ND = neutral density filter, KG3 = infra-red blocking filter,
CP = corona poling needle, RS = rotation stage, S = sample

overlap on the investigated material. If the material is photorefractive then there should be an asymmetric energy transfer between the two beams.

The experimental set up is shown in Figure 4.6. The beam of a 10 mW He-Ne laser operating at 632.8 nm was p polarized, for maximum two-beam coupling gain, and split using a beam splitter at 45°. This way the original beam was split into two equal intensity, p polarized, coherent beams. The two beams overlapped on the polymer sample with an angle of 15°, except for the measurement of DED - doped materials, where the angle between the two beams is 30°. This was because, due to the low solubility of DED, the films obtained were thinner and the grating spacing needed to be increased. The sample was tilted 45° to give a component of the grating vector parallel to the externally applied field. For the signal detection a Si photo-diode connected to an EG&G lock-in amplifier was used. A chopper, connected to the lock in amplifier was used to chop one of the beams to act as a reference, while the signal of the second beam is monitored through the detector. This way if there is any energy transfer from the chopped beam to the detected beam, the lock-in amplifier separates it from the background and amplifies it.

The gain coefficient can be calculated using equation (2.39) for two beams of equal intensity. That gives

Figure 4.6 The experimental set-up fro two beam coupling. P = polarizer, BS = beam splitter, M = mirror, C = chopper, S = sample, D = detector

$$\Gamma = \frac{1}{L}\left[\ln(\gamma_0) - \ln(2 - \gamma_0)\right]$$ (4.22)

For the two-beam coupling measurements of ULTRA-DEMI doped materials, where any measurements in the red part of the optical spectrum are impossible because of the high absorption of the composite at that spectral region, the same experiment was set up using an Argon-ion laser operating at 488 nm.

4.4.4 Degenerate Four-Wave Mixing

In order to measure the diffraction efficiency, a degenerate four wave mixing was performed. In this experiment, a grating was created by overlapping two coherent beams. The grating was then read using a lower power laser of the same wavelength.

The experimental set-up is shown in Figure 4.7. The beam of a 10 mW He-Ne laser operating at 632.8 nm was s polarized, so as to minimize two-beam coupling effects, and split into two equal intensity coherent beams using a beam splitter at 45°. The two beams overlapped on the polymer sample with an angle of 15°, except in the case of DED-doped materials, where the angle between the two beams was 30°, for the reasons explained in Section 4.7. The sample was tilted 45° to give a component of the grating vector parallel to the electric field. The beam of a 5 mW, p polarized He-Ne laser operating at 632.8 nm was used to probe the grating. The power of the beam was reduced using a 0.7 dB neutral density filter and was chopped, in order to provide a reference. The probe beam,
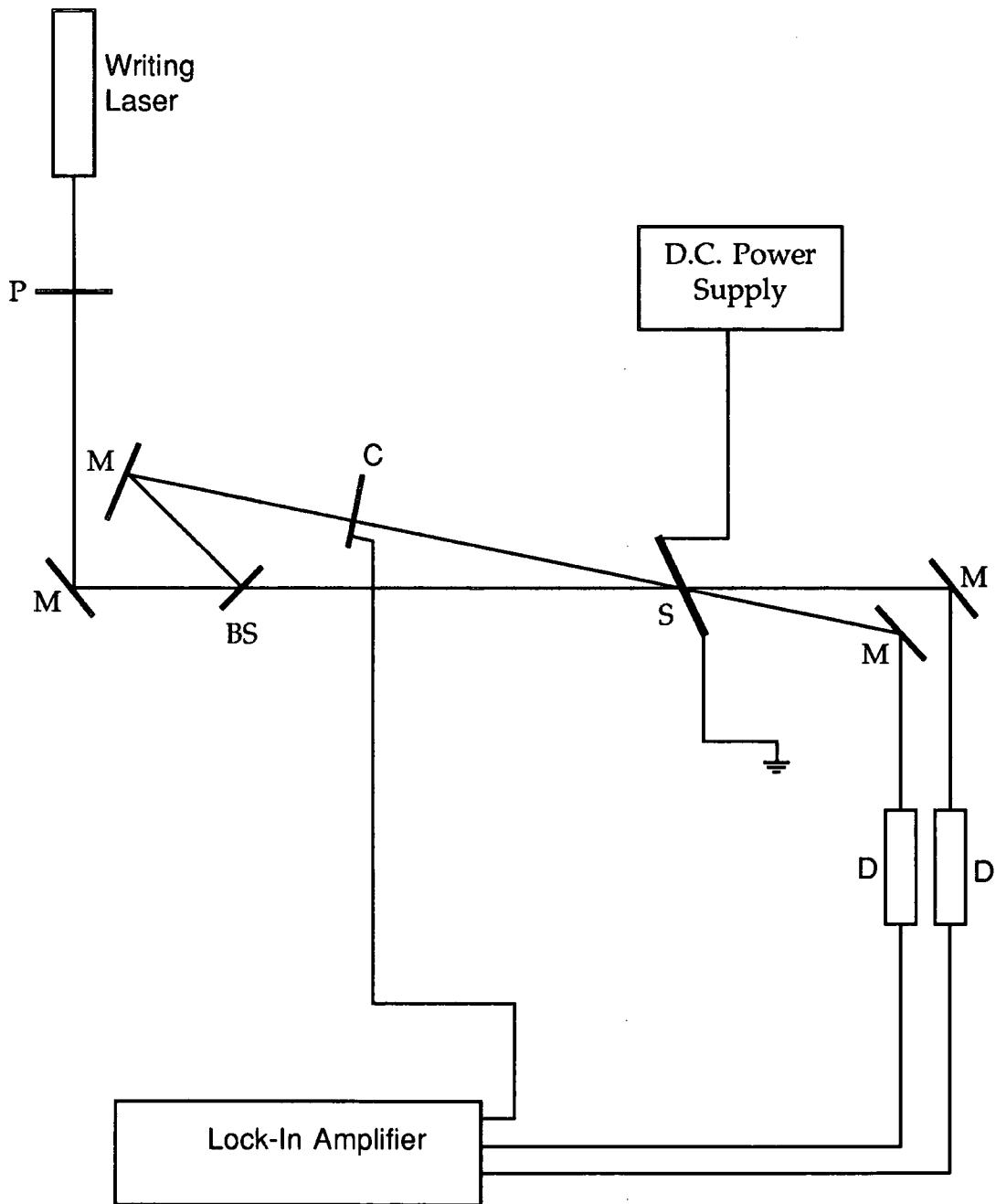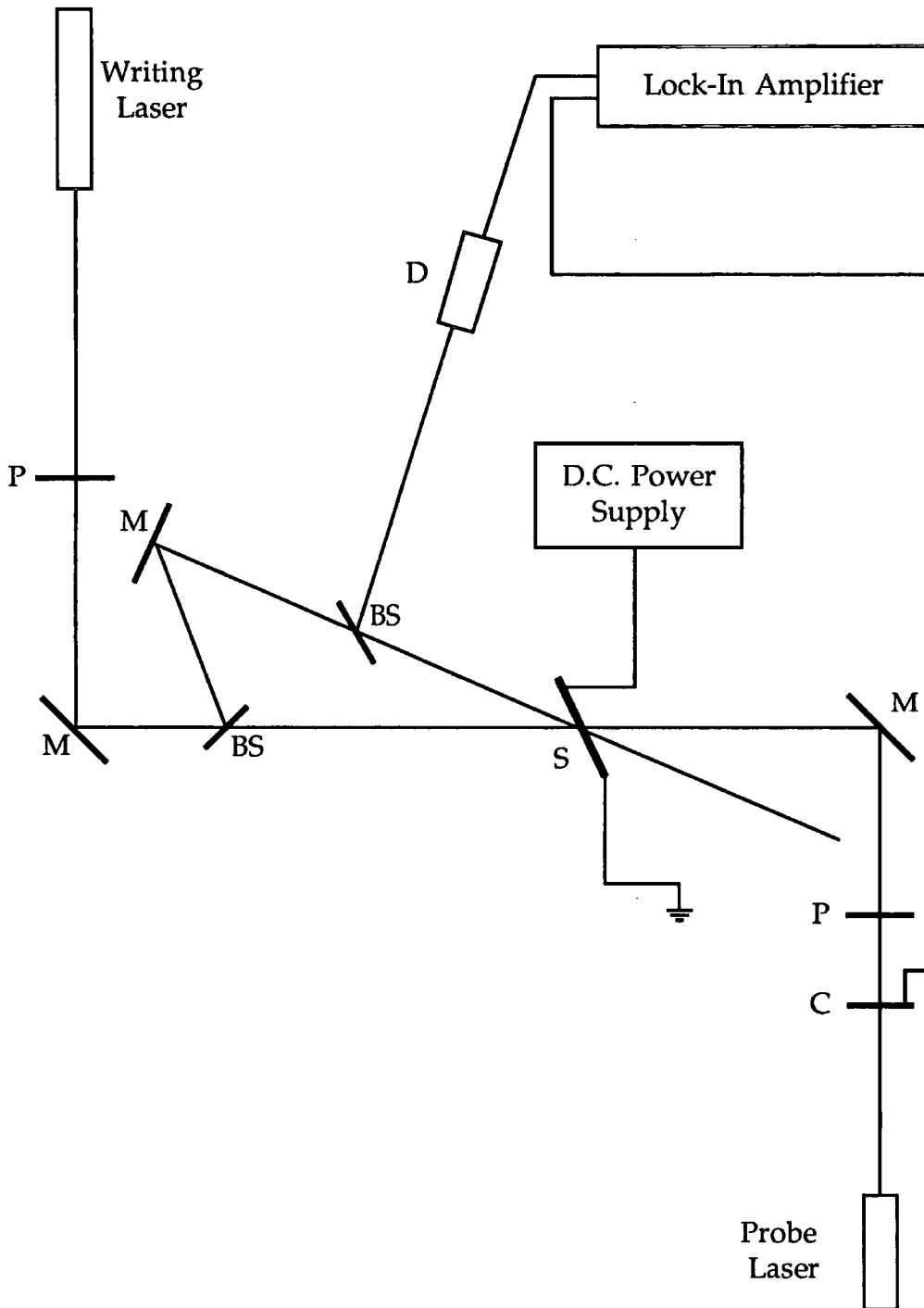
Figure 4.7 Experimental setup for degenerate four-wave mixing. P = polarizer, BS

= beam splitter, M = mirror, C = chopper, S = sample, D = detector

because of the four wave geometry, satisfied the Bragg condition and is diffracted by the grating with an efficiency η. The diffracted beam was directed as a background - free signal into a Si photodiode detector connected to the lock-in amplifier.

Degenerate four-wave mixing is a very sensitive experiment and it requires very stable laser beams and a very high stability optical bench.

4.5 References

[1]   C. J. F. Böttcher, pp. 1-44, *Theory of electric polarization*, Elsevier, **1952**.

[2]   J. D. Jackson, *Classical Electrodynamics*, pp. 27-53, John Wiley & Sons, **1975**.

[3]   J. Joo and A. J. Epstein, 'Complex dielectric constant measurements of samples of various cross-sections using a microwave impedance bridge', *Dev. Sci. Instrum.*, vol. 65, pp. 2653-2657, **1994**.

[4]   S. K. Mohapatra, C. V. Francis, K. Hahn, and D. Doffi, 'Microwave loss in nonlinear optical polymers', *J. Appl. Phys.*, vol. 73, pp. 2569-2571, **1993**.

[5]   J. D. Jackson, *Classical Electrodynamics*, pp. 334-390, John Wiley & Sons, **1975**.

[6]   P. K. Tien, R. Ulrich, and R. J. Martin, 'Modes of propagating light in thin deposited semiconductor films', *Appl. Phys. Lett.*, vol. 14, pp. 291-294, **1969**.

[7]   R. Morita, N. Ogasawara, S. Umegaki, and R. Ito, 'Refractive indices of 2-Methyl-4-Nitroanaline (MNA)', *Jap. J. Appl. Phys.*, vol. 26, pp. L1711-L1713, **1987**.

[8] C. Bosshard, K. Sutter, P. Prêtre, J. Hulliger, M. Flörsheimer, P.Kaatz, and P. Günter, *Organic Nonlinear Optical Materials*, pp. 106-114, Gordon and Breach, **1995**.

[9] M. A. Mortazavi, A. Knoesen, S. T. Kowel, B. J. Higgins, and A. Dienes, 'Second-harmonic generation and absorption studies of polymer-dye films oriented by corona-onset poling at elevated temperatures.', *J. Opt. Soc. Am. B*, vol. 6, pp. 733-741, **1989**.

[10] P. T. Dao, D. J. Williams, W. P. Mc Kenna, and K. Goppert - Berarducci, 'Constant current corona charging as a technique for poling organic nonlinear optical thin films and the effect of ambient gas', *J. Appl. Phys.*, vol. 73, pp. 2043-2050, **1993**.

[11] K. Meerholz, B. L. Volodin, Sandalphon, B. Kippelen, and N. Peyghambarian, 'A photorefractive polymer with high optical gain and diffraction efficiency near 100-percent', *Nature*, vol. 371, pp. 497-500, **1994**.

[12] Y. Zhang, C. A. Spencer, S. Ghosal, M. K. Casstevens, and R. Burzynski, 'Thiapyrylium dye sensitization of photorefractivity in a polymer composite', *App. Phys. Lett.*, vol. 64, pp. 1908-1910, **1994**.

[13] D. Gray, *Molecular organic photonics*, Ph.D. thesis, University of Durham, **1994**.

[14] C. C. Teng and H. T. Man, 'Simple reflection technique for measuring the electro-optic coefficient of poled polymers', *Appl. Phys. Lett.*, vol. 56, pp. 1734-1736, **1990**.

[15] J. S. Schildkraut, 'Determination of the electro-optic coefficient of a poled polymer film', *Applied Optics*, vol. 29, pp. 2839-2841, **1990**.

[16] B. Kippelen, Sandalphon, K. Meerholz, and N. Peyghambarian, 'Birefringence, Pockels and Kerr effects in photorefractive polymers', *Appl. Phys. Lett.*, vol. 68, pp. 17481750, **1996**.

[17] P. D. Maker, R. W. Terhune, M. Nisenoff, and C. M. Savage, 'Effects of dispersion and focusing on the production of optical harmonics', *Phys. Rev. Lett.*, vol. 8, pp. 21-22, **1961**.

[18] J. Jerphagnon and S. K. Kurtz, 'Maker Fringes: A detailed comparison of theory and experiment for isotropic and uniaxial crystals.,' *J. Appl. Phys.*, vol. 41, pp. 1667-1681, **1970**.

[19] W. N. Herman and L. M. Hayden, 'Maker fringes revisited: second harmonic generation from birefringent or absorbing materials', *J. Opt. Soc. Am. B*, vol. 12, pp. 416-427, **1995**.

[20] I. Shoji, A. Kitamoto, M. Shirane, T. Kondo and R. Ito, 'Absolute scale of the second-order nonlinear optical coefficient', *OSA Technical Digest Series*, vol. 11, pp. 126-128, **1996**.

Chapter 5

Sample Preparation

5.1 Introduction

In this chapter the methodology of the substrate, solution and sample preparation is described.

In order to reduce scattering during optical measurements it is very important to avoid any sort of contamination of the samples and keep foreign particles to a minimum. It is also important that substrates are clean, to promote adherence of the polymer to the substrate. For these reasons, all the preparations were carried out in a clean room environment.

5.2 Substrate Preparation

The several different experiments required the use of different substrates, varying from plain glass slides for the absorption measurements to Teflon discs for the high frequency dielectric measurements. However, the same preparation procedure was followed in all cases.

Each piece of substrate was placed individually in a glass sample bottle with chloroform and left in an ultrasonic bath for thirty minutes. Then they were wiped using lint free paper and were placed in a sample bottle again with 5% Decon 90 and de-ionized water, and left in the ultrasonic bath for an hour. They were then rinsed with de-ionized water and the excess water was blown off with a nitrogen gun. After they were dried, they were placed in a sample bottle again with chloroform and left in the ultra-sonic bath for ten minutes. Eventually they were left to dry for several hours in a drying cabinet.

5.3 Solution Preparation

In the case of the photorefractive materials, several solvents were investigated for their suitability for the preparation of thin and thick films. Both the host polymer and the different dopants were soluble in a variety of solvents such as DCM, chloroform, TCP, DMF and TMU. It was discovered, however, that volatile solvents such as DCM and chloroform caused phase separation in films thicker than a few microns. Non-volatile solvents such as TCP, DMF and TMU produced in general very high quality thin and thick

films. TMU was chosen as the main solvent because it dissolved all the materials under investigation and because it is a very low-hazard solvent.

The sample bottles and magnetic stirrers were cleaned out with chloroform and placed in an ultrasonic bath for ten minutes. Solutions were prepared with 0.07-2.0 g of polymeric mixture to 10 ml of TMU, depending on the solubility of the nonlinear optical material and the required film thickness (PVK, C_{60} and TNF are very soluble in TMU and they did not affect the solution concentration). The solutions were left stirring overnight. To remove any dust particles and any coagulant the solution was filtered through a 0.5 μm pore Millipore disposable filter. The solutions were prepared under nitrogen environment in a glove-box, to avoid the absorption of any water.

For the two electro-optic polymers, TCP was used as a solvent. In the case of polymer (I), solutions 1-2% (w/w) were prepared and left stirring for several days. They were then boiled to 140°C and filtered through a 0.5 μm pore size disposable filter. In the case of polymer (II), solutions 15% (w/w) were prepared. They were left stirring for several days and then filtered through a 0.5 μm pore size disposable filter.

5.4 Sample Composition

In order to determine the amount of dopant required to add to the polymer to reduce the T_g of the composites to room temperature, PVK was doped with different concentrations of NPP (25%, 30%, 40%, 50% w/w). The different solutions were prepared as above (1g composite for 10 ml TMU) and

films approximately 3 μm thick were prepared by simple solvent casting using ITO-coated glass as a substrate. The films were left to dry in a vacuum oven for several days and then silver electrodes were applied on them by evaporation. To determine the T_g of the different composites, a 50 Volts DC electric field was applied across the sample and the current through the film was monitored with an electrometer as the sample was heated. A sharp increase of the current flowing through the sample is an indication that the temperature of the film was approaching the T_g of the composite. There was no need to heat the film for a 50% w/w concentration of NPP. For the rest of the material preparation, a maximum concentration 50% of PVK was maintained.

The nonlinear response of the composite increases with nonlinear optical material concentration [1]. For this reason, the concentration of the nonlinear optical material in the different composites investigated is the highest possible, and it depends on its solubility and its tendency to crystallize.

It has been shown that the diffraction efficiency of a photorefractive PVK-based polymer in the visible part of the spectrum increases with the increasing concentration of sensitizer [2,3]. However, very high sensitizer concentration results in high absorption of the polymer, which competes with the two beam coupling gain. In the case of TNF used as a sensitizer, most commonly 1-2% w/w is used [4] and in this work, 2%. In the case of C_{60} used as a sensitizer, it was found that the maximum amount that could be used is 0.2% w/w. Any higher concentration caused phase separation.

nlo material	nlo (% w/w)	PVK (% w/w)	TNF (% w/w)	ECZ (% w/w)
NPP	50	48	2	-
DAN	20	50	2	28
DED	5	50	2	43
DCNQI	0.5	50	2	47.5
DI-DEMI	2	50	2	46

Table 5.1 Composition of the TNF-sensitized polymeric composites examined

nlo material	nlo (% w/w)	PVK (% w/w)	C_{60} (% w/w)	ECZ (% w/w)
NPP	50	49.8	0.2	-
DAN	20	50	0.2	29.8
DED	5	50	0.2	44.8
DCNQI	0.5	50	0.2	49.3
ULTRA-DEMI	5	50	0.2	44.8
DI-DEMI	2	50	0.2	47.8

Table 5.2 Composition of the C_{60}-sensitized polymeric materials examined

The composition of the TNF-sensitized polymeric materials examined in this work is shown in Table 5.1, while in Table 5.2 the composition of the C_{60} sensitized composites is shown. It should be pointed out that TNF was banned before ULTRA-DEMI was firstly synthesized, as a result there are no measurements on ULTRA-DEMI:TNF containing composites.

5.5 Film Preparation

In the following sections the film preparation for the different experiments described in Chapter 4 is presented. The sample preparation refers to both TNF and C_{60}-sensitized composites, except in the case of ULTRA-DEMI, where only C_{60} was used as a sensitizer.

5.5.1 Film Preparation for Low Frequency Dielectric Measurements

In order to perform the dielectric measurements at 1 KHz and 1 MHz, films of the polymeric mixtures were prepared using ITO glass substrates. The ITO glass was cut into 2.0x2.0x0.1 cm square pieces using a diamond scribe and cleaned using the procedure described in § 5.2. Solutions of the different composites were prepared as in § 5.3. Their concentration is shown in Table 5.3. Then films of the polymeric mixtures were prepared by solvent casting and left to dry under vacuum for several weeks.

In the case of DCNQI and DI-DEMI, because of the low concentration of the solutions, which was due to the low solubility of the nonlinear optical material and the polymer respectively, multiple layers of the composite needed to be applied, in order to achieve the desired film thickness. It was

found that up to three layers could be applied, without affecting the quality

of the film. The thickness of the films were measured using a surface pro-

filer and were found to be between 20 and 40 μm, except in the case of

DCNQI, where the films were approximately 10 μm.

In the case of the two electro-optic polymers, films 20-40 μm were

prepared by multiple solvent casting and dried for several days in a vacuum

oven at 120°C.

5.5.2 Film Preparation for High Frequency Dielectric Measurements.

For the high frequency dielectric measurements, a low dielectric constant

substrate was required, so that it would not distort significally the electric

field in the cavity. Originally 1 cm diameter, 1 cm thick silica discs were

used. Silica, however, is very brittle and the substrates tended to fragment

nlo material	polymeric composite in 10 ml of TMU (g)
NPP	2.0
DAN	2.0
DED	1.0
DCNQI	0.07
ULTRA-DEMI	0.3
DI-DEMI	0.1

Table 5.3 Composition of the solutions used in the preparation of films for dielectric
and nonlinear optical measurements

cleaning and during the insertion of the sample in the cavity. For this reason they were replaced by Teflon discs of the same dimensions.

The substrates were prepared as described in § 5.2. Polymer films of between 20 and 40 µm were deposited by solvent casting and slow evaporation using the same solutions as for the low frequency dielectric measurements (Table 5.3). For drying the solvent and to minimize water inclusion, the samples were kept under vacuum for several weeks. Following the dielectric measurements, the film thicknesses were determined. As for the films for low frequency dielectric measurements, multiple layers of the composite needed to be applied in the case of DCNQI and DI-DEMI.

In the case of the two electro-optic polymers, films of 20-40 µm were prepared by multiple solvent casting and dried for several days in a vacuum oven at 120°C.

5.5.3 Film Preparation for Linear Optical Measurements

For the different absorption and refractive index measurements, polymer films were prepared using microscope glass slides as substrates. Firstly the glass slides were cut into halves 1.5x3.75x0.1 cm using a diamond scribe. The substrates were cleaned following the procedure described in § 5.2. The films were prepared by spin coating at 2000-4000 revs per minute for 5-40 seconds and left to dry under vacuum for 48 hours. In the case of DI-DEMI, three layers of polymer had to be applied, because of the low concentration of the solution, while in the case of DCNQI, no films were possible, for the same reason.

nlo material	polymeric composite in 10 ml of TMU (g)
NPP	1.2
DAN	1.2
DED	1.0
DCNQI	0.07
ULTRA-DEMI	0.3
DI-DEMI	0.1

Table 5.4 Composition of the solutions used in the preparation of films for linear optical measurements.

The different solution concentrations are shown in Table 5.4.

5.5.4 Film Preparation for the Nonlinear Optical Measurements

For the nonlinear optical measurements, polymer films of between 2 and 60 μm were deposited using ITO-coated glass as a substrate. Firstly the glass was cut into 1.0x3.5x0.1 cm pieces and cleaned following the procedure described in § 5.2. The solutions prepared were the same as for the dielectric measurements (Table 5.3). The films were prepared by simple solvent casting and slow evaporation. For drying the solvent, the film samples were kept under vacuum for approximately a week.

It should be pointed here that, as it has already been mentioned in Chapter 3, TNF was banned before any nonlinear optical measurements were performed. Therefore, this preparation refers only to C_{60}-sensitized composites.

5.6 References

[1] D. S. Chemla and J. Zyss, 'Nonlinear optical properties of organic molecules and crystals', vol. 1, pp. 405-435, Academic Press, **1987**.

[2] S. M. Silence, C. A. Walsh, J. C. Scott, and W. E. Moerner, 'C_{60} sensitization of a photorefractive polymer', *App. Phys. Lett.*, vol. 61, pp. 2967-2969, **1992**.

[3] S. M. Silence, M. C. J. M. Donckers, C. A. Walsh, D. M. Burland, R. J. Twieg, and W. E. Moerner, 'Optical properties of poly(N-vinylcarbazole)-based guest-host photorefractive polymer systems', *Applied Optics*, Vol. 33, p. 2218-2222, **1994**.

[4] W. E. Moerner and S. M. Silence, 'Polymeric photorefractive materials', *Chem. Rev.*, vol. 94, pp. 127-155, **1994**.

Chapter 6

Linear Measurements

6.1 Introduction

In this chapter the results for the dielectric measurements and linear optical experiments described in Chapter 4 are presented. The dielectric measurements were performed at 1 KHz and 1 MHz using a bridge capacitance meter and at 10 GHz, at ambient and elevated temperatures, using a resonant cavity technique. The experimental techniques have been described in § 4.2.1 and § 4.2.2 respectively. The linear optical measurements were performed using a Perkin Elmer Lambda 9 spectrophotometer. The experimental technique for the measurements of the refractive index has been described in § 4.3.1

6.2 Low Frequency Dielectric Measurements

For the low frequency dielectric measurements, the effective distance between the sample surface and the top electrode was firstly calculated (c.

§4.2.1). The capacitance of the polymer film was then measured as a function of the electrode distance and the dielectric constant was calculated using equation (4.7). The results of these measurements for the PVK:TNF and PVK:C_{60} composites are presented in Table 6.1 and Table 6.2 respectively. The results for the two electro-optic polymers are presented in Table 6.3. The value of the dielectric constant presented here is the mean value of the ones measured for five samples, while for the errorbars, the standard error was calculated. The accurancy of the method was found to increase with film thickness.

The results of these measurements show that the dielectric constants of the different PVK based polymeric composites are low, as would be expected from a polymeric material. Additionally, there seems to be very small variation between the dielectric constants of the different composites.

nlo material	1 KHz	1 MHz
NPP	4.40±0.40	4.32±0.11
DAN	4.02±0.33	3.91±0.09
DED	4.04±0.42	3.92±0.12
DCNQI	3.86±0.52	3.67±0.24
DI-DEMI	4.01±0.48	3.92±0.18

Table 6.1 The dielectric constant of the different PVK:TNF based composites at 1 KHz and 1 MHz

nlo material	1 KHz	1 MHz
NPP	4.26 ± 0.36	4.10±0.0 8
DAN	3.82±0.38	3.61±0.12
DED	4.06±0.42	3.86±0.12
DCNQI	3.90±0.49	3.62±0.20
ULTRA-DEMI	4.02 ±0.46	3.80±0.16
DI-DEMI	4.09±0.45	3.76±0.14

Table 6.2 The dielectric constant of the different PVK:C_{60} based composites at 1 KHz and 1 MHz

nlo material	1 KHz	1 MHz
polymer (I)	5.22±0.24	4.52±0.17
polymer (II)	4.35±0.24	4.30±0.17

Table 6.3 The dielectric constant of the two electro-optic polymers 1 KHz and 1 MHz

6.3 High Frequency Dielectric Measurements at Ambient and Elevated Temperatures

For the high frequency dielectric measurements, the bare Teflon disk was firstly placed on the sample holder and inserted into the cavity through a hole at the side. The sample was placed approximately at the centre of the side of the cavity, where the electric field is assumed to be parallel to the surface so that minimum distortion of the field is caused. The cavity microme-

ter was moved until a resonance at 10 GHz was observed and the resonant frequency and quality factor of the cavity were measured. A polymer film was then deposited on the Teflon disc which was placed again on the sample holder and the new position of the resonant frequency as well as the new quality factor were measured.

In order to calculate the permittivities, the unknown quantities $F(x,y,z)$ and V_0 (c. §4.2.2) which have unique values for every setting of the micrometer, were measured experimentally using a quartz cube of known volume and relative permittivity at 10 GHz. The value for ε_{r11} (ε_{r11}= 4.423 [1]) for quartz was assumed in this work after experimentally determining the crystal orientation from the frequency shifts. The resonant frequency of the cavity was measured with and without the quartz reference and the factor $V_0F(x,y,z)$ determined from equation (4.10). This way any errors in the measurement of the volume of the cavity and in the calculation of $F(x,y,z)$ were eliminated.

The results obtained for the different PVK:TNF and PVK:C_{60} polymeric composites are given in Table 6.4 and 6.5, respectively, while the results for the two electro-optic polymers are given in Table 6.6. The value of the dielectric constant presented here is the mean value of the ones measured for five samples and for the errorbars, the standard error was calculated.

nlo material	ε_r'	$\varepsilon_r''/10^2$
NPP	3.62±0.24	55±12
DAN	3.42±0.27	47±11
DED	3.64±0.33	86±14
DCNQI	3.43±0.38	79±22
DI-DEMI	3.47±0.31	92±18

Table 6.4 The dielectric constant and loss of the PVK:TNF composites at 10 GHz

nlo material	ε_r'	$\varepsilon_r''/10^2$
NPP	3.38 ± 0.28	89 ± 11
DAN	3.28 ± 0.32	78 ± 13
DED	3.81 ± 0.30	75 ± 8
DCNQI	3.54±0.41	88±18
ULTRA-DEMI	3.64 ± 0.30	73 ± 16
DI-DEMI	3.42±0.34	56±11

Table 6.5 The dielectric constant and loss of the PVK:C_{60} composites at 10 GHz

nlo material	ε_r'	$\varepsilon_r''/10^2$
polymer (I)	4.42±0.29	0.145±0.025
polymer (II)	3.25±0.29	0.035±0.012

Table 6.6 The dielectric constant and loss of the two electro-optic polymers at 10 GHz

In order to confirm the experimental validity of the technique and to estimate the errors, films of poly(methyl methacrylate), PMMA, were also measured. The real part of the permittivity measured was 2.92 ±0.16, which differs by less than 15% from the published value of 2.59 [2]. The imaginary part of the permittivity, or dielectric loss, measured was $(76 \pm 42) \times 10^{-2}$ which is of the same order of magnitude as the published value of 29×10^{-2} [2].

The results of the dielectric measurements at 10 GHz are in agreement with those of the dielectric measurements at lower frequencies. The dielectric constant is, as expected, decreasing slightly and the order of magnitude of the dielectric loss is typical of polymeric materials [2].

For the 10 GHz dielectric measurements at elevated temperatures, the same procedure was followed. The results for the temperature dependent dielectric constant and loss are presented in Figure 6.1 and Figure 6.2 respectively.

Material (I) was found to exhibit a rapid increase of its dielectric constant and loss at temperatures over 40°C. This makes material (I) unsuitable for industrial applications This is not the case with material (II) whose permittivity did not increase significally with temperature.

In conclusion, the temperature dependence of the microwave relative permittivity of two polymers considered as candidates in electro-optic devices was measured. A novel adaptation of the resonant cavity method for measuring the temperature dependence of the dielectric permittivity at 10 GHz was employed. The use of the cavity perturbation method and the removal of the need for complicated sample preparation make this technique
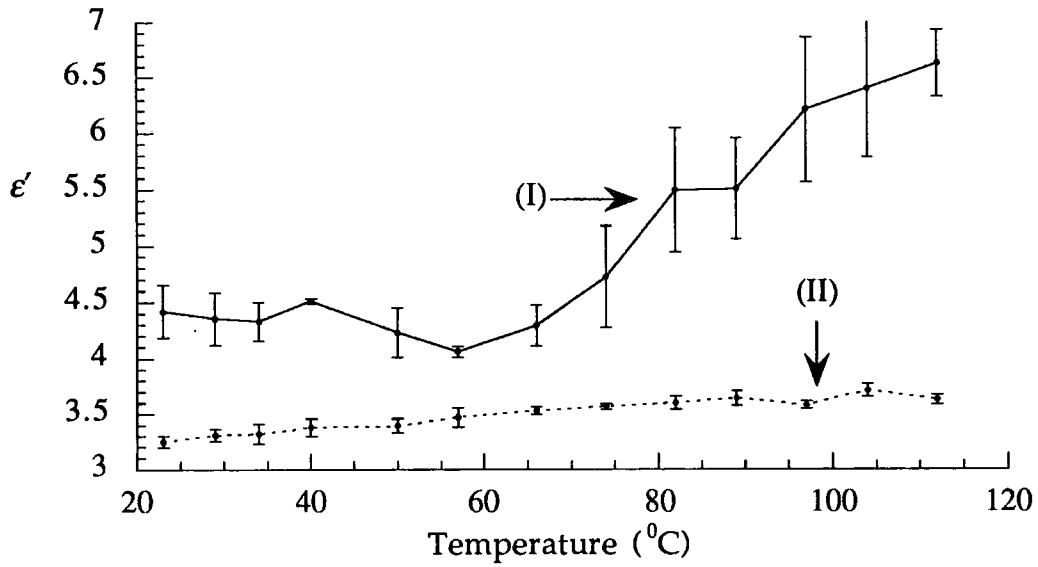
Figure 6.1 Dependence of the dielectric constant at 10 GHz of polymers (I) and (II) on temperature
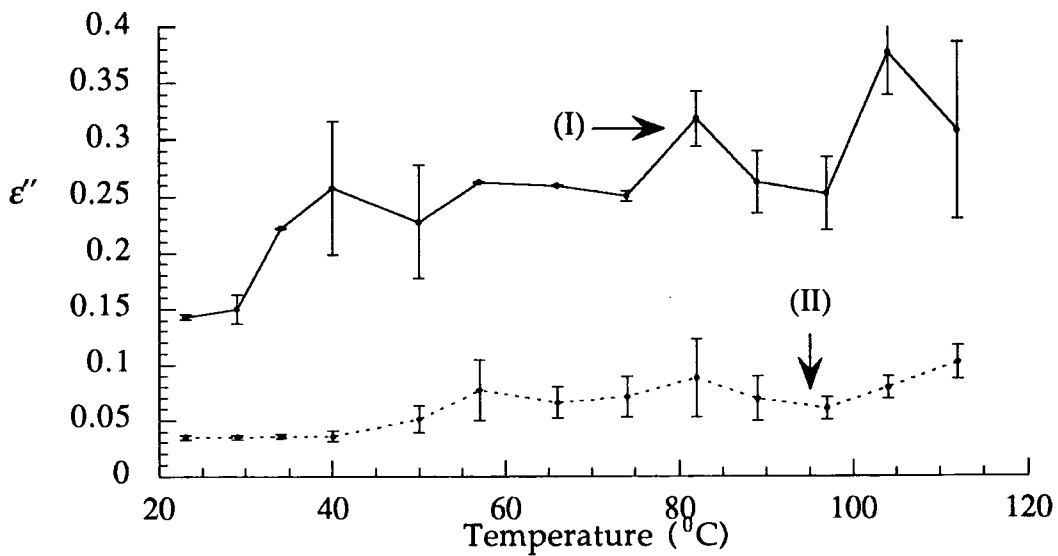

Figure 6.2 Dependence of the dielectric loss at 10 GHz of polymers (I) and (II) on temperature

attractive for wider application. This method may help in the earlier identification of fundamental constraints on the use of newly developed materials.

6.4 Absorption

For the absorption measurements, the spectrophotometer was firstly calibrated to zero absorption using a glass slide as a reference. Then the absolute absorption spectrum was taken and the absorption coefficient α was calculated by dividing the absorption at the required wavelength with the film thickness. In practice, the absorption coefficient is needed to be known at 1064 nm and 532 nm, where the second harmonic generation experiment is operating and at 632.8 nm where the photorefractive measurements take place except in the case of ULTRA-DEMI and DI-DEMI doped composites, where the photorefractive experiments are carried out at 488 nm, because of the high absorption of the materials at the red part of the spectrum. The results of the absorption measurements are shown in Tables 6.7 and 6.8, for the TNF and C_{60} doped composites respectively. The value of the dielectric constant presented here is the mean value of the ones measured for four samples, while for the errorbars, the standard error was calculated.

It can be seen that the TNF doped composites have significally higher absorption coefficient than the ones doped with C_{60}. This is mainly because of the much higher concentartion of TNF (2%, instead of 0.2% in the case of C_{60}).

nlo material	488 nm (cm^{-1})	532 nm (cm^{-1})	632.8 nm (cm^{-1})	1064 nm (cm^{-1})
NPP		136.6±3.1	71.2±4.9	35.4±3.9
DAN		112.8±3.2	64.2±3.8	29.8±2.9
DED		177.7±5.8	86.4±4.2	36.2±7.7
DI-DEMI	512±14.8	608.0±26.9		45.6±6.3

Table 6.7 Absorption coefficient α of the different PVK:TNF composites at the required wavelengths

nlo material	488 nm (cm^{-1})	532 nm (cm^{-1})	632.8 nm (cm^{-1})	1064 nm (cm^{-1})
NPP		31.3 ± 1.3	12.4 ± 0.9	5.6 ± 0.5
DAN		25.8 ± 0.9	12.8 ± 0.9	5.6 ± 0.4
DED		87.4 ± 1.3	19.1 ± 1.2	10.7 ± 0.5
ULTRA-DEMI	249.8±8.5	459.5 ± 19.5		27.7 ± 2.3
DI-DEMI	312.4±9.2	526.0±18.6		24.8±2.4

Table 6. 8 Absorption coefficient α of the different PVK:C$_{60}$ composites at the required wavelengths

Another quantity is the wavelength of the maximum absorption λ_{max} (electronic resonance) of the different PVK:C$_{60}$ composites and its comparison with the λ_{max} of the respective nonlinear optical material. In order to find the peak absorption of the nonlinear optical material, small quantities

nlo material	λ_{max} in 1,4 dioxane (nm)	λ_{max} of PVK:C$_{60}$ films (nm)
NPP	386	440
DAN	355	422
DED	458	443
DCNQI	416 (in TMU)	-
ULTRA-DEMI	719	733
DI-DEMI	720	711

Table 6. 9 Absorption peak of the different nonlinear optical materials and doped PVK composites (DCNQI is not soluble in 1,4 dioxane)

of it were dissolved in 1,4 dioxane. 1,4 dioxane is a very low polarity solvent that would induce a negligible solvatochromic shift and is often used as a reference [3,4]. The spectra of the different solutions were taken in a similar manner to that of the films. The results of these measurements are shown in Table 6.9.

As expected, for a polar host such as PVK, the λ_{max} of NPP-doped and DAN-doped polymers is shifted to longer wavelengths compared to the λ_{max} of the solutions. The λ_{max} of DED-doped PVK:C$_{60}$ has shifted to lower wavelengths, but this is not surprising since DED is a zwitterionic material (c. §3.4.3), therefore negative solvatochromism is expected.

Negative solvatochromism would also be expected for ULTRA - DEMI-doped PVK:C$_{60}$, since ULTRA-DEMI is also a zwitterionic material (c.

§3.4.5). However, instead there is a small shift to *higher* wavelengths. To investigate this phenomenon, solutions of ULTRA-DEMI:PVK:C_{60}, ULTRA-DEMI: PVK and ULTRA-DEMI:PVK:ECZ were prepared, thin films were made by spin-coating on a glass substrate and their spectra were taken. The shift to higher wavelengths remained even when all the dopants except ULTRA-DEMI were omitted, and in fact there was a small shift to even higher wavelengths (Figure 6.3). This indicates that the shift is not due to an interaction between ULTRA-DEMI and any of the other dopants, but due to an interac- tion between PVK and ULTRA-DEMI. Further research is needed to investigate the nature of this interaction.
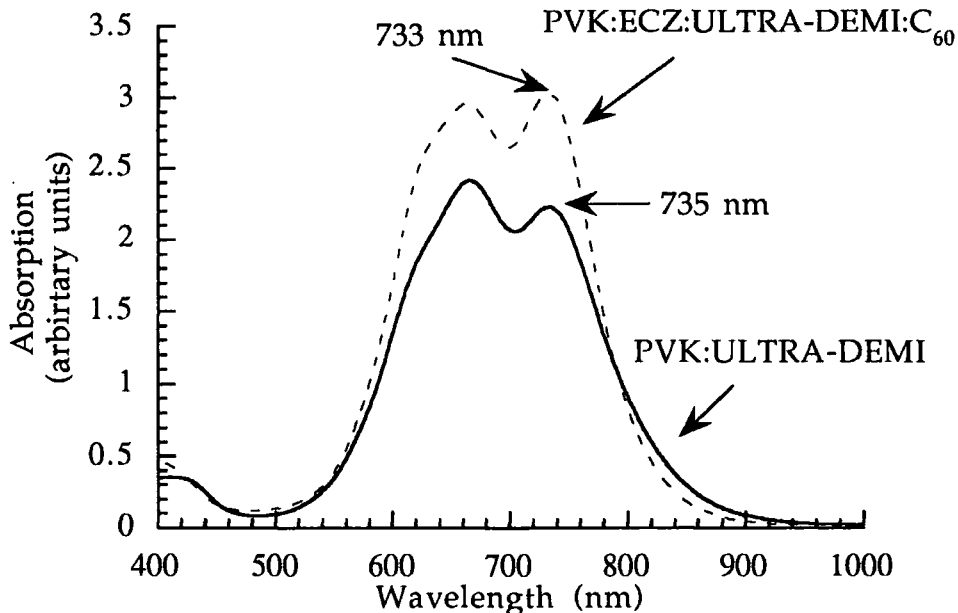

Figure 6.3 The absorption spectrum of PVK:ULTRA-DEMI:ECZ:C_{60} and ULTRA-DEMI:PVK. The shift to higher wavelengths can be seen when all the dopants except ULTRA-DEMI were omitted.

6.5 Refractive Index Measurements

The spectrophotometer was firstly calibrated to zero absorption by using a glass slide as reference. Then the spectrum of the thin films was taken between 300-2000 nm wavelength. An example of the form of the spectrum is shown in Figure 6.4. The position of the minimum and maximum absorption peaks near the required wavelengths were taken and the respective refractive index was calculated using equation (4.13). The results of these calculations are shown in Table 6.10 and 6.11. The value of the dielectric constant presented here is the mean value of the ones measured for eight samples, while for the errorbars, the standard deviation was calculated.
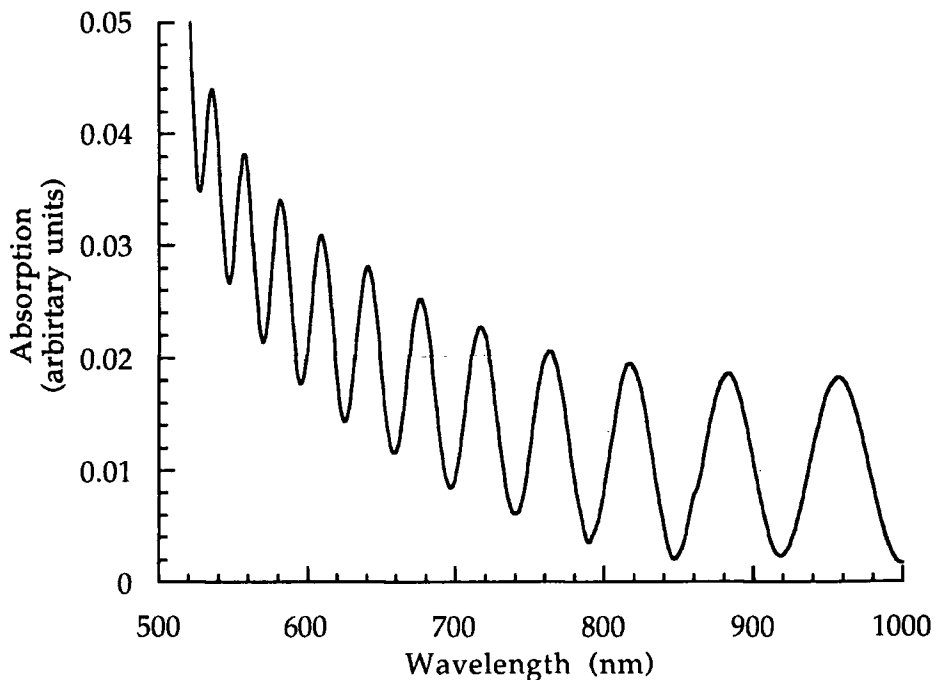
Figure 6.4 An example of the form of the spectrum required for the refractive index measurements. The fringes are due to the reflection of light from the film and the glass surface. Films of very high quality and flatness are required for these measurements.

nlo material	488 nm	532 nm	632.8 nm	1064 nm
NPP		2.19±0.05	1.89±0.04	1.74±0.04
DAN		2.10±0.05	1.75±0.05	1.71±0.04
DED		1.93±0.06	1.86±0.06	1.72±0.5
DI-DEMI	2.15±0.05	2.24±0.06		1.73±0.06

Table 6.10 The refractive index of the different PVK:TNF composites at the operating wavelengths

nlo material	488 nm	532 nm	632.8 nm	1064 nm
NPP		2.16±0.04	1.88±0.04	1.71±0.04
DAN		2.04±0.04	1.76±0.04	1.70±0.04
DED		1.89±0.07	1.84±0.07	1.72±0.7
ULTRA-DEMI	2.10±0.05	2.15±0.05		1.71±0.05
DI-DEMI	2.12±0.05	2.18±0.06		1.72±0.05

Table 6.11 The refractive index of the different PVK:C_{60} composites at the operating wavelengths

6.6 References

[1]   The quartz cube was supplied and calibrated for this purpose by GEC Wembley, Herst Research Centre, London.

[2]   D. E. Gray, *Handbook of the American Institute of Physics*, **1957**.

[3]   E. Bungel and S. Rajagopal, 'Solvatochromism and solvent polarity scales', *Acc. Chem. Res.*, vol. 23, pp. 226-231, **1990**.

[4]   C. Reichard, 'Solvatochromic dyes as solvent polarity indicators', *Chem. Rev.*, vol. 94, pp. 2319-2358, **1994**.

Chapter 7

Nonlinear Measurements

7.1 Introduction

In this chapter the results for the nonlinear optical experiments described in Chapter 4 are presented. The second order susceptibility is measured using second-harmonic generation at 1064 nm and the electro-optic coefficient at the required wavelengths is inferred from these measurements. Finally, the two-beam coupling gain coefficient and the diffraction efficiency are presented as a function of the applied electric field.

Second harmonic generation, two-beam coupling and degenerate four-wave mixing are a series of experiments required to characterize every potential photorefractive film. These three experiments were performed *in situ* and the one following the other. Firstly the optical nonlinearity of the film was examined with second harmonic generation and the second order susceptibility was measured. After the film was proven electro-optic, the two-beam coupling experiment was set-up and the two beam coupling coef-

ficient was measured. Once the film demonstrated photorefractive response, the degenerate four-wave mixing experiment was performed and the diffraction efficiency was measured.

The nonlinear optical measurements are very film-thickness dependent, and various factors had to be taken into consideration. For the geometry adopted in this experiment (c. § 4.4.4) the diffraction efficiency varies according to the relation [1]

$$\eta_p \propto d r_{eff}{}^2 E_{SC}^2$$

where d is the film thickness, r_{eff} is the effective electro-optic coefficient and E_{SC} the space-charge field. It can be seen that in general the diffraction efficiency increases with film thickness. However, with corona poled films, where the internal electric field is limited by the maximum density of deposited charge on the film surface, the maximum electro-optic coefficient that can be obtained reduces dramatically with increasing film thickness. The optimum film thickness therefore has to be investigated.

In this work, films of different thickness were investigated for their electro-optic and photorefractive properties. The results presented here are of those films that gave the highest diffraction efficiency, as is in line with previously reported work (c. Table 1.1, for examples).

7.2 Second Harmonic Generation

The theory and the set up of the second harmonic generation experiment have been described in § 4.4.2. The film under investigation was firstly placed on the corona poling holder with an angle of 45° between the sample normal and the laser beam. The laser beam was polarized in the plane of incidence (i.e. p polarized) and the power of the beam was set to levels adequate to generate second harmonic without destroying the polymer film.

The voltage of corona poling was switched on and the second harmonic generation of the film was monitored as a function of time. The output maximized and stabilized after 2-5 minutes. Then the beam was focused on the sample with the use of a lens and the maximum harmonic generation was measured for different values of the corona poling voltage.

After the second harmonic generation of the polymer film as a function of the applied corona poling film was recorded, the film was removed and replaced by a quartz wedge set at 0°. The quartz wedge was aligned so that the electric field vector was parallel to the $\chi_{11}^{(2)}$ coefficient of the quartz. Then the quartz wedge was translated relative to the beam until maximum second harmonic generation was achieved. The second-harmonic generation obtained was used as reference, in order to calculate the second order susceptibility of the polymeric films relevant to that of quartz, using equation (4.14).

The response of the $\chi_{33}^{(2)}$ as a function of the corona poling field of an approximately 60 μm thick film of NPP-doped PVK:C_{60} is presented in Fig-

ure 7.1. NPP-doped films showed high nonlinear optical response and toler-ance to the electric field. The $\chi_{33}^{(2)}$ increased almost linearly with the electric field up to approximately 13 kV needle voltage, and then started to increase very rapidly up to 16 kV needle voltage, where saturation occurred. This was a reproducible behaviour that was not observed for any other materials' combination. The reason for this rapid increase in second-harmonic genera-tion is not known, it might however have something to do with the very high concentration of the nonlinear optical material in the composite. Pre-vious work by Giacometti et al. [2,3] on the polar ferroelectric polymer poly-vinylidene fluoride (PVDF) and its copolymers has shown that, when the material was corona poled, its surface potential increased in a similar fash-ion to that of the $\chi^{(2)}$ of NPP in Figure 7.1. In this case, the electric field inside the material would have a similar increase, which would cause a propor-tional increase of the value of $\chi^{(2)}$. This is however only a suggestion and further work is needed to explain the phenomenon properly.

DAN doped films demonstrated a relatively low nonlinear optical re-sponse and small tolerance to the corona voltage. No second-harmonic gen-eration could be observed for a corona poling voltage lower than 10 kV and any voltage higher than 13 kV could not be applied due to electrical break-down. The $\chi_{33}^{(2)}$ response as a function of the electric field for a 45 μm thick film is presented in Figure 7.1.
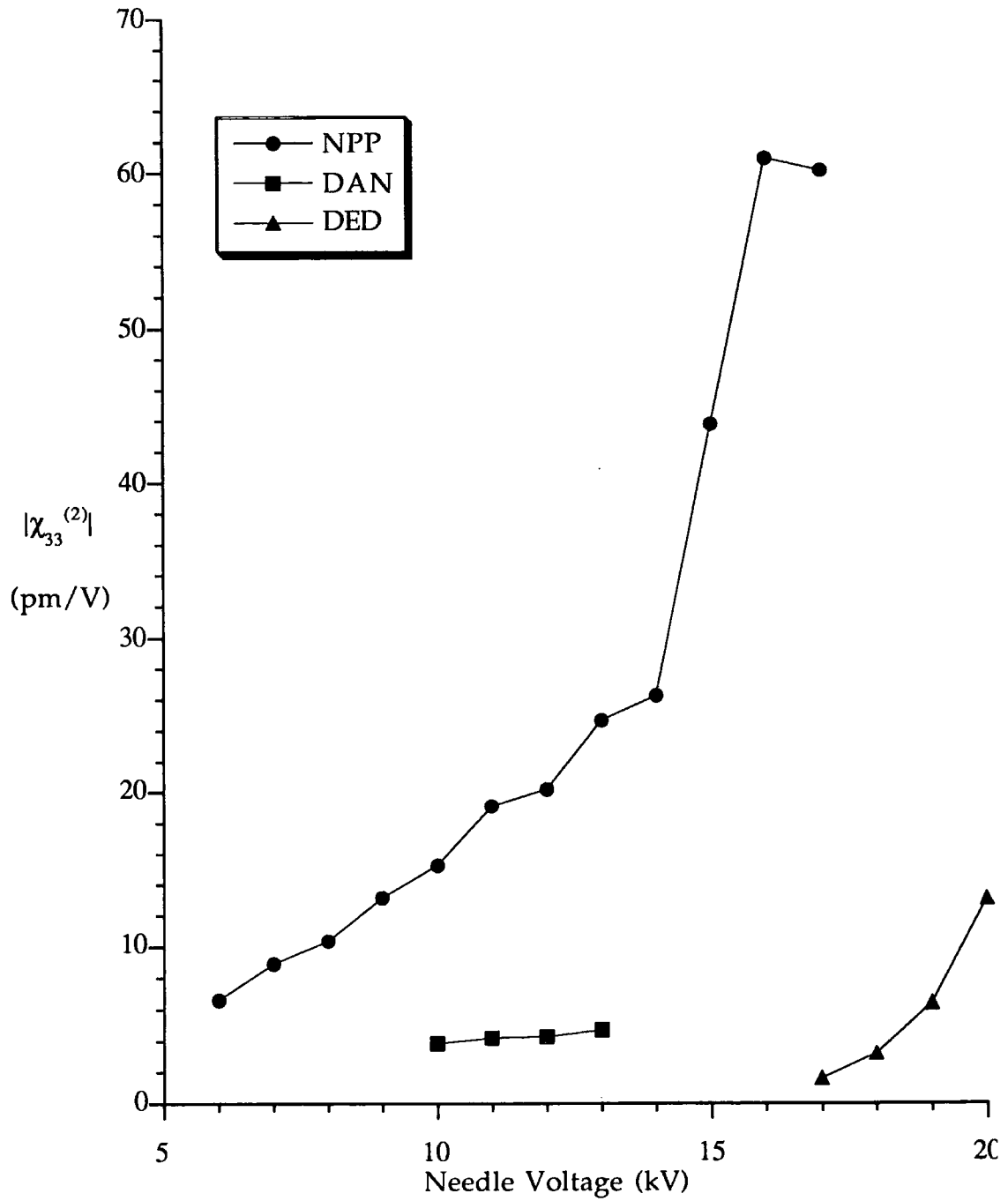
Figure 7.1 The $\chi_{33}^{(2)}$ as a function of the applied field for NPP, DAN and DED doped polymer films. Film thickness; NPP: 60 μm, DAN: 45 μm, DED: 30 μm
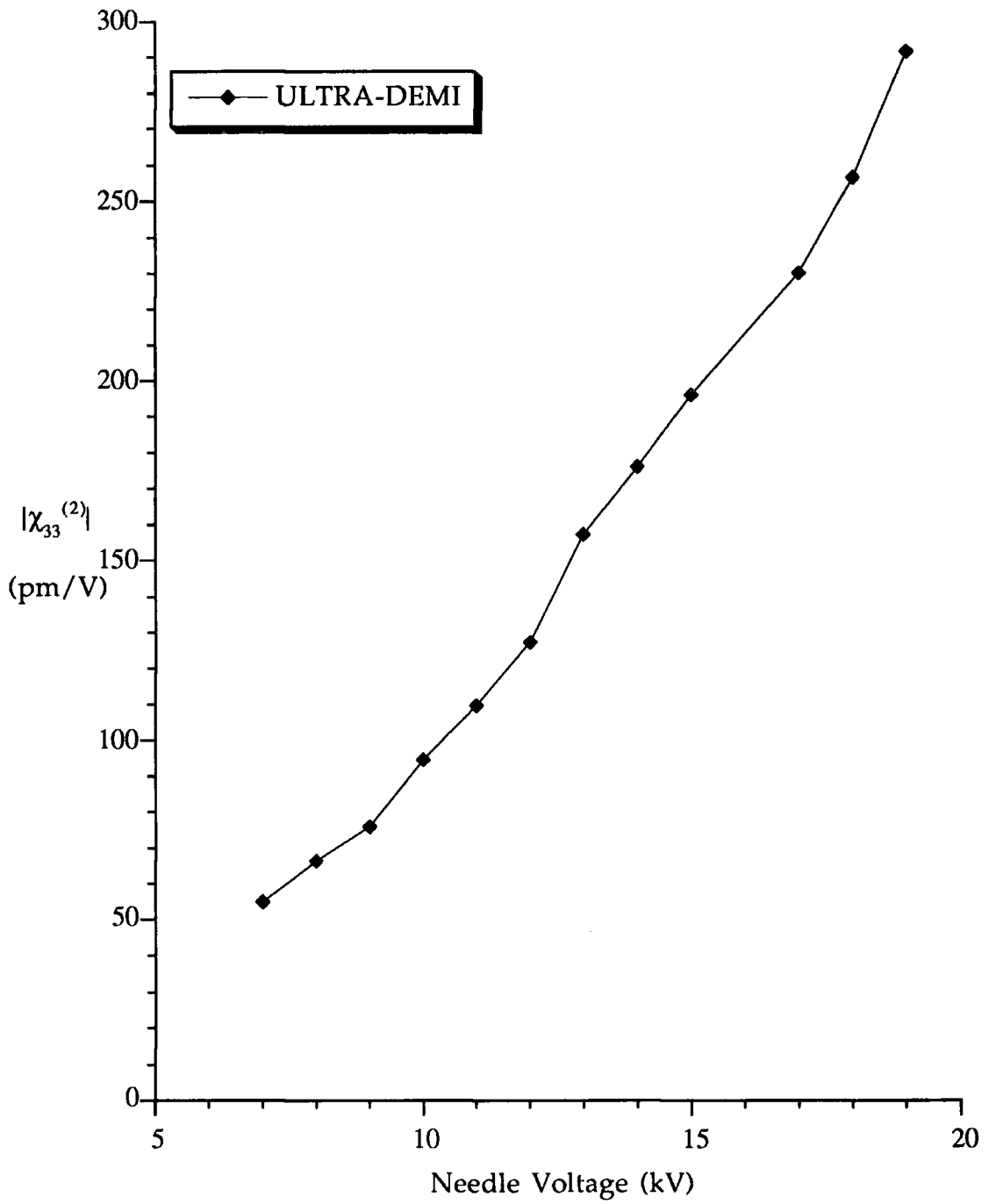
Figure 7.2 $\chi_{33}^{(2)}$ as a function of the poling field for a 6 μm thick ULTRA-DEMI doped film.

DED doped films showed a quite high nonlinear optical response, considering that the doping level of DED was only 5%. They also showed very high tolerance to electric field and fields up to 20 kV could be applied. The $\chi_{33}^{(2)}$ as a function of the applied field for a 30 μm film is presented in Figure 7.1.

The DCNQI films prepared were very thin (2-5 μm) and of very low quality. These, in combination with the fact that the doping level of DCNQI was only 0.5%, had as a result that, even though a very high nonlinearity was expected, no second harmonic light was produced during the experiments.

ULTRA-DEMI doped PVK:C_{60} films showed a very high nonlinear optical response (Figure 7.2) and tolerance to the applied electric field. Difficulties in the film preparation limited the film thickness to a maximum of 6 μm, which meant that the ULTRA-DEMI results could not be compared directly with any of the other materials' results.

As in the case of DCNQI, no second harmonic light could be produced from DI-DEMI doped films, even though the films investigated were of reasonable quality and thickness (approximately 5 μm). No second harmonic light was produced even when PMMA was used as a host [4]. These lead us to believe that the nonlinearity of the DI-DEMI molecule might be very low.

The voltages used in this experiment are higher than the ones usually employed in corona poling experiments [11]. There are two reasons for this. Firstly, the distance between the needle and the sample (2.5 cm, c. Fig-

ure 4.3), is larger than that normally used in second-harmonic generation experiments. This is in order to obtain a more uniform charge distribution and avoid edge effects. Secondly, low T_g polymeric materials have higher conductivity than the high T_g ones and as a result the poling process is less efficient.

7.3 Derivation of the Electro-Optic Coefficient

The second order nonlinear optical susceptibility $\chi_{ij}^{(2)}$ and the electro-optic coefficient r_{ij} are frequency dependent. When the frequency of the second harmonic and the operating frequency of the electro-optic effect are the same, the relation between the two quantities can be approximated as [5]

$$-r_{ij}(-2\omega;2\omega,0) \approx \frac{2\chi_{ij}^{(2)}(-2\omega;\omega,\omega)}{n^4(2\omega)} \tag{7.1}$$

where ω is the frequency of the fundamental. In this work, the wavelength of the second harmonic is 532 nm and the operating wavelength of the electro-optic effect is 632.8 nm, in the case of NPP, DAN and DED doped PVK:C_{60} and 488 nm in the case of ULTRA-DEMI doped PVK:C_{60}. In this case, equation (7.1) has to be modified to take account of the dispersion. If ω is the frequency of the electro-optic effect and ω' the frequency of the second-harmonic generation measurements, then the relation between $\chi_{ij}^{(2)}$ and r_{ij} can be expressed as [6,7]

$$r_{ij}(-\omega;\omega,0) = -\frac{2\chi_{ij}(-2\omega',\omega',\omega')}{n^4(\omega)} f_g D_\omega \qquad (7.2)$$

where f_g is a factor taking account of the local field correction and in the case of this experiment is

$$f_g = \frac{(f^\omega)^2 f^0}{f^{2\omega'}(f^{\omega'})^2} \qquad (7.3)$$

and D_ω describes the dispersion of the electro-optic coefficient

$$D_\omega = \frac{(3\omega_0^2 - \omega^2)(\omega_0^2 - \omega'^2)(\omega_0^2 - 4\omega'^2)}{3\omega_0^2(\omega_0^2 - \omega^2)^2} \qquad (7.4)$$

where ω_0 is the frequency of electronic resonance of the material. The local field correction terms can be calculated using Onsager's formula for static fields

$$f^0 = \frac{\varepsilon_r(n_\omega^2 + 2)}{2\varepsilon_r + n_\omega^2} \qquad (7.5)$$

and Lorentz-Lorenz formula for optical frequency fields

$$f^\omega = \frac{n_\omega^2 + 2}{3} \qquad (7.6)$$

The quantities f^0, f^ω, $f^{\omega'}$, $f^{2\omega'}$, f_g and D_ω can be calculated using information from Tables 6.2, 6.9 and 6.11. These calculations are presented in Table 7.1. The only notable point in these calculations is the negative sign

nlo material	f^0	f^ω	$f^{\omega'}$	$f^{2\omega'}$	f_g	D_ω
NPP	1.96	1.84	1.64	2.22	1.10	0.82
DAN	1.78	1.70	1.63	2.05	0.94	0.86
DED	1.90	1.79	1.65	1.86	1.20	0.81
ULTRA-DEMI	2.07	2.14	1.64	2.14	1.65	-0.07

Table 7.1 The local field and dispersion factors required for the derivation of the electro-optic coefficient

and the very low value of the dispersion of ULTRA-DEMI doped films. It occurs because the frequency of the measurement of the electro-optic effect is higher than the frequency of the electronic resonance of the material (c. Table 6.9). As a result, this resonance is not contributing to the electro-optic effect.

Using this information the electro-optic coefficient of the different composites can be calculated at the required wavelengths. These results are presented in Figure 7.3.

It should be stressed that regardless of the corrections, equation (7.2) is still an approximation. Even though it serves well in demonstrating the potential of a electro-optic material at a certain wavelength, it is not good enough for device design. It was necessary because the low T_g of the material and the required film thickness for photorefractive measurements did not allow the use of the usually employed methods [8,9] for the measurement of the electro-optic coefficient. Recently, Kippelen and coworkers [10] have
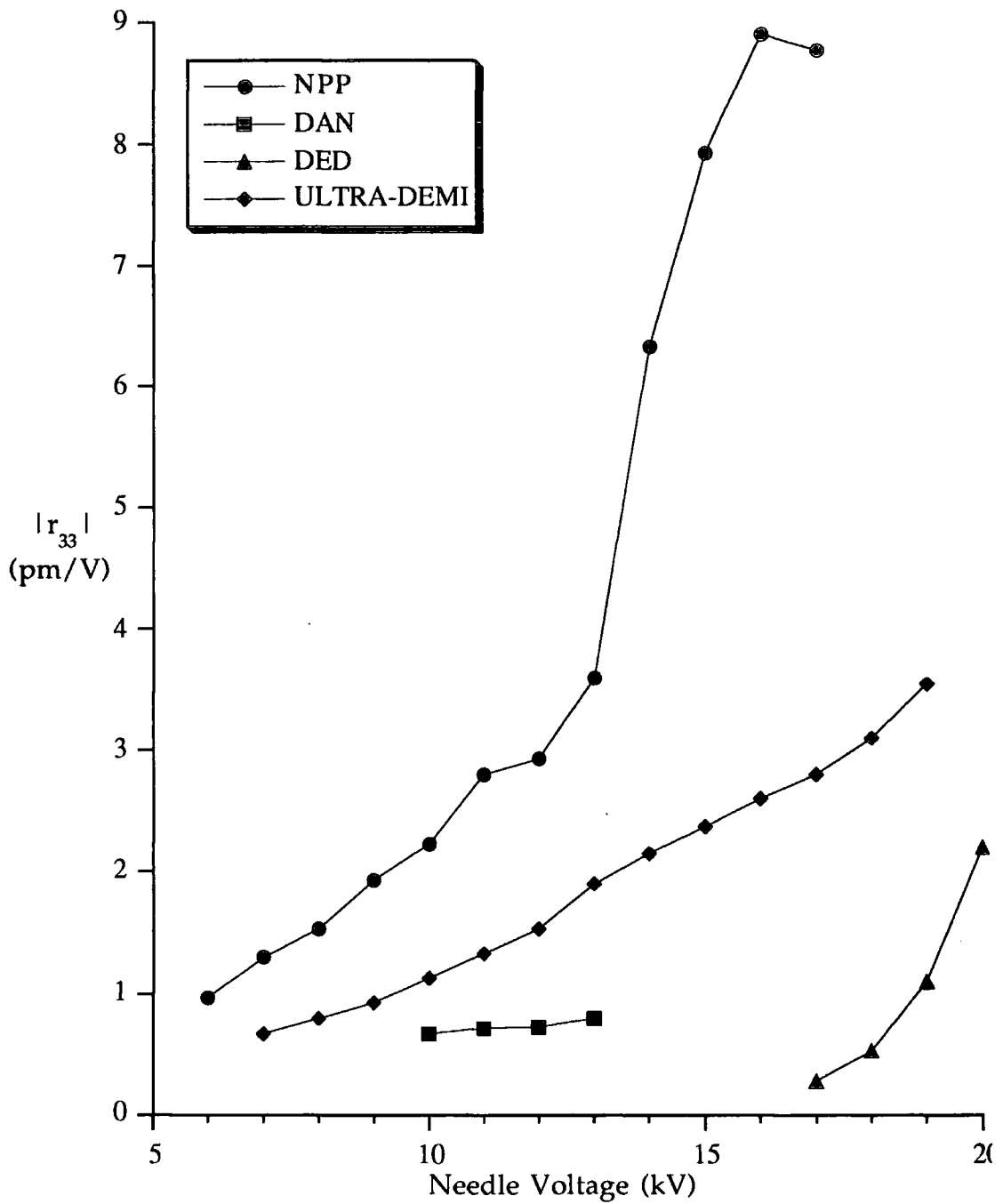
Figure 7.3 The r_{33} at 632.8 nm as a function of the applied field for NPP, DAN, DED and and at 488 nm forULTRA-DEMI doped PVK:C_{60} films. Film thickness; NPP: 60 μm, DAN: 45 μm, DED: 30 μm, ULTRA-DEMI: 6μm.

developed a new method which enables the direct measurement of the electro-optic coefficient of low T_g thick films.

7.4 Calculation of the Effective Electro-Optic Figure of Merit

A common way of comparing the electro-optic potential of a material is the means of an electro-optic figure of merit Q, which may be described by the relation [12]

$$Q = n^3 r_{eff} \tag{7.7}$$

where n is the refractive index of the material at the wavelength of the photorefractive measurements and r_{eff} is the effective electro-optic coefficient. The effective electro-optic coefficient is dependent on the experimental setup and in the case of a p polarized readout in a tilted geometry is given by the equation [1]

$$r_{eff} = r_{13}\left(\cos\theta_2 \sin(\theta_G + \theta_2) + \sin\theta_1 \cos\theta_2 \cos\theta_G\right) + \\ r_{33}\left(\sin\theta_1 \sin\theta_2 \cos\theta_G\right) \tag{7.8}$$

where θ_1 and θ_2 are the angles at which beams 1 and 2 respectively are propagating inside the sample (Figure 7.4). θ_G is the angle between the grating wave vector and the applied electric field. θ_1, θ_2, and θ_G can be calculated using Snell's law and the refractive index information from Table 6.11. The angle calculations for each materials' combination are presented in Table 7.2.
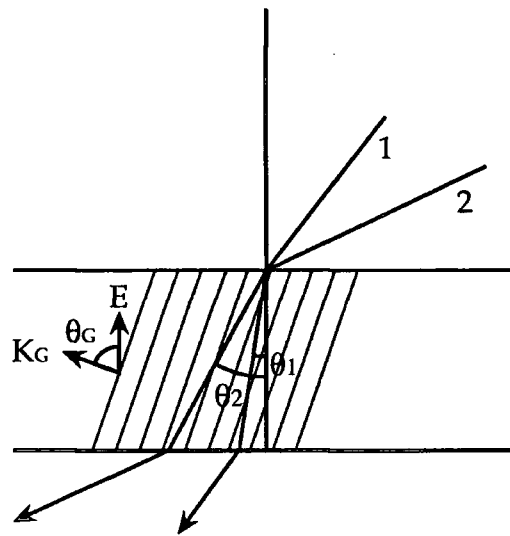
Figure 7.4 The tilted geometry used for the study of the photorefractive effect

nlo material	θ_1	θ_2	θ_G
NPP	15°	22°	72°
DAN	16°	24°	70°
DED	16°	28°	68°
ULTRA-DEMI	14°	20°	73°

Table 7.2 The different angles that the writing beams are propagating in the photorefractive material and the angle between the grating vector and the electric field, for each materials' combination

In this experiment, the r_{33} coefficient has been derived from the second-harmonic generation measurements. The r_{13} coefficient can be calculated using the standard assumption for linear chromophores in the small field limit $r_{33}=3r_{13}$ [1]. This assumption is known not to be valid in the case of ULTRA-DEMI doped polymers, where the relation depends on the field strength [11]. For the present conditions the relation is taken as $r_{33}=4r_{13}$, which is a reasonable mean value. Combination of equation (7.7), the information from Table 7.2 and the relation between r_{33} and r_{13} leads to the following relations for r_{eff}

for NPP $r_{eff} = 1.00r_{13} + 0.03r_{33} = 0.36r_{33}$ (7.9)

for DAN $r_{eff} = 1.00r_{13} + 0.04r_{33} = 0.37r_{33}$ (7.10)

for DED $r_{eff} = 0.97r_{13} + 0.05r_{33} = 0.37r_{33}$ (7.11)

for ULTRA-DEMI $r_{eff} = 1.04r_{13} + 0.02r_{33} = 0.31r_{33}$ (7.12)

Using equations (7.7), (7.9)-(7.12) and the information from Figure 7.3, the figure of merit for each materials' combination as a function of the applied corona poling field can be calculated. The results of these calculations are presented in Figure 7.5.

In order to be able to compare the potential of the investigated composites as photorefractive materials, the maximum figures of merit obtained
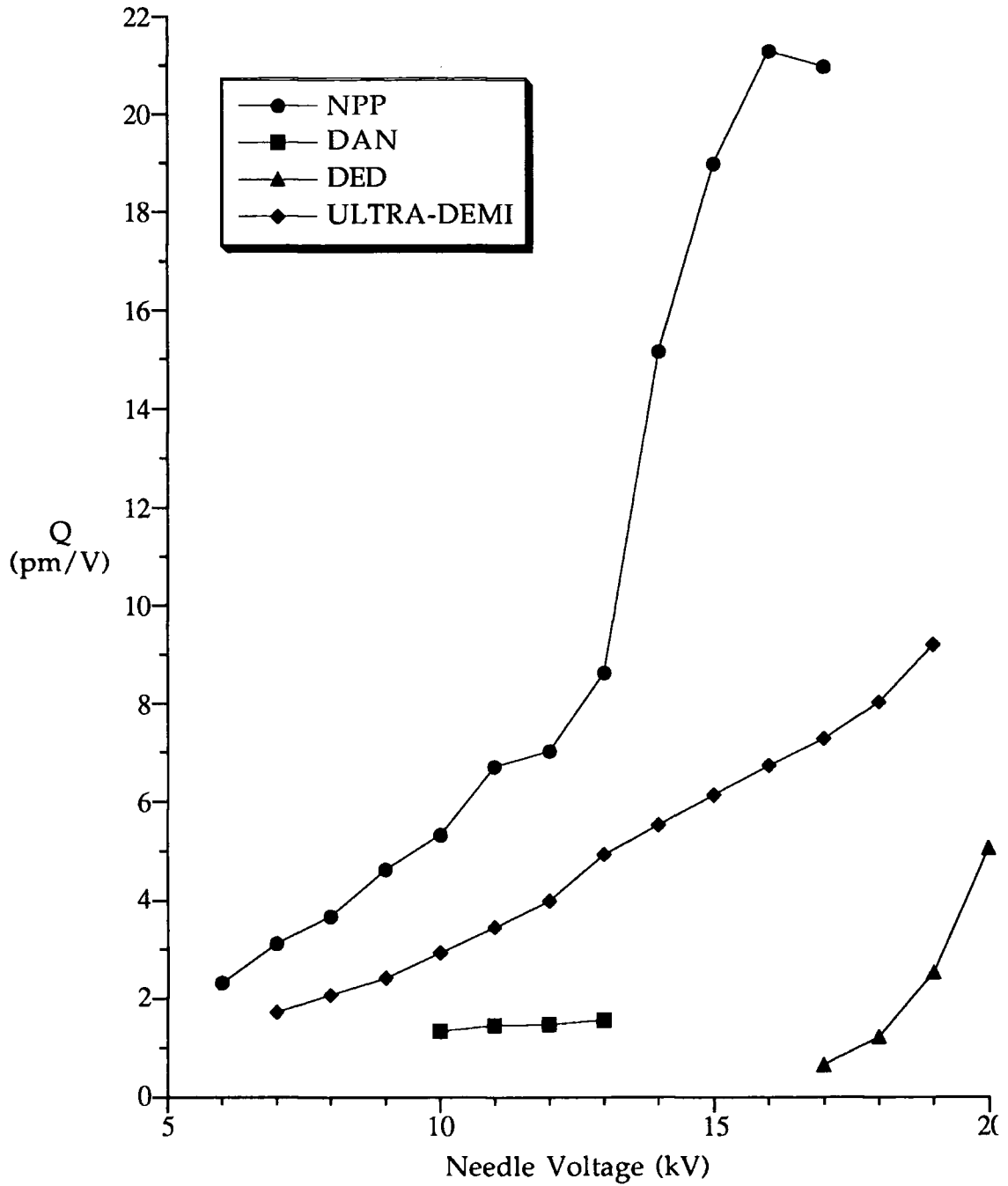
Figure 7.5 The figure of merit as a function of the applied field for NPP, DAN, DED
and ULTRA-DEMI doped PVK:C_{60} films. Film thickness; NPP: 60 μm,
DAN: 45 μm, DED: 30 μm, ULTRA-DEMI: 6μm.

Material	λ (nm)	r. index	max. r_{33} (pm/V)	max. $n^3 r_{eff}$ (pm/V)
NPP:PVK:C_{60}	632.8	1.88	8.77	20.97
DAN:PVK:ECZ:C_{60}	632.8	1.76	0.80	1.48
DED:PVK:ECZ:C_{60}	632.8	1.84	2.20	5.07
ULTRA-DEMI:PVK:ECZ:C_{60}	488	2.10	3.55	9.20

Table 7.3 The refractive index, the maximum r_{33} and the maximum $n^3 r_{eff}$ of the investigated materials at the operating wavelength of the photorefractive effect.

are presented in Table 7.3. In the same table are presented the operating wavelength, the refractive index and the r_{33} coefficient of these composites, to help comparison with the existing data of other polymeric photorefractive materials.

In Table 7.4 the refractive index, the maximum r_{33} coefficient and maximum electro-optic figure of merit of some other previously documented materials is presented. At the top two rows of Table 7.4, the theoretically predicted maximum values and the predicted maximum practical values are shown [12]. It can be seen that the electro-optic properties of the materials under investigation is lower than the maximum predicted but they are comparable with those of the existing photorefractive materials. There is generally however a lack of data of the electro-optic properties of the existing most efficient photorefractive polymers [13,14], which does not enable comparison with them.

Table 7.4 The refractive index, maximum r_{33} and maximum $n^3 r_{eff}$ of some photorefractive polymers

Material	refractive index	maximum r_{33}	maximum $n^3 r_{eff}$	References
theoretical limit	1.6-2.4		7600	[17]
typical estimation	2		800	[17]
DEANST:PVK:TPY	1.7	4.2		[20, 21]
DEANST:PVK:C$_{60}$	1.74	10		[22]
polyurethane	1.812	4.0	24.3	[23]
dialkyninonitrostilbene	1.72	38		[24]
PVK:F-DEANST:TNF			3.1	[25]
bisA-NAT:DEH			6.9	[26]
PMMA-PNA-DEH-C$_{60}$			0.3	[27]

7.5 Two-Beam Coupling Measurements

The two-beam coupling experiment was performed after the second-harmonic generation experiment had indicated a nonlinear optical response of the film under investigation. The experimental set-up has been described in § 4.4.3.

For the measurement of the two-beam coupling response of NPP, DAN and DED doped $PVK:C_{60}$ films, a He-Ne laser operating at 632.8 nm was used. The experiment was set up and the two beams were overlapped on the sample. One of the beams was blocked and the other beam was monitored as it was switched on again. This was before the corona poling voltage was applied, in order to investigate the existence of any gratings due to photochromic and thermal effects. These effects are not reversible or electric field dependent. No such gratings were found for any of the materials investigated. This was not, however, a definite proof for photorefractivity, since reversible, electric-field dependent, light induced non-photorefractive gratings have been reported in the past [23].

Unambiguous proof of the existence of the photorefractive effect was provided with the demonstration of a phase shifted refractive index grating [1]. As discussed in Chapter 2, the nonlocal character of the photorefractive effect results in the asymmetric energy exchange between the two writing beams. This was found to be the case for the NPP, DAN and DED doped polymeric composites. When the electric field was switched on, there was an energy transfer between the two beams. This energy transfer took several minutes to maximize, which was mainly due to the time needed for the es-

tablishment of the electric field, as shown at the second-harmonic genera-

tion measurements. This energy transfer disappeared once the electric field

was switched off. The same procedure was repeated for different values of

the applied field. The ratio γ_0 of the change of the power of each of the two

beams as a function of the applied electric field is shown in Figure 7.6.

Once the photorefractivity of the different polymeric composites was

proved, the two-beam coupling coefficient was then calculated using equa-

tion (4.21). These calculations are presented in Figure 7.7.

For the two-beam coupling measurements on ULTRA-DEMI doped

PVK:C_{60}, an Argon-ion laser operating at 488 nm was used[*]. In this case,

however, once the experiment was set up and the film was illuminated, the

material started discolouring and a clear spot appeared where the two beams

were joining. The phenomenon, a sign of photo-oxidation, took place only a

few seconds after the initial illumination of the film and made any photore-

fractive measurements impossible. This comes in contradiction with the

second-harmonic generation measurements, where no such effect was ob-

served, even though a much higher power laser was employed (c. § 4.4.2).

The explanation is that the photons of the 1064 nm light do not have

enough energy to photo-oxidize the ULTRA-DEMI molecules, and the pho-

tons of the 488 nm light do.

---

[*] The measurements involving an Argon-ion laser were performed at Heriot-Watt
University, Edinburgh, where the appropriate facilities were available. Thanks are
due to Dr. C. H. Wang and Dr. A. Kar for their hospitality and help.

In many photorefractive applications, such as beam amplification, it is required that the two-beam coupling coefficient exceeds the optical absorption coefficient at the wavelength of the photorefractive effect. The information for the optical absorption can be found in Table 6.8 and are noted on Figure 7.7. It can be seen that only NPP doped $PVK:C_{60}$ demonstrated net gain.
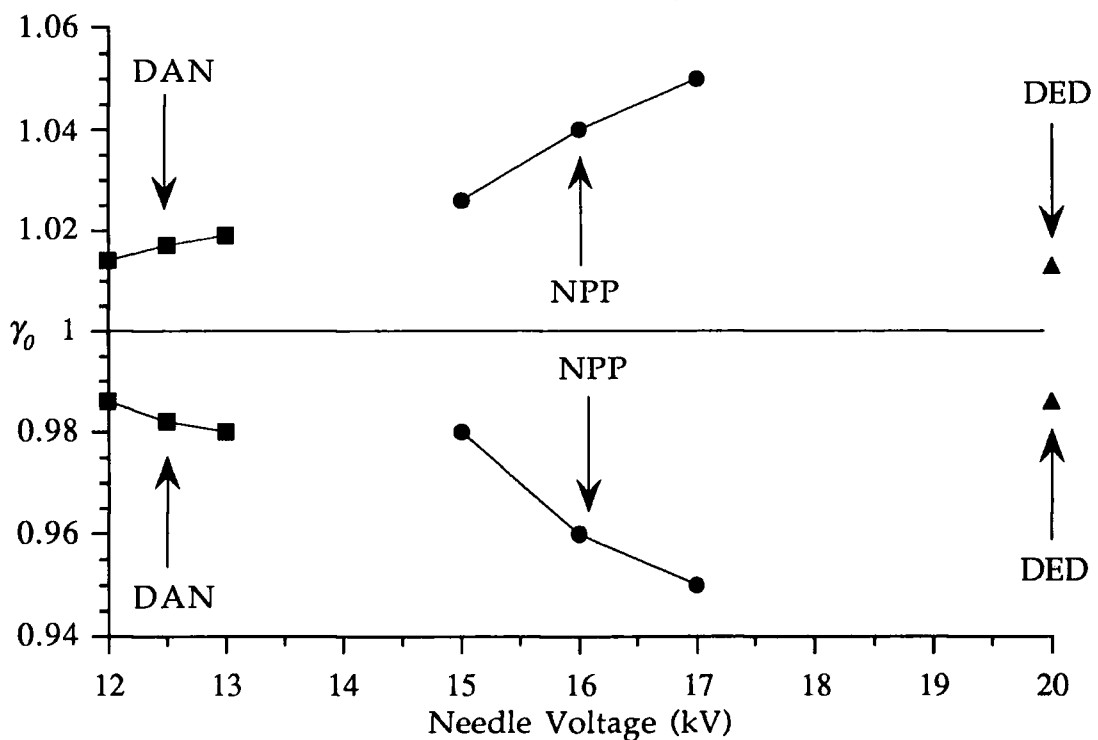

Figure 7.6 The ratio γ_0 of the change of the power of each of the two writing beams as a function of the applied electric field
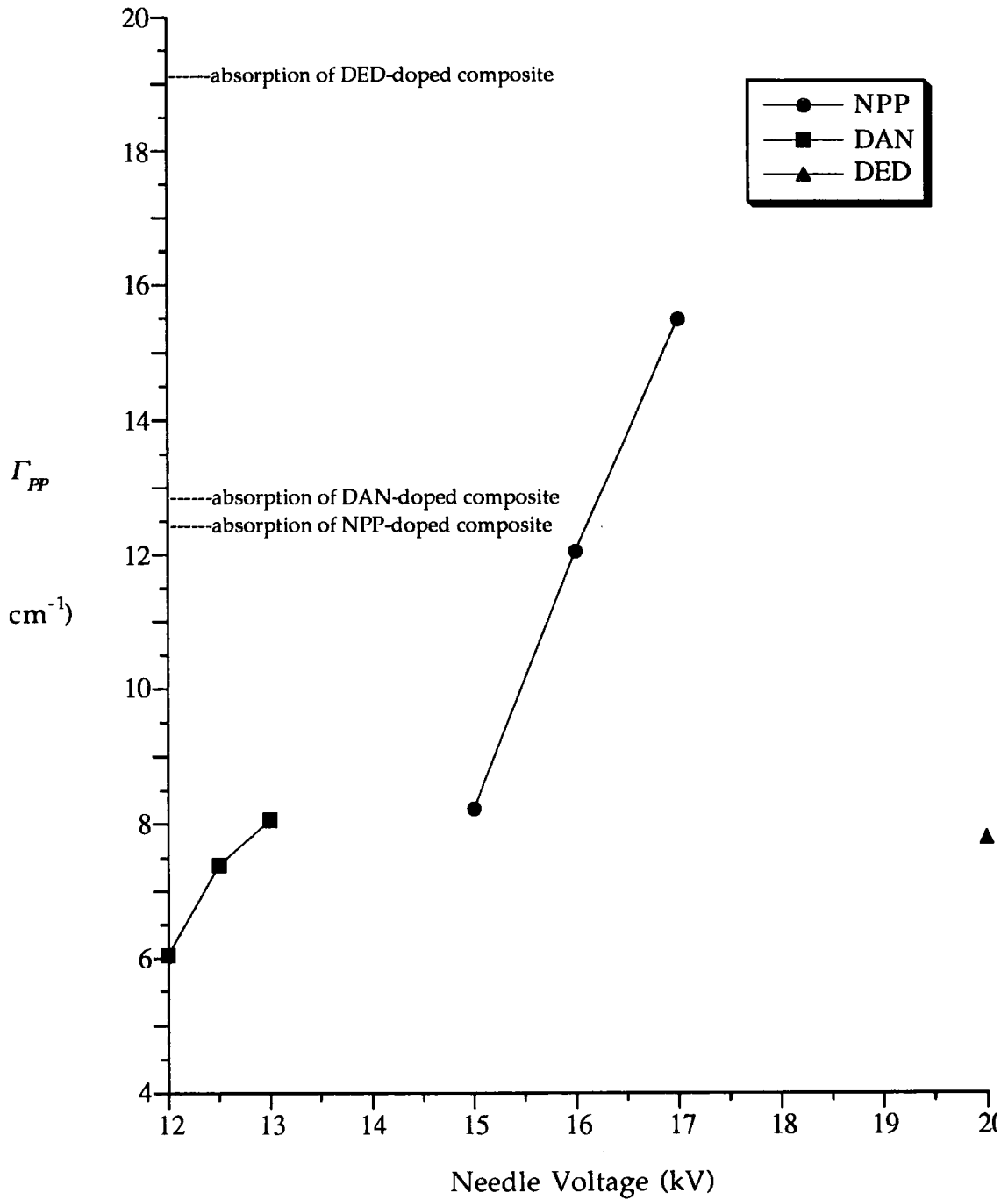
Figure 7.7 The two-beam coupling coefficient as a function of the applied field for NPP, DAN and DED doped PVK:C_{60} films. Film thickness; NPP: 60 μm, DAN: 45 μm, DED: 30 μm.

7.6 Degenerate Four-Wave Mixing Measurements

Once the photorefractivity of the polymeric composites was proven, their diffraction efficiency was measured using the degenerate four-wave mixing experiment described in § 4.4.4.

The two writing beams were overlapped on the sample and the corona poling voltage was switched on. Adequate time was left for the nonlinear chromophores to align with the electric field and the grating to form. Then a much weaker beam of the same wavelength counterpropagating one of the writing beams was used to probe the grating. Because of the existence of the photorefractive grating and the four-wave mixing geometry, part of the beam was diffracted at the direction of the other writing beam. The power of the beam was measured using the lock-in amplifier.

In order to measure the power of the probe beam with the lock-in amplifier, the corona poling was switched off and the probe beam was directed to counterpropagate the other writing beam. The power was measured employing the same set-up used earlier for the detection of the diffracted beam. In order to avoid any nonlinear response of the detector, neutral density filters were used to reduce the power of the probe beam to the same order of magnitude as the diffracted beam. This way, the absolute power of the two beams need not be known and the diffraction efficiency can be calculated from the ratio of the power of the diffracted beam over the power of the probe beam. The measurement was taken for several values of the electric field and the results are presented in Figure 7.8.

The NPP doped polymeric composite gave the highest value of diffraction efficiency, 7.8×10^{-5} for a corona poling voltage of 17 kV. No diffraction could be measured for any voltage less that 15 kV.

DAN doped polymeric composite gave a maximum diffraction efficiency of 0.9×10^{-5}, for a corona poling voltage of 13 kV. A higher voltage could not be applied because of electrical breakdown. No diffraction could be measured for any voltage lower than 12 kV.

Finally, the DED doped film gave a diffraction efficiency of 2.1×10^{-6} for a corona poling voltage of 20 kV. No diffraction could be measured for a lower poling field.

The poling technique employed in this experiment does not allow the measurement of the applied film across the sample, so it is difficult to estimate the contribution of the orientational enhancement to the total diffraction. The diffraction efficiencies measured are comparable with those of most of the existing photorefractive polymers but several orders of magnitude lower than those of the most efficient ones (c. Table 1.1)
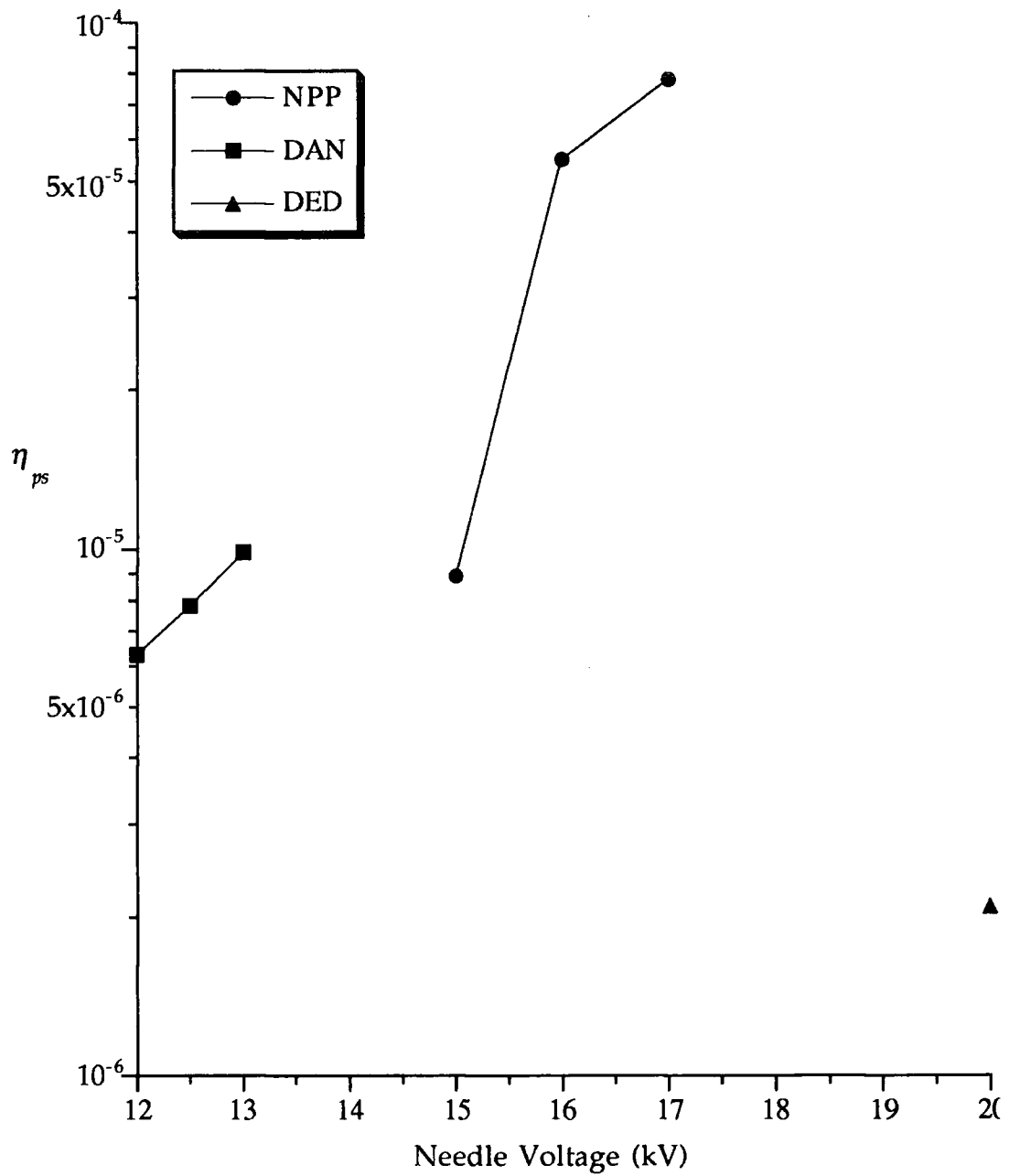
Figure 7.8 The diffraction efficiency as a function of the applied field for NPP, DAN and DED doped PVK:C_{60} films. Film thickness; NPP: 60 μm, DAN: 45 μm, DED: 30 μm.

7.7 References

[1] W. E. Moerner and S. M. Silence, 'Polymeric photorefractive materials', *Chem. Rev.*, vol. 94, pp. 127-155, **1994**.

[2] J. A. Giacometti and O. N. Oliveira, 'Corona charging of polymers', *IEEE Transactions on Electrical Insulation*, vol. 27, pp. 924-943, **1992**.

[3] G. M. Sessler, D. K. Das-Gupta, A. S. DeReggi, W. Eisenmengei. T. Furukawa, J. A. Giacometti, and R. G. Multhaupt, 'Piezo and pyroelectricity in electrets; Caused by charges, dipoles or both?', *IEEE Transactions on Electrical Insulation*, vol. 27, pp. 872-897, **1992**.

[4] D. Healy, University of Durham, personnal communication

[5] P. N. Prasad and D. J. Williams, *Introduction to nonlinear optical effects in molecules & polymers*, pp.102-104, John Wiley & Sons, **1991**.

[6] D. S. Chemla and J. Zyss, *Nonlinear Optical Properties of Organic Molecules and Crystals*, volume 1 of *Quantum Electronics*, pp. 437-468, Academic Press, **1987**.

[7] F. Kajzar, P. A. Chollet, I. Ledoux, J. L. Moigne, A. Lorin, and G. Gadret, 'Organic thin films for quadratic optics', *Proceedings of the NATO advanced research workshop on organic molecules for nonlinear optics and photonics*, pp. 403-432, **1990**.

[8] C. C. Teng and H. T. Man, 'Simple reflection technique for measuring the electro-optic coefficient of poled polymers', *Appl. Phys. Lett.*, vol. 56, pp. 1734-1736, **1990**.

[9] J. S. Schildkraut, 'Determination of the electrooptic coefficient of a poled polymer film', *Applied Optics*, vol. 29, pp. 2839-2841, **1990**.

[10] B. Kippelen, Sandalphon, K. Meerholz, and N. Peyghambarian, 'Birefringence, Pockels and Kerr effects in photorefractive polymers', *Appl. Phys. Lett.*, vol. 68, pp. 17481750, **1996**.

[11] D. Healy, P. R. Thomas, M. Szablewski, and G. H. Cross, 'Molecular $\mu\beta$ figure-of-merit studies of solid solutions', *SPIE Proceedings*, vol. 2527, pp. 32-40, **1995**.

[12] C. Bosshard, K. Sutter, P. Pr tre, J. Hulliger, M. Fl rsheimer, P.Kaatz, and P. G nter, *Organic Nonlinear Optical Materials*, pp. 211-212, Gordon and Breach, **1995**.

[13] K. Meerholz, B. L. Volodin, Sandalphon, B. Kippelen, and N. Peyghambarian, 'A photorefractive polymer with high optical gain and diffraction efficiency near 100%, *Nature*, vol. 371, pp. 497-500, **1994**.

[14] S. M. Silence, M. C. J. M. Donckers, C. A. Walsh, D. M. Burland, R. J. Twieg, and W. E. Moerner, 'Optical-properties of poly(N-vinylcarbazole)-based guest-host photorefractive polymer systems', *Appl. Optics* , vol. 33, pp. 2218-2222, **1994**.

[15] Y. Zhang, C. A. Spencer, S. Ghosal, M. K. Casstevens, and R. Burzynski, 'Thiapyrylium dye sensitization of photorefractivity in a polymer composite', *Appl. Phys. Lett.*, vol. 64, pp. 1908-1910, **1994**.

[16] Y. Zhang, C. A. Spencer, S. Ghosal, M. K. Casstevens, and R. Burzynski, 'photorefractive properties of a thiapyrylium -dye- sensitized polymer composite', *J. App. Phys.*, vol. 76, pp. 671-679, **1994**.

[17] M. E. Orczyk, J. Zieba, and P. N. Prasad, 'Fast photorefractive effect in PVK:C_{60}:DEANST polymer composite', *J. Phys. Chem.*, vol. 98, pp. 8699-8704, **1994**.

[18] Y. M. Chen, Z. H. Peng, W. K. Chan, and L. P. Yu, 'New photorefractive polymer-based on multifunctional polyurethane', *Appl. Phys. Lett.*, vol. 64, pp. 1195-1197, **1994**.

[19] M. J. Sansone, C. C. Teng, A. J. East, and M. S. Kwiatek, 'Observation of the photorefractive effect in a dialkylaminonitrostilbene copolymer', *Optics Letters*, vol. 18, pp. 1400-1402, **1993**.

[20] M. C. J. Donckers, S. M. Silence, C. A. Walsh, F. Hache, D. M. Burland, W. E. Moerner, and R. J. Twieg, 'Net two-beamcoupling gain in a

polymeric photorefractive material', *Optics Letters,* vol. 18, pp. 1044-1046, **1993**.

[21] Ducharme, B. Jones, J. M. Takacs, and Z. Lei, 'Electric-field stabilization and competition of gratings in a photorefractive polymer', *Optics Letters,* vol. 18, pp. 152-154, **1993**.

[22] S. M. Silence, C. A. Walsh, J. C. Scott, and W. E. Moerner, 'C_{60} sensitization of a photorefractive polymer', *Appl. Phys. Lett.,* vol. 61, pp. 2967-2969, **1992**.

[23] B. E. Jones, S. Ducharme, M. Liphardt, A. Goonesekera, J. M. Takacs, L. Zhang, and R. Athalye, 'Photoconductivity and grating response-time of a photorefractive polymer', *J. Opt. Soc. Am. B,* vol. 11, pp. 1064-1072, **1994**.

Chapter 8

Conclusion

8.1 Conclusion

Polymeric photorefractive materials are often investigated in compart-mentalized fashion. The photorefractive properties are measured but the other properties of these materials are ignored. In this work, a more complete approach to the subject was attempted. The dielectric and linear and nonlinear optical properties of a series of potential photorefractive composites were investigated.

The materials investigated were a series of PVK:C_{60} based composites. High doping level of the nonlinear optical material was possible only in the case of NPP, and in all the other cases was limited by the low solubility of the dopant. The materials were plasticized so as to reduce their glass transition temperature. This is a common practice and has proven to enhance the performance of polymeric photorefractive materials. It can

prove however to be a drawback when it comes to applications, since low T_g materials cannot be poled permanently and a high voltage is required for the photorefractive effect to operate.

The measurements carried out in this work could be divided into three main categories; dielectric measurements, linear optical measurements and nonlinear optical measurements.

The dielectric measurements were carried out at three frequencies and two different methods were employed. The capacitance bridge method employed for the measurements at 1 KHz and 1 MHz proved to be extremely accurate, especially for films thicker than 20 μm. For the dielectric measurements at 10 GHz, a new adaptation of the resonant cavity method was employed. This method gave very accurate results without requiring complicated sample preparation, as is the case with most other techniques. The design of the sample holder allowed measurements at elevated temperatures. The metod was confirmed with the determinationof the dielectric properties at elevetated temperatures of two electro-optic polymers.

The linear optical measurements consisted of absorption measurements and refractive index measurements. The absorption measurements revealed an interesting interaction between PVK and ULTRA-DEMI signified in a shift of the absorption spectrum. The nature of this interaction is not known and further research is needed to understand it. We suspect however that it might be due to a weak charge interaction between the two molecules.

The refractive index of the different composites was measured using a fringe technique. This is not a very accurate method, but it was found to be necessary because of the high absorption of the composites at the operating wavelengths. This is a general problem with photorefractive materials, which by definition are absorptive at the wavelength that the photorefractive effect operates. This might be the reason that in most published work the measurement is ignored and a value of 1.7 is assumed. We have proven this to be wrong in the case of PVK based photorefractive polymers; the refractive index is very much wavelength-dependent in the visible part of the spectrum and it only approaches 1.7 at wavelengths higher than 700 nm.

The nonlinear optical measurements consisted of second harmonic generation, to prove the nonlinearity of the composites and calculate the electro-optic coefficient, two-beam coupling measurements, to prove that the dominant grating mechanism was the photorefractive effect and degenerate four-wave mixing measurements, to measure the diffraction efficiencies of the composites.

From the second harmonic generation measurements the second order susceptibility was calculated and the electro-optic coefficient was inferred using the two level model. This model works quite well for materials such as NPP, DAN and DED, but not for complicated molecules such as ULTRA-DEMI, especially at frequencies higher than the electronic resonance frequency of the material, where the electronic resonance is not a dominating factor contributing to the electro-optic effect and higher

resonances are not taken into account. As a result, the value given for the electro-optic coefficient of the ULTRA-DEMI-doped composite, is only a rough estimation. A better estimation of the real value would be obtained if the three-level model was used for the calculations. The three-level model however does not have a general solution; research is under way for its calculation in the case of the ULTRA-DEMI molecule.

The two-beam coupling measurements proved the photorefractivity of the NPP, DAN and DED composites and that net gain could be obtained only for the NPP composite. The fourth nonlinear optical material, ULTRA-DEMI, photoxidized before any photorefractive measurements were possible. The diffraction efficiencies measured through the four-wave mixing experiment were at least three orders of magnitude lower than the existing most efficient photorefractive polymer (c. Table 1.1).

The optical performance of the materials investigated in this work was limited by the fact that the samples were corona poled. Corona poled thin films have a better response than contact poled films because of limited electrical breakdown, but this is not the case for thicker films, such as the ones required for photorefractive measurements, where the applied voltage is limited by the maximum charge density of the film surface. As has already been explained earlier, contact poling was not possible because DED and ULTRA-DEMI suffered electrochemical reduction by charges induced from the electrodes. This problem could be eliminated with the use of a passivating layer that would block those charges. It is very difficult however to find a suitable material since it would have to have a T_g

lower than the photorefractive material (that is, room temperature), otherwise during poling most of the electric field would drop across the passivating layer and the poling would be very inefficient.

One subject that has not been addressed in this work is the speed of the photorefractive effect. It is generally a very complicated subject and depends mainly on the power of the laser and also on the applied voltage, the host polymer, the dopant and the doping level and the thickness of the film. The laser used in this experiment was of quite low power, which would lead to a slow grating formation.

In conclusion, PVK host polymer doped with C_{60}, ECZ and four different nonlinear optical compounds exhibited second order nonlinearity and good processibility. The use of the dopants resulted in the observation of the photorefractive effect, which was confirmed by two-beam coupling and four-wave mixing experiments for three of the nonlinear optical materials (NPP, DAN, DED). The nonlinear optical performance of these materials was limited by the corona poling and the low solubility of the nonlinear optical compounds.

8.2 Further Work

From the above it is obvious that the current setup is not ideal for photorefractive materials, and further research is needed to optimize their photorefractive performance. This research should point at two directions; optimizing the chemical properties of the materials and investigat-

ing ways to reduce the electric field required for the photorefractive effect to operate.

As far as the chemistry of the materials is concerned, there are two main problems to be solved; stability and solubility. Stability was a problem in the case of ULTRA-DEMI, and further work is needed to understand the electrochemistry of this material. Solubility was a problem with all materials except NPP. This problem could be solved by either adding to the structure of the material components that would make the material more soluble, or by chemically incorporating the nonlinear optical molecule at the side chain of PVK, or other photoconducting polymers.

This is probably the way to the solution of the other problem and reduction of the electric field required for the operation of the photorefractive effect. By avoiding doping of the material, high T_g can be obtained. These materials do not need *in situ* poling; the material could be poled beforehand and only a much smaller voltage would be required for the application. Another approach to this problem would be to experiment with different sample structures. Samples with multiple layers or samples in a waveguide geometry are easy to fabricate and would require a lower operating voltage.